2011-10-14

# Telomere Length Dynamics in Human T Cells: A Dissertation

Joel M. O'Bryan
*University of Massachusetts Medical School*

# TELOMERE LENGTH DYNAMICS IN HUMAN T CELLS

A Dissertation Presented

By

JOEL M. O'BRYAN

Submitted to the Faculty of the

University of Massachusetts Graduate School of Biomedical Sciences, Worcester

in partial fulfillment of the requirements for the degree of

DOCTOR OF PHILOSOPHY

OCTOBER 14, 2011

IMMUNOLOGY AND VIROLOGY

TELOMERE LENGTH DYNAMICS IN HUMAN T CELLS

A Dissertation Presented

By

JOEL M. O'BRYAN

The signatures of the Dissertation Defense Committee signifies
completion and approval as to style and content of the Dissertation

Anuja Mathew, Ph.D., Thesis Advisor

Kendall L. Knight, Ph.D., Member of Committee

Timothy F. Kowalik, Ph.D., Member of Committee

Raymond M. Welsh, Ph.D., Member of Committee

Loren D. Fast, Ph.D., Member of Committee

This signature of the Chair of the Committee signifies that the written dissertation meets
the requirements of the Dissertation Committee

Katherine Luzuriaga, M.D., Chair of Committee

The signature of the Dean of the Graduate School of Biomedical Sciences signifies
that the student has met all graduation requirements of the school.

Anthony Carruthers, Ph.D.,
Dean of the Graduate School of Biomedical Sciences

Program in Immunology Virology
October 14, 2011

## ACKNOWLEDGEMENTS

This has been a much longer endeavor than I imagined seven years ago when I started. In hindsight, it has been a “slog” at times, but fully worth the effort as I near the end of one chapter in my life and look forward to the next. The excitement of science “discoveries,” even as small as they are for a grad student, is what I found along the way to make it a fulfilling and worthy effort. For that effort to have even had a chance, I certainly must thank those who were instrumental along the way.

My two mentors, Alan Rothman and Anuja Mathew, have wisely guided me though this process since joining the lab six years ago. Their mentorship has been essential to my development as a scientist; a process I now realize can never be complete, even in a lifetime of science. Alan’s thoughtful advice combined with guiding directions and questions allowed me to find insights to questions I had not seen in my own data. I realize that is the essence of a philosophy of science which Alan has shown me -- to see beyond what we are taught and ask the essential, most pertinent questions, not merely what is preconceived by existing biases in a jumble of data. Anuja’s skills of patience and persistence, coupled with her healthy skeptical scientific rigor, have been equally essential into my investigations and views of my own data. She taught me how to think like a scientist and be skeptical of what I think I see. The probing questions she asked has kept me grounded in the reality that good science is really about “show me, prove it to me.” For all this and for both of their many hours of discussions, corrections, and patient listening to my long explanations, I am forever grateful to Alan and Anuja.

I want to thank and acknowledge the help of Marcia Woda and her patience in teaching me how not just to use the FACS Aria flow cytometer, but to understand it as well. I do not know if the road that lies ahead of me has “flow” on it, but if it does, Marcia has me well prepared. Thank you, Marcia.

Acknowledgement of my time in CIDVR would not be complete without thanking Kim West. Her absolutely critical help and training with cell cultures, their reagents, and always helping me to find that one cryo-preserved sample among ten of thousands of frozen vials was a major factor in my simply not flailing and failing as I worked to get cell culture experiments and projects off and running. I wish her the best as she has moved on ahead of me to new opportunities in science.

Of course, I save the last acknowledgement, and the most important, for my wife and best friend. I cannot thank Terri enough for the patience and love she has given me through these years. Her gracious acceptance of the many Friday nights I had to spend with my other girlfriend “Ms. Aria”, instead of with her, was truly a sacrifice. She would always ask if my experiment worked or not when I came dragging home, and she would still love me even when it usually didn’t.  As anyone who knows me knows, I could go on and on, but I will conclude with a simple, “Thank you, my Love,” to Terri, my beloved wife and partner.

# ABSTRACT

Telomere length has been shown to be a critical determinant of T cell replicative capacity and in vivo persistence in humans. We evaluated telomere lengths in virus-specific T cells to understand how they may both shape and be changed by the maintenance of memory T cells during a subsequent virus re-infection or reactivation. We used longitudinal peripheral blood samples from healthy donors and samples from a long-term HCV clinical interferon therapy trial to test our hypotheses.

To assess T cell telomere lengths, I developed novel modifications to the flow cytometry fluorescence in situ hybridization (flowFISH) assay. These flowFISH modifications were necessary to enable quantification of telomere length in activated, proliferating T cells. Adoption of a fixation-permeabilization protocol with RNA nuclease treatment prior to telomere probe hybridization were required to produce telomere length estimates that were consistent with a conventional telomere restriction fragment length Southern blot assay.

We hypothesized that exposure to a non-recurring, acute virus infection would produce memory T cells with longer telomeres than those specific for recurring or reactivating virus infections. We used two acute viruses, vaccinia virus (VACV) and influenza A virus (IAV) and two latent-reactivating herpesviruses, cytomegalovirus (CMV) and varicella zoster virus (VZV) for these studies. Combining a proliferation assay with flowFISH, I found telomeres in VACV-specific $CD4^+$ T cells were longer than those specific for the recurring exposure IAV; data which support my hypothesis.

Counter to my hypothesis, CMV-specific $CD4^+$ T cells had longer telomeres than IAV-specific $CD4^+$ T cells.

We assessed virus-specific $CD4^+$ T cell telomere length in five donors over a period of 8-10 years which allowed us to develop a linear model of average virus-specific telomere length changes. These studies also found evidence of long telomere, virus-specific $CD45RA^+$ T cell populations whose depletion may precede an increased susceptibility to latent virus reactivation.

I tested the hypothesis that type I interferon therapy would accelerate T cell telomere loss using PBMC samples from a cohort of chronic hepatitis C virus patients who either did or did not receive an extended course of treatment with interferon-alpha. Accelerated telomere losses occurred in naïve T cells in the interferon therapy group and were concentrated in the first half of 48 months of interferon therapy. Steady accumulation of $CD57^+$ memory T cells in the control group, but not the therapy group, suggested that interferon also accelerated memory turnover.

Based on our data, I present proposed models of memory T cell maintenance and impacts of T cell telomere length loss as we age.

# TABLE OF CONTENTS

# LIST OF TABLES

# LIST OF FIGURES

# ABBREVIATIONS

| | |
|---|---|
| $1^o$ | primary |
| $2^o$ | secondary |
| AICD | activation induced cell death |
| ALT | alanine aminotransferase |
| APC | antigen presenting cell |
| AST | aspartate aminotransferase |
| BMI | body mass index |
| BrdU | bromodeoxyuridine |
| CFSE | carboxy fluorescein succinimidyl ester |
| CMV | cytomegalovirus |
| CTL | cytotoxic T lymphocyte |
| CV | coefficient of variation |
| DDR | DNA damage response |
| DNA | deoxyribonucleic acid |
| HALT-C | Hepatitis C Antiviral Long-term Treatment against Cirrhosis |
| HCV | hepatitis C virus |
| HIV | human immunodeficiency virus |
| IAV | influenza virus A |
| IFN | interferon |
| LN | lymph node |

| | |
|---|---|
| M21 | HALT-C trial randomization period month 21 |
| M45 | HALT-C trial randomization period month 45 |
| MESF | molecules of equivalent soluble fluorescence |
| MFI | mean fluorescence intensity |
| PBMC | peripheral blood mononuclear cells |
| PBS | phosphate buffered saline |
| PCR | polymerase chain reaction |
| peg-IFNα | pegylated-interferon alpha |
| PNA | peptide nucleic acid |
| RNA | ribonucleic acid |
| RPMI | Roswell Park Memorial Institute cell culture media |
| RTE | recent thymic emigrant |
| S00 | screening visit for HALT-C trial |
| SVR | sustained virologic response |
| TA | telomerase activity |
| TCR | T cell receptor |
| $T_{EMRA}$ | T cell effector memory re-expressing $CD45RA^{+}$ |
| TL | telomere length |
| TNF | tumor necrosis factor |
| TRF | telomere restriction fragment |
| VACV | vaccinia virus |
| VZV | varicella zoster virus |

# PREFACE

Parts of this thesis have appeared in separate publications:

**Chapter III (portions) and Chapter IV.**

O'Bryan JM, Woda M, Co M, Mathew A, Rothman AL (2011). Telomere length dynamics in human memory T cells specific for viruses causing acute or latent infections. *Submitted for publication.*

**Chapter III (portions) and Chapter V.**

O'Bryan JM, Potts JA, Bonkovsky HL, Mathew A, Rothman AL, for the HALT-C Trial Group (2011). Extended Interferon-Alpha Therapy Accelerates Telomere Length Loss in Human Peripheral Blood T Lymphocytes. *PLoS One*; 6(8):e20922. Epub 2011 Aug 4. PMID: 21829595.

Other work performed during thesis studies that is not presented in this dissertation has appeared in a separate publication:

Mathew A, O'Bryan J, Marshall W, Kotwal GJ, Terajima M, Green S, Rothman AL, Ennis FA (2008). Robust intrapulmonary CD8 T cell responses and protection with an attenuated N1L deleted vaccinia virus. *PLoS One.* 2008 Oct 2;3(10):e3323. PMID: 18830408.

# CHAPTER I

# INTRODUCTION

## A. Biology of peripheral T lymphocytes

$CD4^+$ and $CD8^+$ T cells have many overlapping, but also distinctly different and indispensable functional roles in the control of viral infections (1). However, both share the common characteristic of providing long-lived adaptive immunity for the host (2, 3). The establishment of stable pools of memory $CD4^+$ and $CD8^+$ T cells, able to recognize a specific pathogen, allows for a faster response on future pathogen-specific re-encounters. Thus antigen-experienced memory T cells spare the host the serious delay and consequences of mounting a new response with each re-infection or re-exposure. In order to carry out their functions, limited numbers of naïve T cells (for a primary response) or memory T cells (for a secondary response) must rapidly proliferate under settings of T cell receptor (TCR) mediated activation in a race for survival against infection.

### i. Building the T cell repertoire

The T cell compartment is built and continuously replenished by new, naïve T cell production from the thymus starting before birth and continuing well into adulthood (4, 5). The repertoire of naïve T cells contains a vast diversity in TCR sequence, allowing for high probability that some naïve T cells will exist to recognize any foreign epitope originating from an infecting virus or microbe (6). Naive T cells lack critical immediate

effector functions and have a homing phenotype that keeps them recirculating though lymph nodes to enable recognition of pathogen epitopes presented on lymph node-resident professional antigen presenting cells (APCs) (7). When first activated, naïve T cells must rapidly replicate and produce growth factors, such as IL-2. It is not the naïve T cell, but the multitude of clonally expanded daughter cells that carry the immune response forward and become armed with effector functions as they pass though the cell cycle with some eventually become the antigen-experienced memory T cells (8). In this regard, proliferation serves two critical roles -- amplification of numbers and continued differentiation of T cell effector functions. Understanding what influences the output of memory T cells thus necessitates understanding the input: naïve T cells, the "compartment" in which they reside, and how they are maintained (Figure 1.1).

**ii. Thymic involution as we age**

Our thymus undergoes a process after puberty that is termed involution, which steadily reduces the number of recent thymic emigrants (RTEs) in the naïve T cell compartment. Involution is the gradual shrinking and structural architecture change of the thymus as we age, thought largely due to accelerating senescence of thymic epithelial cells and loss of the cytokines they produce (5). A consequence of age-related thymic involution is an increasing reliance on homeostatic maintenance of the existing naïve T cell compartment (9, 10).

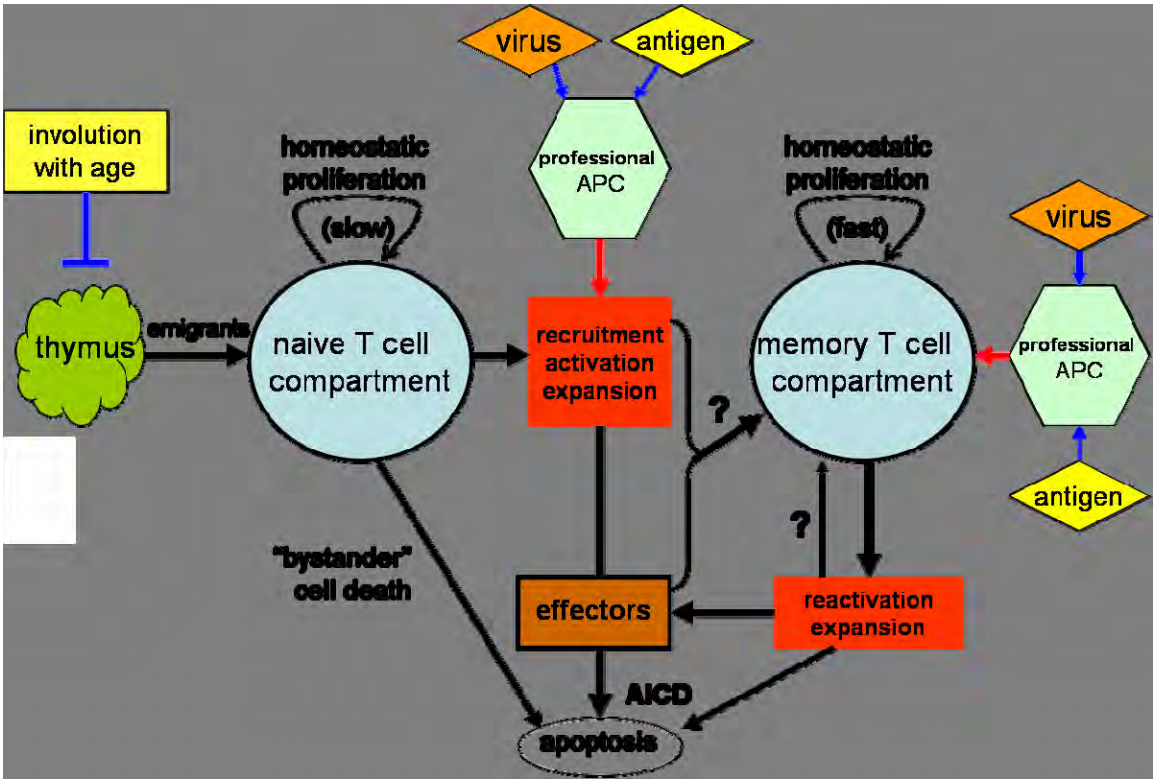


**Figure 1.1 The dynamics of peripheral T cells**

Naïve T cells emigrate from the thymus with an undifferentiated molecular phenotype, i.e. other than a high capacity to proliferate they lack most immediate effector functions such as interferon secretion or cytolytic killing capacity. Naive T cell numbers are maintained by the inflow of recent thymic emigrants (RTEs) and by slow homeostatic proliferation. Naïve T cell homeostatic proliferation is controlled by limiting levels of growth and survival cytokines, thus regulating total numbers. T cell loss from the naïve compartment can occur as a result of bystander death or by recruitment to become effectors or memory T cells. In the context of viral infections or immunization with viral antigen, professional antigen presenting cells (APC) provide signals for naïve T cell recruitment, activation, and expansion. Effector T cells generated during activation may be short-lived and undergo activation-induced cell death (AICD) or become effector memory cells for homeostatic maintenance within the memory compartment by survival cytokines. During memory responses, professional APCs can re-activate memory cells and drive further expansions. Age-related thymic involution results in a steady decline of RTEs. Homeostatic proliferation within the memory T cell compartment proceeds 5-10 times faster than in the naïve T cell compartment. Essential questions (?) exist in understanding “how” and “which” activated, reactivated, or effector T cells “decide” to become longer-lived memory T cells.

### iii. Memory T cells

#### a. Immediate effector responses of memory T cells

Memory T cells are capable of varying levels of immediate effector functions since they have already undergone a program of activation-induced expansion (11, 12). $CD8^+$ T cells act primarily through inducing programmed death of infected cells; a response termed a type 1 response (1). $CD8^+$ T cells deliver direct and indirect cytotoxic and antiviral signals to infected cells, while releasing signals to recruit other effector cells to these tissues.

$CD4^+$ T cells have been similarly described with all the helper type 1 (Th1) effector functions of $CD8^+$ T cells, but also are capable of other "helper" functions to guide, control, and limit immune responses of innate and adaptive immunity. $CD4^+$ T cells have been termed the master regulators of the immune system where they "license" and regulate many facets of activation in both adaptive and innate immunity. $CD4^+$ T cells are essential in the development of long-lived memory $CD8^+$ T cells with cytotoxic capacity and to B cells in generating long-lived antibody-secreting cells, the classically described Th1 and Th2 $CD4^+$ T cell responses, respectively (13-15). More recently, this B cell antibody supporting role has been expanded to include $CD4^+$ T cell helper functions necessary in the lymph node follicle termed a T follicular helper (Tfh) response (16).

Human memory $CD4^+$ T cells have been divided into two subsets of memory T cells with distinct homing potentials and effector functions based on the L-selectin receptor expression, CD62L (17). More differentiated, Th1 effector memory T cells lack

CD62L; conversely $CD62L^+$ expression is associated with a less differentiated central memory T cell phenotype (18, 19). In this regard, human activated $CD62L^+$ $CD4^+$ memory T cells mainly produce IL-4 and IL-5 associated with supporting B cell responses, whereas $CD62L^-$ $CD4^+$ T cells produce interferon-gamma, the signature Th1 cytokine (13, 16, 20). Importantly, formation of $CD62L^-$ effector memory $CD4^+$ T cells has been reported necessary for recovery of immune-suppressed transplant recipients from a cytomegalovirus (CMV) reactivation (21). The essential anti-viral effect of CD62L downregulation from T cells is also seen in experimental mice models of influenza virus infection (22). Furthermore, acquisition of tumor infiltrating cytolytic activity in T cells is associated with the shedding of CD62L from the T cell surface (23, 24). In mice and in humans, in vivo IL-2–derived signals promote the downregulation of CD62L and formation of the effector memory $CD4^+$ and $CD8^+$ T cell population (24, 25). Taken together, these data support the model that differentiation of T cells with more cytotoxic Th1, effector-like, $CD62L^-$ properties are likely critical aspects in the control of viral infections.

Small numbers of virus-specific T cell clones must rapidly proliferate over several days to produce a large number of activated, virus-specific T cells to carry-out the anti-viral effector functions. After the pathogenic microbes are eliminated, T cell numbers typically contract to only a small percentage of their maximal size through apoptosis; only a limited number of antigen-experienced cells remain to form the memory pool. How newly activated T cells become memory T cells is controversial and appears to depend on many factors (26).

### b. Rapid recall of memory T cells

Differentiated T cells undergo multiple cycles of DNA replication where T cells can progressively alter their chromatin and gain functions as they cycle (8, 27-29). Naive and less differentiated memory T cells express a range of cell surface co-stimulatory molecules, most notably CD28 and CD27, which provide signaling from stimulated APCs that enhances cellular metabolic functions during activation-induced proliferation. Highly differentiated T cells are often characterized by the loss of one or both of these molecules (30).

The proliferative capacity is quite low or even non-existent in highly differentiated T cells, especially those with high cytotoxic capacity (19, 31). Accordingly, in order for quiescent memory T cells to retain robust proliferative capacity in response to TCR signaling, the maintenance of memory T cells with a less than a fully differentiated state would appear to be a necessary prerequisite. How T cells of the same clonal origin decide different fates on the path to division and differentiation, with some as differentiated effectors and others as long-lived memory cells maintaining replicative capacity, is a central and critical question in T lymphocyte research.

### c. Reactivation of memory T cell responses

Re-vaccination or boosting is a common vaccination strategy to induce robust immunity. Many vaccines, particularly those with inactivated or highly attenuated pathogens, produce weak responses with a single inoculation. Most vaccines seek to attain high levels of virus neutralizing antibody levels via B cells to provide protective

immunity. However, a successful, high affinity antibody response is still dependent on T cell help to “license” the obligate B cell affinity maturation and isotype switching reactions (16, 32). Thus antigens from the vaccine preparations must simultaneously stimulate $CD4^+$ T cells to assist the B cell reactions.

### d. Homeostasis in the control of peripheral T cell compartments

A key feature of both naïve and memory T cell compartments is their relatively stable size over periods of many years (33). This overall homeostasis, or stability, occurs despite periodic infections inducing activation-driven clonal expansions to specific pathogens (34, 35), cytokine signaling from severe infections inducing infrequent episodes of lymphopenia, as well as thymic involution reducing the supply of RTEs (9, 36). The stable size of T cell compartments has been shown in mouse models to be dependent on the maintenance of a stable cytokine environment, notably IL-7 levels (9, 37). Effector T cells are also dependent to varying degrees on IL-15 and/or IL-21 for survival and growth (9). While IL-2 provides a critical growth and differentiation signal to effector T cells undergoing activation-induced expansion, its role in homeostasis appears largely confined to regulating the size of $CD4^+$ regulatory T cell numbers (38, 39). Thus the general picture is one of heterogeneous T cell compartments sustained and maintained by a milieu of soluble cytokines.

## B. Model Viral Infections of Humans

Some virus infections are acute – they are resolved quickly within a week or two and the pathogen is no longer detectable in the host, whereas other viral infections lead to persistent infections with a prolonged pathogen and antigenic presence providing chronic T cell stimulation (40). Finally, there are the latent-reactivating herpesviruses. In their natural host reservoirs, herpesviruses initially infect in an acute manner and then play a highly evolved game of "hide and seek" with the immune system after the acute phase resolves (41). How each of these virus-host models produce the persistence of virus-specific memory T cells likely relies on common mechanisms of T cell biology during induction. However each "model" may then play out in a different manner with time and re-exposure of the immune system to that specific or similar pathogen(s).

### i. Acute virus infections

Acute virus infections are those which are eliminated by the immune response, usually within a period of several weeks or less. In this context, seasonal influenza A virus (IAV) is considered an acute virus, one that healthy individuals are able to clear and which induces long-lived immunity. However, due to a process termed "antigenic drift," various IAV surface proteins slowly change each year, resulting in seasonal outbreaks of IAV (42). Thus, we are typically re-exposed to closely related IAV variants each season in a recurring pattern (43).

Existing high affinity antibodies would neutralize any virus that made its way past physical surface barriers, and then may present that viral antigen to memory T cells by

APCs and B cells. This would provide periodic TCR stimulation of T cells during the flu season even in the absence of productive infection. Overall, the effect of these periodic re-exposures, both infectious virus and vaccine antigens, may be such that virus-specific memory T cells become activated and expand, without a need for recruitment of new T cells to memory. Understanding how these recurring antigenic encounters may affect maintenance of T cell memory to IAV may be crucial to elucidating what factors may limit successful seasonal influenza immunizations.

Live vaccinia virus (VACV) is another acute infecting virus; it was used as the immunizing agent to eradicate smallpox. Individuals born before 1970 were routinely vaccinated with live VACV via skin scarification (44, 45). Since that time, VACV immunizations have been limited to medical, laboratory, and military personnel (46). Re-exposure of the immune system to VACV is generally assumed to be non-existent outside of known vaccinations. Immunization with VACV has been described as inducing life-long immunity through the production of virus-specific antibodies and memory T cells (44, 47).

**ii. Chronic viral infections and exhaustion**

Some viruses, such as human immunodeficiency virus (HIV), induce a state of chronic infection. HIV primarily infects $CD4^+$ T cells and causes a persistent viremia leading eventually to severe immune deficiency (48, 49). Hepatitis B and C viruses (HBV and HCV) initiate a chronic infection in the liver with sustained viremia, which can produce sustained liver damage and cirrhosis (50-53). Type I interferon is the accepted

clinical therapy for chronic HCV infection, and is also used for some patients with chronic HBV infection (54, 55). Additionally, elevated production of circulating type I interferons by innate cells in response to chronic viremia maintains the immune system in a continuous non-specific activated state (56, 57). This chronic immune activation in HIV infection by interferon is suspected as one of the causes leading to the depletion of T cells during the descent to immune deficiency (58, 59). Related to this effect, type I interferons have been shown in mice to produce bystander effects of apoptosis and/or reduced proliferative responses to TCR-signaled activation in T cells (60, 61).

These chronic virus infections have competing effects on the formation of specific T cell memory. Although HIV, HBV, and HCV initially drive a potent acute phase immune response, in the chronic phase long-term T cell memory fails to be either fully established and maintained by unclear mechanisms (62). This failure to maintain the T cell response has been termed clonal exhaustion, as the replicative capacity and effector functions of virus specific T cells diminishes with time (becomes exhausted) as the infection continues. With clonal exhaustion, virus-specific T cell numbers eventually fall to near undetectable levels.

**iii. Latent virus infections and periodic reactivation**

Herpesvirus infections, while having an acute primary phase with large scale virion production which seeds the virus throughout the body, eventually establish a life-long infection in specific target cells. Latency occurs after the immune response successfully eliminates lytically infected cells (those producing virus). Viral latency is a

state in which the virus hides from the host immune system by maintaining its viral DNA genome in the cell nucleus but expressing few if any viral epitopes on the cell surface (63-65). Two very common latent-reactivating herpesviruses differ in their host interactions, such as the frequency of reactivation and sites of latency. Cytomegalovirus (CMV) is thought to establish latency in a wide range of tissues and cell types, especially ubiquitously dispersed myeloid lineage innate immune cells, and to reactivate frequently (41). Varicella zoster virus (VZV), the virus of both chickenpox and shingles, establishes latency in ganglionic neurons and likely reactivates infrequently (66-68). Nevertheless, both viruses require life-long T cell-mediated immunity for their control (41, 69). Memory T cells reactive to these two herpesviruses are readily detectable in seropositive individuals (70). CMV is thought to form the basis of T cell memory clonal expansions seen in aging populations, where high frequencies of $CD8^+$ CMV-reactive T cells are common (66, 71). The basis for this T cell memory "inflation" is still poorly understood, but may relate to the frequency of reactivation of CMV and thus restimulation of T cell proliferation (41).

**C. Telomere biology**

Cellular DNA damage response (DDR) machinery must repair chromosome strand breaks that occur due to damaged nucleotides, replication fork stalls, or cross linked DNA. In doing so, the DDR machinery efficiently recognizes and ligates two DNA strands in an end-joining reaction (72, 73). In contrast, in order to maintain a stable genome through mitosis, the true termini of the chromosomes must not be fused.

Accordingly, cells have evolved a unique end structure - the telomere. Through complex mechanisms, functional telomeres prevent the end-joining DDR reactions between chromosomes. Telomeres are repetitive DNA sequences, consisting of hundreds to thousands of double-stranded repeats, found at both ends of every chromosome (74).

The normal diploid (2n) human cell has 46 chromosomes, and thus 92 telomeres. For every molecular solution, though, new complications arise – each telomere must be maintained during DNA replication. Telomere-associated proteins, termed the shelterin complex, recognize the unique six base pair (bp) telomere repeat sequence, 5'-TTAGGG-3', with high specificity and affinity. In addition to the long double-stranded repeats, the very end of the telomere terminates in a 3' G-rich overhang of up to several hundred bases formed by an unknown nucleolytic processing reaction (Figure 1.2.A) (74, 75). Shelterin complexes use poorly understood conformational changes to protect and safeguard the telomeres and their single-strand 3' DNA overhang from being recognized as DNA damage by the DDR pathways. When a telomere becomes exposed, this has been described as an "uncapped" state due to an altered shelterin-telomere configuration (76). Thus, if the telomere sequence reaches a critically short length and shelterin is unable to "re-cap" the telomere, a sustained DDR signaling cascade results in cell cycle arrest, i.e., a normal cell with too short, uncapped telomeres can no longer divide (Figure 1.2.B).

**i. Telomere length encodes replicative potential**

A normal cell's replicative potential has been linked to a combination of its telomere length (TL) and the ability to maintain that length, usually through expression of

the telomerase enzyme (77-79). Steady telomere shortening during cellular division, termed erosion, with the imposition of cell cycle arrest when telomeres get too short, protects chromosomal integrity and forms a barrier to unlimited growth of normal human cells (77). Telomere erosion and subsequent cell cycle arrest by critically short telomeres provided the molecular explanation to the so-called Hayflick limit observed almost 50 years ago -- the replicative limit observed when fibroblasts, continually grown in culture, slow their replication and eventually stop cycling, unable to further divide (78, 80). Telomere erosion occurs due to both the end-replication problem and the nucleolytic processing of the telomere ends. Telomere erosion during chromosomal replication typically results in 50-120 bp of telomere loss per cell cycle. Thus telomere erosion in human cells during replication is effectively a molecular cell cycle counting device which imposes limits on a normal cell's replicative capacity in the absence of some mechanism to reverse telomere erosion.

**ii. Telomerase assists in telomere maintenance**

Telomerase is a unique reverse transcriptase enzyme that elongates the G-rich 3' end of telomeres to assist in telomere maintenance during replication (Figure 1.2.C) (79, 81-83). The enzymatic action of telomerase on telomeres has been shown to be dose-dependent; high levels of telomerase during replication have been shown to arrest telomere erosion during rapid cell cycling and at very high levels telomerase can produce telomere elongation. B and T lymphocytes are among the few human somatic cells that

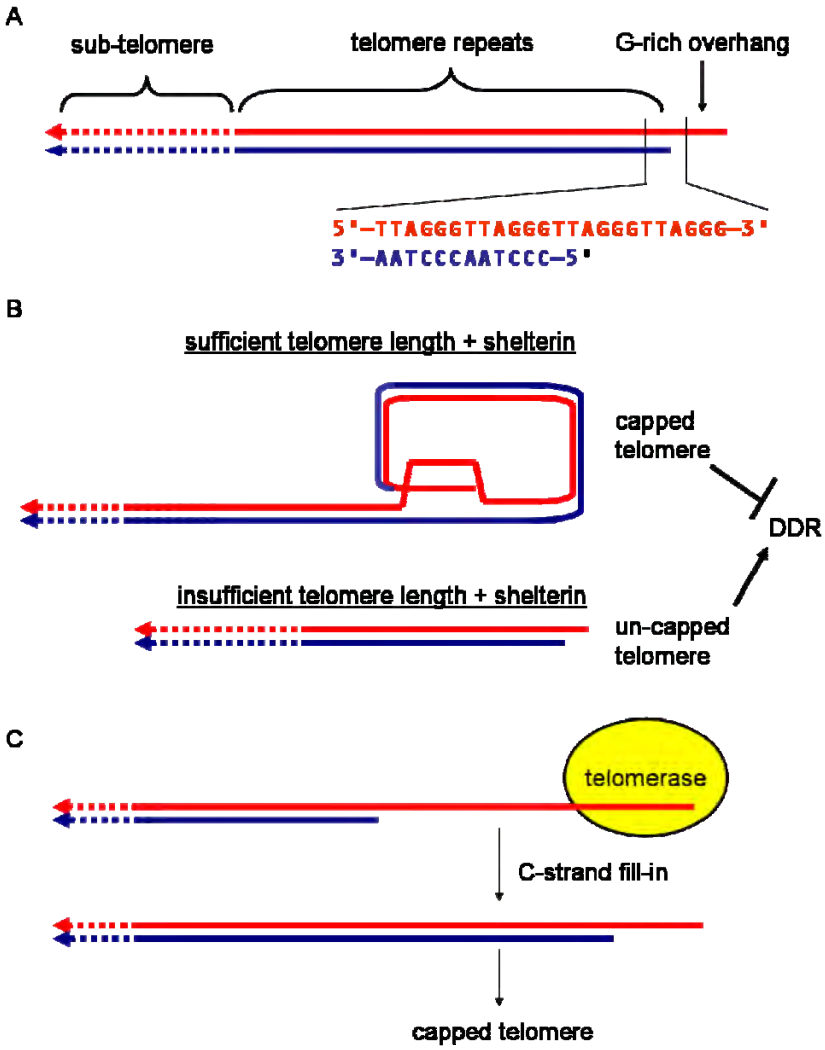


**Figure 1.2 Telomeres provide a unique structure to protect chromosomes**

(A) Every chromosome end contains thousands of double strand repeats of the 5-TTAGGG-3' sequence. The G-rich single-strand overhang is nucleolytically formed by end-processing reactions. (B) Multiple shelterin protein complexes (not shown for clarity) recognize the telomere sequence and catalyze the folding reaction to form a capped telomere which suppresses the DNA Damage Response (DDR) signal. Telomeres with insufficient length are not able to be capped by shelterin. Uncapped telomeres activate the DDR which precipitates cell cycle arrest. (C) Telomerase, if expressed, elongates the G-rich strand during replication. Unknown C-strand fill-in reactions complete the telomere maintenance and elongation process during late S-phase and $G_2$-phase allowing the telomere to regain a capped state.

are capable of expressing significant amounts of telomerase during activation-induced proliferation. During clonal expansion, telomerase activity and maintenance of telomeres are crucial to a sustained $CD4^+$ and $CD8^+$ T cell memory response (79, 81, 84). However, telomerase activity in activated T cells has been shown to be dependent on many factors including how many times a T cell has undergone activation-induced proliferation and the cytokine signaling environment (82, 85, 86).

### a. Telomerase inhibition

Type I interferons (IFN), in addition to anti-viral and anti-proliferative effects, inhibit expression and activity of telomerase (86). IFN also commonly causes lymphopenia (87), which is a stimulus for homeostatic proliferation (9). How these competing phenomena of telomerase inhibition, anti-proliferative effects, and stimulated homeostatic proliferation may affect naïve and memory T cell telomere lengths is unclear. In addition to cytokines such as interferons, repeated T cell activation-induced proliferation also leads to repression of telomerase expression and activity in human T cells. After 4 or more rounds of in vitro TCR-signaled activation, T cells have been shown to have mostly lost telomerase activity, with a gradual diminishment of telomerase activity occurring at each sequential activation (79, 84, 85).

### b. T cell telomere kinetics

TL in naïve T cells in adults, typically measured as an average or mean TL, ranges from 6000-11000 base-pairs. Mean TL in memory T cells is typically 1200-1500

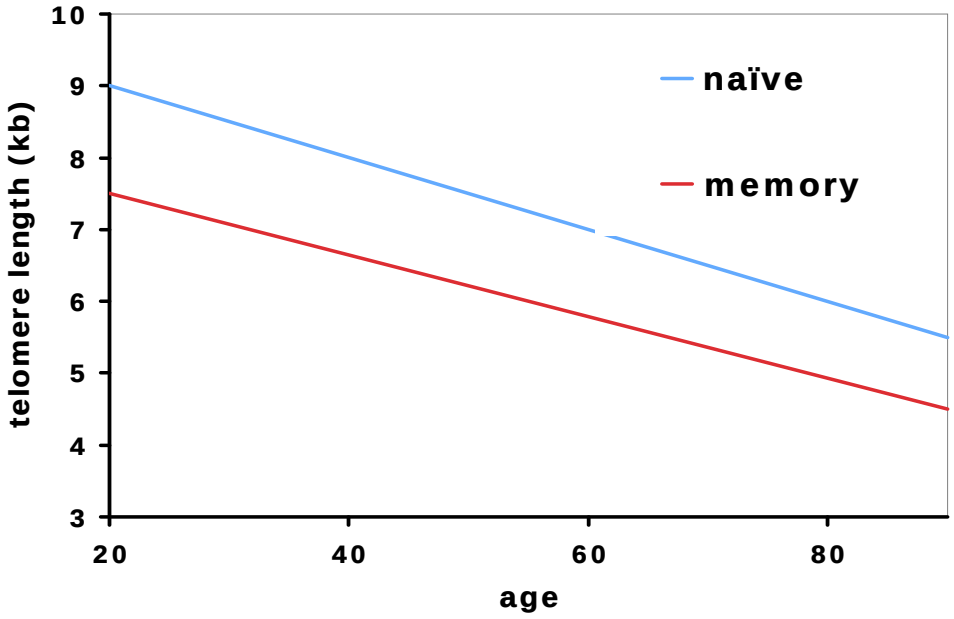


**Figure 1.3 T cell telomere lengths decline with age**

Graph depicts age-dependent decline in peripheral blood in naïve and memory T cell telomere lengths adapted from (88).

base pairs shorter than in naïve T cells (Figure 1.3) (88, 89). T cell differentiation status, seen as a continuum of loss of co-stimulatory markers such as CD27 and CD28, loss of effector functions, cell cycle withdrawal, and expression of higher levels of inhibitory markers, highly correlates to increasing loss of TL (30, 81, 83). In vivo isotopic labeling studies have shown that memory T cells in the peripheral blood turn over much more rapidly than naïve T cells (10, 90, 91). Further, T cells undergoing in vivo homeostatic proliferation do not express the high levels of telomerase believed necessary to arrest the typical 50-120 bases of telomere loss per division (79, 85, 92). Thus, given the established memory T cell TL in adults, these reported turnover rates and the lack of telomerase during homeostatic turnover would theoretically lead to cellular senescence of memory T cells and loss of proliferative capacity within a decade.

### iii. Telomere length maintenance affects in vivo T cell persistence

There are differences in the maintenance of $CD4^+$ and $CD8^+$ T cell memory. Despite similarly robust $CD8^+$ T cell responses during a primary infection, $CD4^+$ memory T cell responses are generally more durable than $CD8^+$ memory T cell responses (45, 47, 93, 94). Differing abilities of $CD4^+$ and $CD8^+$ T cells to up-regulate telomerase and limit telomere erosion during activation-induced proliferation have been proposed to account for these differences (95). Further, TL has been shown to be a critical determinant of T cell replicative capacity and in vivo T cell persistence in clinical trials. Adoptive transfer of $CD8^+$ tumor-infiltrating lymphocytes with long telomeres into melanoma cancer patients correlates with better in vivo T cell persistence and proliferation, while excessive

in vitro expansion leading to shortened telomeres correlates with poor in vivo persistence (96, 97).

**iv. Differences between T cell senescence and exhaustion**

Loss of replicative capacity is seen in the phenomenon of clonal exhaustion, as discussed above. However, senescence of T cells due to telomeres reaching critically short lengths appears to be molecularly distinct from clonal exhaustion. It has been shown that clonally exhausted T cells in certain chronic infections can be induced to re-enter the cell cycle if inhibitory signals such as programmed death-1 (PD-1) or IL-10 are blocked or removed at specific, critical times in the immune response (98-103). However, telomere-dependent senescence is irreversible in normal T cells, unless telomerase expression is ectopically forced, for example, by the insertion of a transgene (104-106). Indeed, in the very elderly, where clonally expanded, poorly proliferative, CMV-reactive $CD8^+$ T cells are common, their TL has been described as very short (66, 71, 107, 108). How telomere-dependent senescence may progress to impede the replicative capacity of other virus-specific memory T cells in humans is unclear, especially for T cells specific for acute virus infections such as IAV or VACV.

**D. Measurement of telomere length**

Various molecular techniques have been devised for measuring TL. The telomere restriction fragment (TRF) Southern blot assay represents the oldest and most established assay and, as such, is the gold standard for TL measurement (109). Other TL assays also use DNA extraction from large numbers of cells and then apply quantitative PCR with

carefully designed primers to estimate TL. TRF Southern blot and PCR-based assays suffer from the fact that extraction of DNA from cells erases information regarding TL distribution at the single cell level. One technique developed 13 years ago uses fluorescent in situ hybridization (FISH) of a fluorescent-labeled telomere sequence probe with flow cytometry to enable high speed measurement of TL of a large number of cells, the flowFISH assay (110).

**i. FlowFISH in TL estimation and caveats in its use**

Using flowFISH to analyze TL in peripheral blood cells requires the use of a DNA counterstain to ensure a 2n diploid DNA content (92 telomeres) in every measured cell. Thus in flowFISH TL measurement, it is crucial that TL is not estimated in cells captured during hybridization that were undergoing DNA synthesis (S phase) or in $G_2$/M where the number of chromosomes is no longer diploid. Beyond that caveat, hybridization conditions (heating to 82$^{o}$C in formamide) used to denature the DNA results in the destruction of most protein epitopes available for antibody labeling in flow cytometry. Thus molecules such as CD4 or CD8 must be labeled before hybridization, and the antibody then covalently cross-linked to prevent dissociation at the hybridization temperature. When pre-hybridization staining is employed, the use of heat stable fluorochromes (such as fluorescein or the patented Alexa dyes) is necessary. Together these caveats serve to limit the available phenotypic markers that can be incorporated in flowFISH.

**ii. Identifying low frequency phenotypes**

Low-frequencies of virus-specific T cells and the limited numbers of HLA-peptide tetramers available have restricted the study of TL mainly to $CD8^+$ T cells specific for a few highly immunodominant epitopes, with more limited studies of $CD4^+$ memory T cells (82, 107, 111, 112). In order to study T cell memory across a wide-range of individuals, other methods to evaluate virus-specific T cells are needed. Proliferation-based assays have long been used to identify and quantitate memory T cell responses, but merging these with telomere length measurement and flow cytometry-based phenotyping has been a costly and labor intensive process usually employing cell sorting (109). Merging flowFISH telomere measurements at the single-cell level with phenotypic analysis in a proliferation assay offers the potential to overcome many of these limitations to offer new insight into the TL dynamics of memory T cells.

**iii. Statistical parameters of TL distributions**

Beyond an arithmetic mean TL (mTL), flow cytometry allows for determination and examination of the statistical parameters of distribution such as median TL and coefficient of variation (CV, standard deviation divided by mean). One underappreciated power of flowFISH in TL studies may be the elucidation of TL distributions, i.e. measures beyond a simple mTL. The presence of highly-skewed TL distributions could conceivably be a critical correlate of the maintenance of T cell memory.

**E. Thesis objectives**

The broad objective of this thesis was to investigate the maintenance of memory T cells by studying their telomere biology. This work was driven by the desire to further our understanding of how pathogen re-exposure and the cytokine environment may shape the maintenance of naïve and memory T cells. Toward that goal, I established two hypotheses.

**1) Virus-specific memory T cells that proliferate in response to acute, non recurring infections have longer telomere lengths than T cells that proliferate in response to recurring or reactivating viral infections.**

Rationale: recurring in vivo antigen presentation induces periodic antigen-specific memory T cell proliferation leading to their decreased telomere length.

**2) Long-term exposure to type I interferons result in significant reduction in average telomere lengths in peripheral blood T lymphocytes.**

Rationale: type I interferons inhibit telomerase expression in activated T cells thereby reducing telomere length.

This work is presented in three parts:

**Chapter III: Developing the flowFISH assay**

Questions addressed:

- Can flowFISH protocols be modified to discriminate between $CD4^+$ and $CD8^+$ T cells for TL estimates in naïve and memory compartments?

- Can flowFISH TL measurement be extended to proliferating T cells?
- Can virus-specific T cells that proliferate in response to viral antigens be identified in flowFISH for TL measurements?

Experimental approach

- Compare CD4 and CD8 staining with and without the effects of hybridization to discriminate these two subsets in flowFISH.
- Evaluate flowFISH TL results in proliferating T cells with results from an accepted TL assay.
- Combine a proliferation assay directly with flowFISH to identify virus-specific T cells by their replicative response to virus.

**Chapter IV: Telomere length dynamics in human memory T cells specific for acute and latent viruses**

Questions addressed:

- Does telomere length differ in virus-specific T cells that proliferate in response to acute, non-recurring infections compared to acute recurring virus infections?
- Do telomere length kinetics (rate of TL change) differ between acute, non-recurring virus-specific T cells and recurring virus-specific T cells (Figure 1.4)?

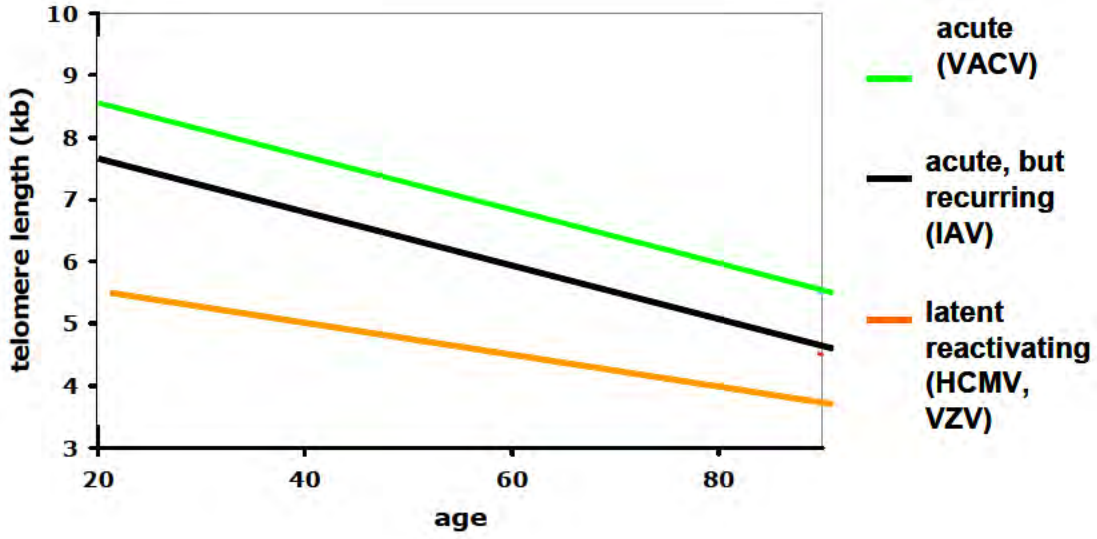


**Figure 1.4 Hypothetical telomere dynamics in memory T cells**

Telomere dynamics hypothesis for acute, non-recurring virus-specific T cells predicts longer telomeres than recurring acute virus-specific or latent-reactivating herpesvirus-specific T cell TLs.

Experimental approach:

- Measure TL in $CD4^+$ and $CD8^+$ T cells that proliferate in response to viruses in a cross-sectional study of healthy donors.
- Longitudinal analysis of TL to assess kinetics of virus-specific T cells.

**Chapter V: Extended interferon therapy accelerates telomere loss in peripheral blood T lymphocytes**

Question addressed:

- Does sustained type I interferon therapy reduce telomere length in peripheral blood T cells?

Experimental approach:

- Use peripheral blood samples from a long-term HCV clinical interferon therapy trial to measure telomere lengths in a representative cohort from those receiving sustained interferon and those in a control, no-therapy group.

# CHAPTER II

# MATERIALS AND METHODS

## A. Ethics Statement

Blood samples were collected and cryo-preserved from healthy donors (Chapters III and IV) in accordance with protocols approved by the University of Massachusetts Medical School Human Subjects Committee. All subjects provided written, informed consent to participate.

All subjects enrolled in the HALT-C trial (Chapter V) provided written, informed consent for participation under protocols approved by the institutional review boards of all participating study centers and which conformed to the ethical guidelines of the 1975 Declaration of Helsinki. PBMC samples for this research came from the following institutions: University of Massachusetts Medical School, Worcester, MA; University of Connecticut Health Center, Farmington, CT; Saint Louis University, Saint Louis, MO; University of Texas Southwestern Medical Center, Dallas, TX; and University of Southern California Health Sciences Campus, Los Angeles, CA.

## B. Donors and Peripheral Blood samples

Peripheral blood mononuclear cell (PBMC) samples for studies in Chapters 3-5 were obtained from fresh whole blood using the protocols described below. PBMC samples from the HALT-C clinical trial used in Chapter 5 were provided as

cryogenically-preserved aliquots from SeraCare Life Sciences (Milford, MA) tissue repository in coordination with the HALT-C Steering Committee and the New England Research Institute (NERI). A description of the HALT-C patient sample cohort is provided below.

**i. Normal donor PBMC**

Whole blood was collected and PBMC separated using Ficoll-PaquePlus (GE Healthcare) or Histopaque-1077 (Sigma). PBMC samples were cryo-preserved in liquid nitrogen in aliquots of $10^7$ cells/vial in 90% Fetal Calf Serum plus 10% dimethyl sulfoxide. All subjects had received the smallpox vaccine at least 3 months prior to blood collection (one donor at 3 months post-DryVax vaccination, all others > 1 year). None had reported a recent influenza infection.

**ii. HALT-C telomere length study**

The HALT-C trial design has been described in detail elsewhere (113). Briefly, enrollment criteria required all subjects to have histologically-confirmed liver fibrosis or cirrhosis (Ishak score ≥3). Subjects who remained viremic after 6 months of "lead-in" therapy with peg-IFNα plus ribavirin were then randomized either to continued maintenance-dose (90 μg/week) peg-IFNα for an additional 3.5 years or a monitor-only control group, for a total study duration of 48 months per patient (Figure 2.1). Thus the randomization phase consisted of these two groups, the peg-IFNα therapy group and the no-therapy control group. Neither subjects nor clinicians were blinded to treatment

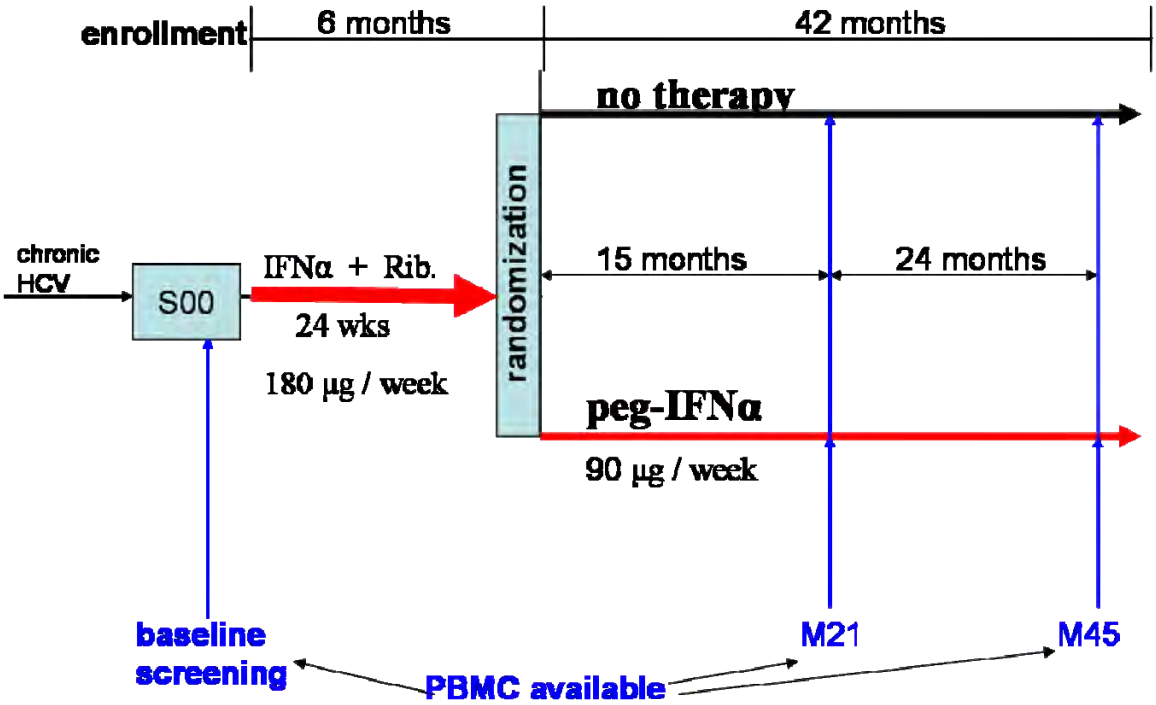


**Figure 2.1 Design of the HALT-C trial and timing of PBMC available for telomere length analysis**

Chronic hepatitis-C virus patients provided blood samples at baseline screening (S00). Upon enrollment, subjects received 24 weeks of lead-in peg-IFNα plus ribavirin therapy. Those who remained viremic were randomized into one of two arms -- no-therapy monitoring-only (control group), or continuous peg-IFNα therapy at a reduced maintenance dose for an additional 3½ years. PBMC for these TL studies came from S00, month 21 (M21), and month 45 (M45).

assignment during randomization. PBMC samples for telomere length analysis came from a representative subset of the HALT-C cohort consisting of 29 patients who successfully completed the 48 month randomization phase. PBMC were studied from three time points within the trial: baseline (S00), month 21 (M21), and month 45 (M45).

For this telomere length study, subjects from each randomization group, peg-IFNα treatment and control, were selected as matched-pairs, based on age, gender, and Ishak fibrosis score. Subjects for the peg-IFNα therapy group were selected for high compliance (>80%). For TL analysis, we were blinded to treatment group assignment, subject characteristics, and chronological order for each subject until after the completed TL data set was returned to the HALT-C Data Coordinating Center. Subject data (Table 2.1) included: age at enrollment and PBMC collections, gender, race, body mass index (BMI) at enrollment, estimated duration of HCV infection, serum alanine amino transferase (ALT) levels, serum HCV RNA levels, and Ishak fibrosis score (114-116).

**C. BrdU Proliferation Assay**

Thawed PBMC were washed, counted, and plated at $2.75x10^5$ cells per well in 96-well plates in complete media with a final volume of 200 μL per well. Complete media consisted of RPMI-1640 (Gibco-Invitrogen), 10% human AB serum (CellgroMediatech), penicillin-streptomycin, and L-glutamine. Antigens added to wells were gamma-inactivated IAV (A/H3N2/Texas/77/1), gamma-inactivated human CMV (strain AD-169), or gamma-inactivated VZV (strain VZ-10) (all from Microbix Biosystems Inc., Ontario Canada), at a final dilution of 1:100. For VACV stimulation, live virus (strain:

**Table 2.1 Baseline characteristics of the HALT-C study patients**

| Patient Group statistic | All | IFNα therapy | No therapy | p value* |
|---|---|---|---|---|
| *n* | 29 | 14 | 15 | |
| Age | 52.2 ± 6.3 | 52.1 ± 5.9 | 52.4 ± 7.0 | 0.88 |
| Gender (male:female) | 24 : 5 | 11 : 3 | 13 : 2 | 0.65 |
| BMI ($kg/m^2$) | 30.2 ± 5.0 | 32.0 ± 4.5 | 28.5 ± 5.1 | 0.09 |
| Duration of infection (years) † | 32.8 ± 8.3 | 30.0 ± 6.7 | 35.1 ± 9.0 | 0.17 |
| ALT (U/L) | 86.3 ± 42.8 | 95.9 ± 47.0 | 77.4 ± 37.9 | 0.30 |
| HCV RNA ($log_{10}$copies/mL) | 6.6 ± 0.46 | 6.7 ± 0.5 | 6.4 ± 0.4 | 0.09 |
| Ishak fibrosis score | 3.5 ± 0.95 | 3.6 ± 0.9 | 3.4 ± 1.1 | 0.48 |

*Notes:*
*Values are mean ± standard deviation except gender. ALT, blood alanine aminotransferase; BMI, body mass index.*
* *p-value for all IFNα therapy to no-therapy group comparisons by Mann-Whitney test, except gender analyzed by Fisher's exact test.*
† *Duration of infection was unavailable for three patients, two in the IFNα-therapy group and one in the no therapy group.*

NYCBH) was used at an moi = 0.2. Included in all experiments was a medium-only (negative) control to assess background proliferation. On day four of culture, bromo-deoxyuridine (BrdU, BD BioSciences) in complete media was added at a final concentration of 2 μM to all wells. All cultures were harvested on day 7 unless specified otherwise. All virus-stimulated samples from the same subject were analyzed in the same experiment to minimize potential sources of variation. For surface phenotype evaluation, $2x10^5$ cells were processed and analyzed as described below. FlowFISH telomere length analysis was performed on the remainder, typically 2.0-2.5 x $10^6$ cells, as described below. A positive T cell response to virus was defined as proliferation (percent BrdU+ cells) of 5-fold over the media background proliferation.

**D. RNA nuclease treatment and snRNA 7SK FlowFISH analysis**

A small, nuclear localized RNA, 7SK, was chosen to test and optimize RNA nuclease treatments in human PBMC samples for peptide nucleic acid (PNA) probe florescent studies in flowFISH. The 7SK target sequence used has been published by others in fluorescent in situ hybridization studies (117, 118). Peripheral blood mononuclear cell samples were fixed in 4% formaldehyde and 0.05% saponin for 25 minutes at $4^oC$, and then washed twice with 2 mL lithium-based saline with 0.05% saponin to remove fixative. All samples were incubated in lithium-based RNA nuclease buffer plus 0.05% saponin, with RNA nuclease concentration and times as indicated. All incubations were performed at $37^oC$ in sealed tubes with occasional vortexing to re-suspend the cells. The PNA probe sequence for snRNA 7SK hybridization was FAM-

OO-CCTTGAGAGCTTGTTTGG-EE (Panagene, South Korea) and the probe was used at a concentration of 0.7 μg/mL in 70% formamide hybridization buffer at 82$^{o}$C. 7SK probe hybridizations were conducted in triplicate along with no-probe controls using flowFISH hybridization conditions and cytometry settings described in the next section.

**E. FlowFISH telomere length assay on direct ex vivo PBMC samples**

Telomere length (TL) was measured in PBMC samples using a modified flowFISH assay (119). 4x10$^{6}$ PBMC from each sample were stained with anti-hCD4 and anti-hCD8 (eBiosciences, San Diego, CA) as described in Table 2.2, treated with 1mM suberic acid bis(3-sulfo-N-hydroxysuccinimide ester) sodium salt crosslinker, and then quenched with 50 mM Tris-HCl. Cells were fixed in 4% formaldehyde and 0.05% saponin for 25 minutes at 4$^{o}$C, and then washed twice with 2 mL lithium-based saline with 0.05% saponin. All samples were incubated in lithium-based RNA nuclease buffer plus 0.05% saponin with 2 μL RNase One (Promega, Madison, WI) for two hours. Samples were then divided to three probe (+) tubes and one probe (-) tube for hybridization in 70% formamide, 150 mM lithium-chloride buffer at 82$^{o}$C for 12 minutes. Probe (+) tubes contained Cy5-OO-(CCCTAA)$_3$-EE peptide nucleic acid probe at 0.5 μg/mL. After overnight cooling, samples were washed twice in 70% formamide buffer. Samples are washed once with 2 mL PBS, stained with anti-hCD45RA antibody and anti-CD57 as described in Table 2.2, resuspended in PBS-BSA containing 0.1 μg/mL 4′,6-diamidino-2-phenylindole, dihydrochloride (DAPI), and transferred to analysis tubes.

**F. FlowFISH telomere length assay on cultured PBMC**

TL was measured in cultured PBMC subsets using the basic flowFISH assay as described above with the following modifications. For BrdU proliferation assays, multiple wells for each culture condition (typically from 14 to 16 wells for each condition from 96-well plates) were pooled. 2.0 to 2.5 $x10^6$ PBMC from each harvested sample were stained at $4^oC$ with anti-hCD4 and anti-hCD8 (eBiosciences, San Diego, CA) as described in Table 2.2., and washed in cold phosphate-buffered saline (PBS) containing 0.1% bovine serum albumin (BSA). Subsequent cross-linking of antibodies, fixation-permeabilization, washing, RNA nuclease treatment, and hybridizations of samples were carried out as described above in section 3.E. After overnight cooling in the dark, samples were washed twice with 1 mL of 70% formamide, 0.1% BSA, 150 mM sodium chloride wash buffer, then once with 1 mL 1X commercial permeabilization-wash buffer (perm wash, BD Biosciences). Finally, samples were stained with anti-CD45RA and anti-BrdU antibodies (BD Biosciences) as described in Table 2.2, for 1 hour at room temperature in perm wash buffer. Samples were washed twice and resuspended in PBS-BSA containing 0.1 μg/mL of DAPI and transferred to flow cytometry analysis tubes.

**G. Flow cytometry for flowFISH**

All samples were analyzed on a FACS-Aria flow cytometer. DAPI-based DNA content and PNA hybridized probe signals were collected with linear amplification. Calibration beads were run prior to every experiment to configure and verify cytometer baseline alignment and performance. For Chapters 3 and 4, a minimum of 30,000 lymph-

gated events per tube were collected for offline analysis. Each sample probe (-) tube mean fluorescence intensity (MFI) was subtracted from the MFI of the matching probe (+) tube to obtain a specific MFI. For Chapter 5, a minimum of 20,000 lymphocyte-gated events were collected for every tube. Each sample probe (-) tube mean fluorescence intensity (MFI) was subtracted from the average MFI of the matching three probe (+) tubes to obtain a specific MFI. Linear calibration beads (RLP-30-5, Spherotech) were run at the end of all experiments for conversion of experimental mean fluorescence intensities (MFIs) to an inter-experimental standard measure of molecules of equivalent fluorescence (MESF). Mean telomere length (mTL) estimates are made in units of MESF. Using the RLP-30-5 linear calibration bead-derived linear best-fit equation, linear performance in the Cy5 telomere probe channel was verified ($r^2$>0.99) in all analysis runs. Cytometry file analysis was performed with Flowjo v7.2.5 (Treestar, Ashland, OR).

A healthy donor PBMC sample analyzed in triplicate in four separate flowFISH analyses provided inter-assay and intra-assay coefficients of variation (CV). Inter-assay CV for all $CD4^+$ and all $CD8^+$ T cells were 7.4% and 6.6% respectively. Intra-assay CV for all $CD4^+$ and all $CD8^+$ T cells were 1.1% and 1.3% respectively. For in vitro cultured PBMC, samples from each subject's three time points were run in the same assay to minimize the effect of inter-assay variation.

**Table 2.2 Antibody-fluorochrome staining used in flow cytometry studies**

| Label [#] | FlowFISH[1] | BrdU FlowFISH[2] | Standard Flow[2] |
|---|---|---|---|
| CD3 | n/a | n/a | Pacific Blue |
| CD4 | AlexaFluor® 700 | AlexaFluor® 700 | AlexaFluor® 700 |
| CD8 | APC-AlexaFluor® 750 | APC-eFluor® 780 | APC-eFluor® 780 |
| CD45RA | [†]PE-Cy7 | [†]PE-Cy7 | PE-Cy7 |
| CD57 | [†]PE | n/a | n/a |
| CD62L (L-selectin) | n/a | n/a | APC |
| CD27 | n/a | n/a | FITC |
| BrdU | n/a | [†]PE | [‡]PE |
| DNA nuclear stain | DAPI | DAPI | n/a |
| telomere probe | Cy5 | Cy5 | n/a |
| sn7SK probe* | Fluorescein | n/a | n/a |

*Notes:*

*1. Experiments in Chapter 5 – HALT-C studies*

*2. Experiments in Chapter 4– T cell memory studies on cultured PBMC*

*n/a – not applicable*

[#] *- all CD antibodies are anti-human specificity*

[†] *- post-hybridization staining used for these heat labile fluorochromes*

[‡] *- stained post-DNase treatment to enable anti-BrdU antibody epitope binding*

* *- sn7SK probe use was limited to RNA nuclease treatment time-concentration studies.*

® *- AlexaFluor dyes are a registered trademark of Invitrogen-Molecular Probes. eFluor dyes are a registered trademark of eBiosciences.*

**H. Telomere restriction fragment (TRF) Southern Blot**

PBMC and anti-CD3/CD28 activated normal human PBMC (day 4 post-stimulation) samples were magnetically purified using negative selection for $CD3^+$ T cells according to supplied instructions (Pan T cell isolation kit II, Miltenyi Biotec). Cells were split into two aliquots each, one for TRF Southern blot DNA extraction and the other for telomere FlowFISH as described in section 2.E. above.

DNA was extracted from 2 $x10^6$ $CD3^+$ T cells for TRF Southern blotting using the Wizard Genomic DNA purification kit (Promega). DNA preparations were digested overnight with *HinfI* and *RsaI* restriction enzymes (New England BioLabs) in supplied buffers at 37$^o$C. Electrophoresis of one microgram of digested DNA per lane was performed on a 0.8% tris-buffered saline (TBS)-agarose gel with TBS running buffer. Biotinylated-molecular weight (MW) markers were run in adjacent lanes. Samples were depurinated, denatured, neutralized and transferred overnight to a neutral membrane. The next day the membrane was dried, UV cross-linked, and hybridized with a telomere G-strand-specific, fluorescein labeled PNA probe (FAM-OO-$(CCCTAA)_3$). After stringency washes and blocking, the telomere bands were developed and visualized using a commercial chemiluminescence system (lluminator Chemiluminescent Detection System, Stratagene). The membrane was then stripped and biotinylated-MW bands were visualized using streptavidin-alkaline phosphatase chemiluminescence. Both images were overlayed and MW marks transferred to the telomere probe image and then scanned at 1200 pixel per inch resolution. For determination of TRF lengths, the resulting scanned image was analyzed with the MatLab (MathWorks) macro MATELO (120). Using the

MATELO-MatLab computer-aided analysis, three 20 pixel-wide columns were simultaneously analyzed in each telomere band and the resulting TRF length outputs averaged to provide a TRF length result.

**I. Surface phenotype flow cytometry on BrdU labeled PBMC**

Seven-color flow cytometry surface phenotype analyses were performed on all day 7 in vitro, BrdU-labeled PBMC samples. Samples consisting of $2x10^5$ in vitro cultured cells were washed and stained for the following surface markers: CD3, CD4, CD8, CD45RA, CD27, and CD62L as described in Table 2.2. After staining, cells were washed to remove unbound antibodies, then 300 μL fixation-permeabilization solution (fix-perm, BD Biosciences) was applied for 20 minutes at $4^oC$ and then washed in 1X perm-wash buffer (BD Biosciences). Samples were then incubated 10 minutes in perm-wash buffer plus 10% DMSO at $4^oC$, washed, and incubated 5 minutes with 200 μL fix-perm solution. After a perm-wash rinse of the cell pellets, samples were treated with 1 mM DNase I (Sigma) plus 10 mM magnesium chloride in 200 μL perm-wash in sealed tubes for 1 hour at $37^oC$ with occasional gentle vortexing. Samples were then washed one time in perm-wash buffer, and split to two separate staining tubes, one for PE-anti-BrdU and the other for PE-isotype control antibody staining. Samples were stained for 1 hour at room temperature with PE-anti-BrdU antibody or the matched IgG isotype control antibody (BD Biosciences). Samples were washed and transferred to flow cytometry tubes for analysis on a FACS-Aria cytometer (BD BioSciences).

**J. In vitro PBMC activation and telomerase activity measurement**

Telomerase activity in stimulated PBMC was measured using a commercial PCR-based, real-time telomerase repeat activity protocol kit (RT-TRAP, Millipore, Billerica, MA) per manufacturer's instructions. Briefly, $10^6$ PBMC from each sample were stimulated for three days with plate-bound anti-CD3 (clone OKT3, BD) and anti-CD28 (clone 28.1, BD), each at 3 μg/mL in 2 mL complete RPMI-1640 media (Gibco-Invitrogen) with 10% fetal calf serum. Cell lysates were prepared from harvested cell pellets and placed in -80$^{o}$C frozen aliquots per manufacturer's instructions using provided lysis buffer. RT-TRAP was performed per manufacturer's instructions using 2000 cell equivalents per test well on a 96-well PCR plate. Real-time PCR was performed on an ABI Prism 7300 (Applied Biosciences). Using the unit equipped, real-time software (SDS v1.4), triplicate-averaged sample fluorescence threshold crossing values were converted, using kit-provided controls and template standards and the resulting standard curve template control values, to a mean telomerase product quantity for each sample. Telomerase activity (TA) results are a ratio of a triplicate-derived mean quantity to the same-plate, negative control mean quantity.

**K. Statistical analysis**

Statistical tests included linear regression testing, Student's *t*-test, Mann-Whitney unpaired and Wilcoxon paired non-parametric tests, and Fisher's exact test, and were performed using Prism version 5 (Graphpad) software. All tests were two-tailed. For Chapter 5, although subjects within the two randomization groups were initially selected as matched pairs, TL data from one subject was unusable and therefore unpaired analyses were conducted. For linear regression analyses, fitted lines, correlation values, and p values are from linear regression testing. Linear regression equation parameters of slope and intercept were determined by linear trend line fitting in MS Excel (Microsoft).

# CHAPTER III

# MODIFIED FLOWFISH ASSAY DEVELOPMENT

## A. Early obstacles to using the flowFISH assay

The flowFISH assay was originally devised and described by Dr. Peter Lansdorp as a method to estimate TL in large numbers of intact cells using flow cytometry (109, 110). This assay has been used and refined by Lansdorp and others to study TL in ex vivo peripheral blood cells, which are mostly quiescent, non-dividing cell populations (89, 121-123). This chapter is devoted to describing the modification of flowFISH protocols to study TL in PBMC samples from the HALT-C trial (Chapter V) and in PBMC that were stimulated with viral antigens in vitro (Chapter IV).

For the studies of virus-specific memory T cells that will be described in Chapter IV, the major objective was to measure TL in virus-specific T cells that significantly proliferated in vitro. Our initial experiments with the established flowFISH assay met with some obstacles. Foremost among these was our consistent observation that TL estimates from flowFISH were inflated when we used activated, proliferating peripheral blood lymphocytes (cultured blasts). Simultaneous to developing the flowFISH TL assay for proliferated T cells, we also explored various antibody-fluorochrome staining combinations to discriminate $CD4^+$ and $CD8^+$ T cells within the lymphocyte population given the limitations imposed by the telomere probe hybridization conditions. Solutions to these two issues are described in sections B and C below.

A major obstacle was the low frequency of antigen-specific T cells directed against the acute and latent virus infections we proposed to study. Use of HLA-peptide tetramer staining to identify antigen-specific T cells, as has been done by others (112), was not a desirable approach for several reasons. A tetramer would limit the analysis to $CD8^+$ T cells specific for few MHC-restricted epitopes; an area where work on virus-specific T cell TL had already been published by others. An additional consideration was the limited availability of cryopreserved PBMC samples with relevant HLA haplotypes for a longitudinal analysis. We therefore used an antigen stimulation protocol which predominantly stimulated $CD4^+$ T cells for these studies.

Much early effort focused on using carboxy fluorescein succinimidyl ester (CFSE) dye dilution to identify in vitro proliferated cells directly within the flowFISH analysis. There were some early successes with this approach, but visualizing fluorescein in flowFISH-treated cells necessitated high concentration loading of CFSE onto the PBMC sample (data not shown). This high CFSE concentration inhibited antigen-driven proliferation in T cells. We next labeled cells with BrdU and found that the combination of flowFISH with BrdU labeling was suitable to identify T cells that proliferated in response to stimulation with viral antigen and measure their TLs. Section D of this chapter describes these results.

**B. Flow-FISH analysis of T cell telomere length in *in vitro*-expanded T cells**

To determine how in vitro expansion may have affected TL, we initially compared TL in total T cells isolated from fresh PBMC to in vitro-expanded T cells,

using a published flow-FISH protocol (119). We found measures of TL based on probe fluorescence in expanded T cells that were much higher when compared to the same T cells directly ex vivo ($p<0.001$, Fig. 3.1.A left bars). However, TL of expanded T cells calculated from the flow-FISH assay were also higher than TL estimates from TRF Southern blotting (compare Fig. 3.1.B with Fig. 3.1.A left bars), which were similar for expanded T cells and those analyzed ex vivo. This suggested that the inflated flow-FISH TL estimate was an assay artifact rather than a result of in vitro expansion.

Telomeres had recently been shown to be transcribed, thereby creating RNA transcripts of the G-rich sequence telomere sequence (124, 125). In light of this finding, elimination of this potential RNA telomere probe target as a potential source of error in the DNA telomere length estimation in human T lymphocytes was deemed necessary. We therefore tested several modifications to the flow-FISH protocol. Inclusion of a pre-hybridization fixation-permeabilization without RNA nuclease treatment reduced the probe fluorescence, resulting in mean TL estimates closer to the TRF results (Fig. 3.1.A middle bars). The combination of fixation-permeabilization with an optimized RNA nuclease treatment gave minimized background fluorescence for the telomere probe (Fig. 3.1.C) and produced flow-FISH TL estimates in agreement with TRF results (Fig. 3.1.A right bars). Lead-in experiments to establish this optimal RNA nuclease concentration and treatment times are described below.

A series of preliminary experiments were designed and conducted to determine an RNA nuclease treatment time and concentration protocol for PBMC samples. Briefly, a highly abundant small nuclear RNA target, 7SK, was chosen to test RNA nuclease

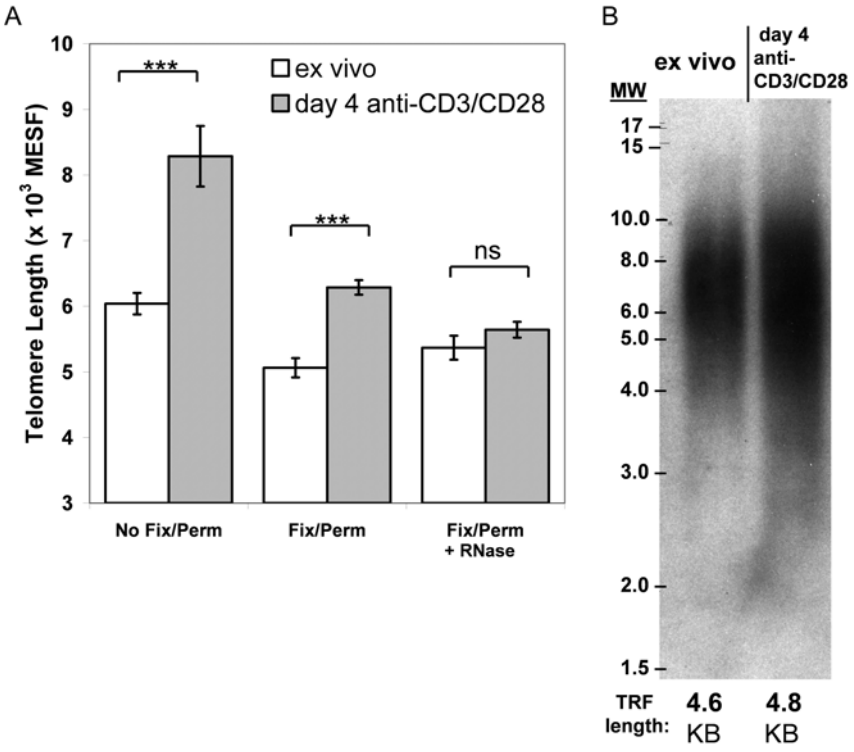


**Figure 3.1 Accurate telomere length (TL) measurement using flowFISH on proliferating T lymphocytes requires fixation-permeabilization and RNA nuclease treatment**

PBMC from healthy adults were divided to two aliquots, either stimulated with immobilized anti-CD3 and anti-CD28 for 4 days or cryogenically preserved on day 0 and thawed for processing on day 4; $CD3^+$ T cells were magnetically sorted from both samples on day 4. Each resulting sample was divided for both flowFISH TL analysis and TRF Southern blotting. (A) FlowFISH analysis using 3 different pre-hybridization conditions: without fixation-permeabilization (no fix/perm), with fixation-permeabilization (Fix/Perm), and with fixation-permeabilization followed by RNA nuclease treatment prior to hybridization (Fix/Perm +RNase). Statistical comparisons were done using unpaired *t*-test, *** $p<0.001$, and ns=not significantly different. These results are representative of four independent experiments. (B) Southern blot telomere restriction fragment (TRF) analysis of $CD3^+$ T cell samples, directly ex vivo or anti-CD3/CD28 stimulated for 4 days used in A. TRF lengths are shown at the bottom of both lanes and are the average of three separate 20 pixel-wide analyses using MatLab software running the MaTelo macro (see Methods).

treatments to verify nuclease access to nuclear-localized RNA and loss of probe signal with flow cytometry measurement. Lithium-based reagents were used to eliminate/prevent nuclease-resistant G-quadruplex structures, which telomeric sequences can readily form (126, 127).

RNA nuclease concentrations tested were 0, 10, 20, 40, and 80 U/mL at a fixed time of three hours. All RNA nuclease concentrations tested reduced the specific 7SK signal to the background fluorescence levels (Figure 3.2.A). RNA nuclease treatment times were tested at 0, 1.5, 3, 5.5, and 7.5 hours incubation time at a fixed RNA nuclease concentration of 20 U/mL. Although all times above 1.5 hours reduced the 7SK specific signal to background levels, background (autofluorescence) in the no-probe samples rose at time points beyond 3 hours (Figure 3.2.B). These data demonstrated that incubation times between 1.5 to 3 hours were optimal.

Using these RNA nuclease treatment concentrations, we tested the telomere PNA hybridization signal to detect a DNA-only signal (Figure 3.2.C). These results indicated that a probe signal minimum for TL estimation occurred at an RNA nuclease concentration of 20 U/mL for 3 hours in agreement with the 7SK RNA nuclease results. Overall, these experiments demonstrated that a DNA-only telomere signal in T lymphocyte flowFISH could best be obtained with fixation-permeabilization followed by an optimized RNA nuclease treatment.

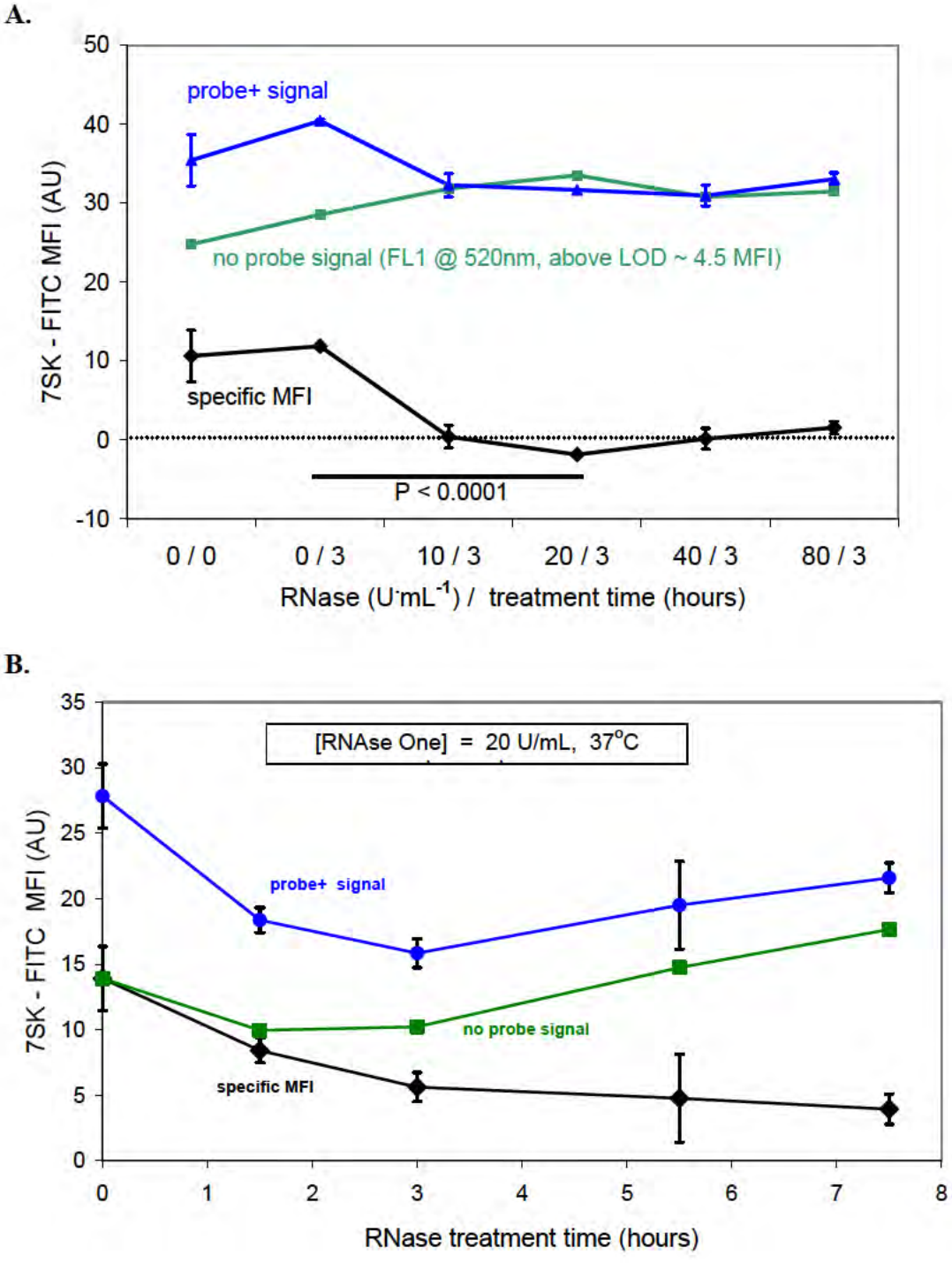


**Figure 3.2 RNA nuclease treatment optimization for detecting a DNA-only telomere probe signal in human T cells** *(continued on next page)*

**C.**

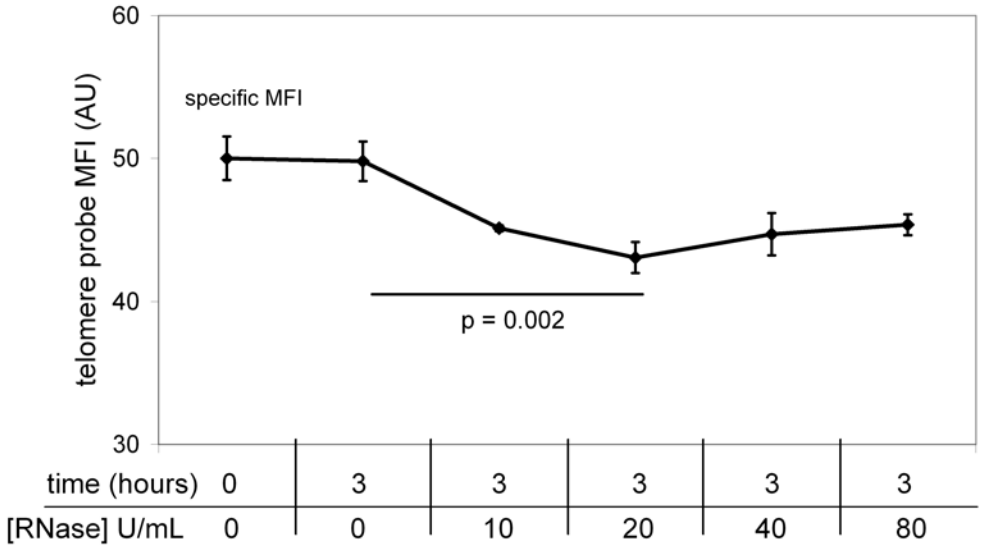


**Figure 3.2 RNA nuclease treatment optimization for detecting a DNA-only telomere probe signal in human T cells**

(A) Effect of RNA nuclease concentrations (units/mL) on the sn7SK RNA target probe fluorescence (black line). Specific MFI is the Probe+ signal (blue line) minus the no-probe (autofluorescence, green line) signal. (B) Effect of RNA nuclease incubation time on the sn7K RNA signal (blue line) and on autofluorescence (green line). (C) Effect of RNA nuclease treatment on the measurement of telomere length signal in T cells analyzed directly ex vivo by flowFISH. Specific MFI is the difference between the average signal in triplicate probe+ tubes and the background fluorescence in the probe-minus tube. These results are from the $CD45RA^{+}$ gate, similar results for RNA nuclease treatment were obtained in the $CD45RA^{-}$ population. T cells were purified from PBMC using magnetic separation. p values were determined by Student's *t*-test on triplicate hybridizations. Limit of detection for mean fluorescence intensity (MFI) was 0.4 arbitrary units (AU). Error bars are standard deviation.

**C. FlowFISH discrimination of $CD4^+$ and $CD8^+$ T cells**

Various anti-CD4 and anti-CD8 antibodies conjugated to heat-stable fluorochromes were tested for adequate discrimination of these two T cell populations (data not shown). Based on these results, we settled upon the staining combinations listed in Table 2.2. The hybridization conditions reduced the intensity of $CD8^+$ staining compared to the same staining without hybridization (Figure 3.3). Nevertheless, $CD4^+CD8^-$ and $CD4^-CD8^+$ T cell subsets could still be clearly discriminated.

CD45RA and CD57 are two of the cell surface phenotypic markers that have been shown to survive flowFISH hybridization and can be stained post-hybridization (123). CD45RA is the high molecular weight isoform of the very abundant surface molecule CD45 and is expressed by naïve T cells and by limited numbers of memory T cells. CD57's role in lymphocyte biology is currently unclear. However, CD57 expression on lymphocytes has been established as a surrogate marker to identify terminally differentiated, high cytotoxic capacity T cells with limited or no replicative potential (128-130).

To enable further subset discrimination, we used post-hybridization staining with antibodies directed against CD45RA and CD57. Within each of these subsets, CD45RA discriminated memory ($CD45RA^-$) T cells from the mostly naïve ($CD45RA^+$) T cell subset and CD57 further enhanced discrimination of naïve ($CD45RA^+$ $CD57^-$) T cells from $CD57^+$ T cell effector-memory re-expressing $CD45RA^+$ ($T_{EMRA}$) (129).

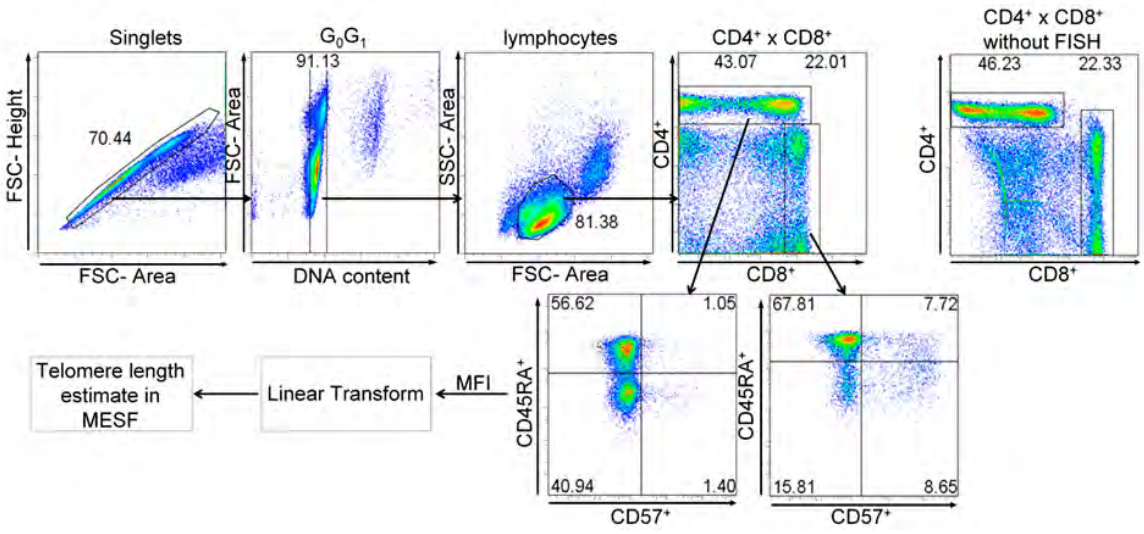


**Figure 3.3 Flow cytometry gating for direct ex vivo analysis of telomere length in $CD4^+$ and $CD8^+$ PBMC subsets**

Forward-scatter area by forward-scatter height gating was used to reduce cell aggregates (doublets). Singlet cells in the $G_0/G_1$ (to ensure diploid DNA content) gate were further selected using a lymphocyte gate based on forward and side scatter profiles. Flow plots of $CD4^+$ by $CD8^+$ staining with and without hybridization are shown. Conversion of mean fluorescence intensities (MFI) to Molecules of Equivalent Soluble Fluorescence (MESF) produced TL estimates for all subsets. A minimum 30 events-per-gate cut-off was used to ensure sufficient numbers of single cell measurements for TL estimation – limit that only limited $CD57^+$ populations estimates. This lower limit on the number of events in a gate serves to ensure the MFI value derived from that gate is of sufficient size to ensure a random sample.

**D. TL measurement in T lymphocytes that proliferated in vitro to viral antigens**

To identify T cells that proliferated to virus antigen, we labeled cells with BrdU during the final 72 hours of incubation and stained with anti-BrdU after telomere probe hybridization. We were able to clearly detect a well separated and distinct population of BrdU+ cells (Figure. 3.4.A). Thus the flowFISH protocol readily accommodated anti-BrdU staining as a post-hybridization step. The use of the CD45RA marker allows for TL measurement in the mostly naïve, non-proliferated ($CD45RA^{+}$ $BrdU^{neg}$) T cell subsets. The mTL of this naïve population provides a point of reference for each individual to assess relative TL differences in the virus-specific BrdU+ populations. Relative changes of naïve T cell TL relative to virus-specific T cell TL changes in an individual could be important in the interpretation and modeling the kinetics of TL gain or loss. Virus-specific $CD4^{+}$ and $CD8^{+}$ BrdU+ cells from a typical subject are shown in Figure 3.4.B.

To elucidate the diversity in telomere lengths in each BrdU+ sample beyond a mean TL, flow-FISH also provides median TL and the coefficient of variation (CV) (Figure 3.4.C). Mean TL fluorescence values greater than median values are an indication of rightward skewed TL distributions, e.g. an elevated frequency of long telomere cells. The long telomere state of a cell becomes a significant consideration when the replicative capacity encoded within an extra kilo-base (kb) of TL would, as rough rule-of-thumb, allow for 10 population doublings of a progenitor cell. Ten population doublings represents a potential 1000-fold expansion capacity. This insight to distribution of

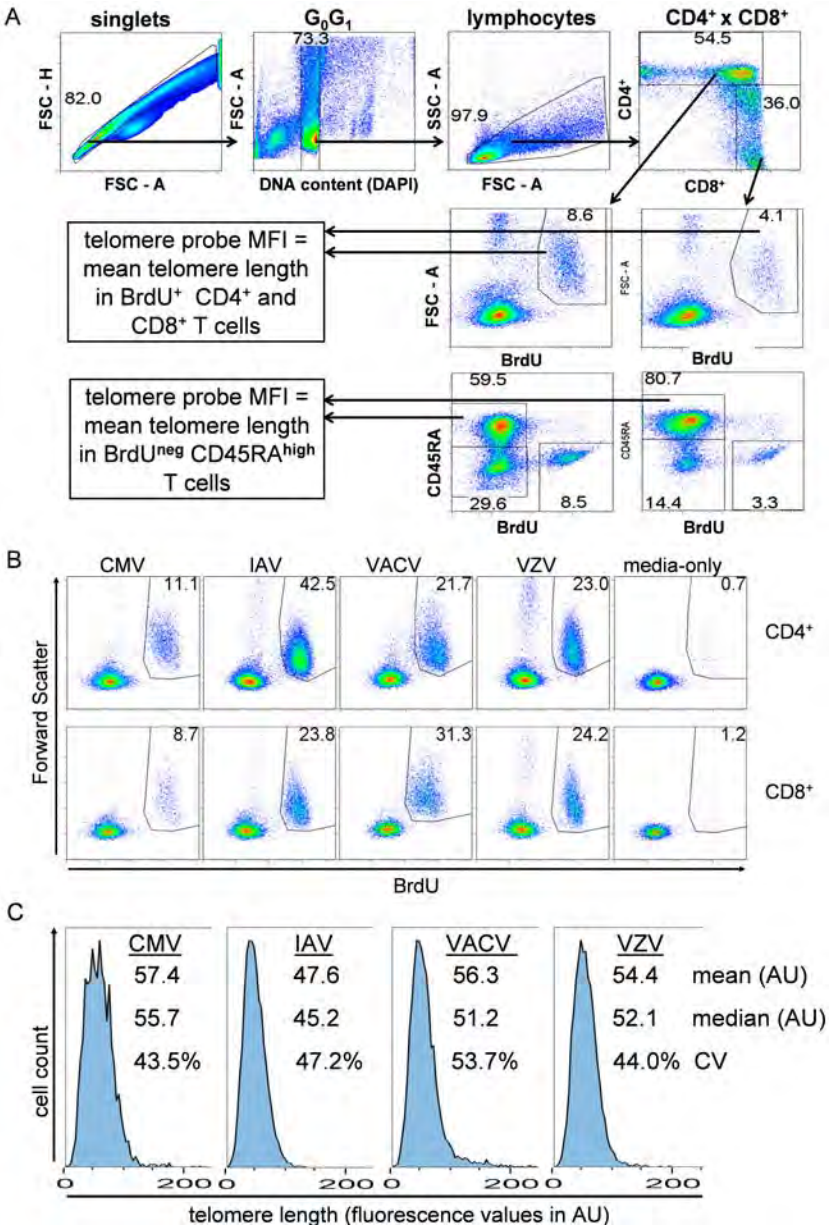


**Figure 3.4 BrdU-flowFISH allows for TL measurement in proliferating T cells**

(A) Flow cytometry gating strategy selects single cells (singlets), $G_0G_1$ diploid cells, and lymphocytes. $CD4^+$ and $CD8^+$ T cells are then gated for FSC-$A^{high}$ BrdU+ as the proliferated virus-specific T cell for TL estimation. (B) Representative proliferative responses (BrdU+ FSC-$A^{high}$ population) of $CD4^+$ and $CD8^+$ T cells to viral antigen. Values shown are frequencies of $CD4^+$ or $CD8^+$ T cells that are BrdU+. (C) Histograms of TL distribution for the virus-specific $CD4^+$ T cell responses shown in B. Mean and median fluorescence intensity values, in arbitrary units (AU), and coefficient of variation (CV) values for each population quantifies virus-specific TL distribution variation.

TLs across heterogeneous cell populations is lost in TL assays such as TRF Southern blotting or quantitative PCR methods (109).

The naïve T cell TL measurement in cells cultured in vitro correlated well with TL measurements in $CD45RA^+$ cells ex vivo (Figure 3.5.A). Replicate experiments using the same donor PBMC samples were performed to understand the variability of the flowFISH assay. Experiments on the same PBMC samples showed that TL measurements in proliferating (virus-specific) T cells were reproducible within and between assays (Figures. 3.5.B and C).

**E. Chapter Summary**

Modification of the flowFISH assay to measure TL in proliferating cells led to the adoption of a fixation-permeabilization with RNA nuclease treatment of the cells. Recent discoveries of telomere biology by others in normal human T lymphocytes may explain the mechanisms behind why this treatment protocol brought the resulting TL estimates into agreement with a TRF Southern blot TL estimate (124, 125, 131). This topic is explored more fully in Chapter VI, Discussion. Further modifications allowed for $CD4^+$ and $CD8^+$ discrimination within the lymphocyte gating strategy. This flowFISH assay subsequently was used to measure T cell TL on direct ex vivo PBMC samples from a clinical trial of interferon therapy (Chapter V). Extension of this assay to incorporate BrdU staining for identification of proliferated cells allowed TL measurements in virus-specific T cells (Chapter IV). The elucidation of TL distributions by flowFISH may be important to understanding the maintenance of replicative capacity in T cell memory.

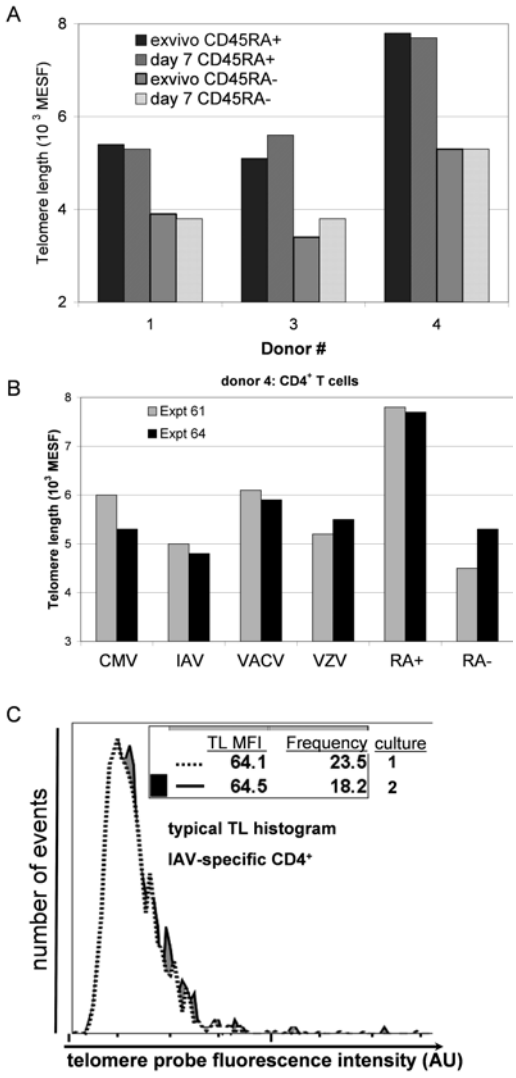


**Figure 3.5 Reproducibility of telomere length measurements by flowFISH assay**

(A) Comparison of TL measured directly ex vivo by flowFISH versus in $BrdU^{neg}$ T cells at day 7 of culture in three different subjects. (B) FlowFISH TL measurements in virus-specific $CD4^+$ T cells and in $CD45RA^+$ ($RA^+$) or CD45RA– ($RA^-$) T cells from the same subject in two different experiments performed several months apart. (C) Intra-assay variability in TL measurement was assessed with replicate influenza virus-stimulated cell cultures tested in the same experiment (dotted and solid lines). Inset panel is the mean telomere probe fluorescence and BrdU+ cell frequencies. Histograms represent distribution of telomere length from diploid-gated BrdU+ $CD4^+$ T lymphocytes. AU is arbitrary units of fluorescence.

# CHAPTER IV

## TELOMERE LENGTH DYNAMICS IN HUMAN MEMORY T CELLS SPECIFIC FOR VIRUSES CAUSING ACUTE OR LATENT INFECTIONS

T cell proliferative responses to acute or latent virus infections have been detected decades after the initial infection (44, 47, 70, 94, 132) but how this T cell memory is established and maintained is not clear. The relationships between T cell proliferation, differentiation status, telomere length (TL) and subsequent ability to maintain effector functions in vivo are areas of intense study. TL has been shown to be a critical determinant of T cell replicative capacity and in vivo persistence in humans; adoptive transfer of tumor-infiltrating lymphocytes with long telomeres correlated with better in vivo persistence and proliferation, while excessive in vitro expansion leading to shortened telomeres correlated with poor in vivo persistence (96, 97).

Here we tested the hypothesis that TLs in T cells specific for acute, non-recurring viruses would be longer than TLs in T cells specific for recurring virus infections. We based this hypothesis on the observations that recurring or re-activating viral infections (or recurring presentation of viral antigens, e.g., from vaccination) drive additional rounds of in vivo clonal expansions thus lowering TL. Using PBMC from healthy adult donors, we examined TLs in T cells that proliferated in vitro to four viruses; two latent-reactivating herpesviruses, CMV and VZV, and two viruses associated with acute infection, influenza A virus (IAV), and VACV. We used bromodeoxyuridine (BrdU)

labeling as described in Chapter III to detect memory T cells that proliferated in vitro in response to these viruses, and then used flowFISH to measure TL in virus-specific (BrdU+) cells. We performed a cross-sectional study of virus-specific memory T cell TL in ten healthy adults, with a longitudinal study involving five of these subjects.

**A. TL measurement in T lymphocytes that proliferate to viral antigens**

Since TL declines in normal somatic cells as a result of cell division, and because our hypothesis was based on TLs in vivo, it was important to understand the effects of in vitro expansion on the measured TL in virus-specific T cells. Prior to day 5, $CD4^+$ BrdU+ cells were not detectable above the background frequency in negative control (unstimulated) cultures (data not shown). Starting at day 5, BrdU+ cells represented a small percentage of total $CD4^+$ T cells but were present as a distinct population compared to unstimulated cultures (Figure 4.1.A); the BrdU+ cell population increased in frequency over the next several days. However, day 5 and 6 cultures had T cell populations with low BrdU+ cell numbers and skewed TL distributions, which combined to produce high variability in measured mean TL at these time points (Figure 4.1.B, and data not shown). In contrast, at day 7 of culture, TL distributions had converged to more Gaussian-like distributions (Figure 4.1.B) where the impact on mean TL of elevated numbers of outlier long telomere cells in a small total number of cell was reduced.

Previous work by others showed that the phenotype of Epstein-Barr virus-, VACV-, and yellow fever virus-specific $CD8^+$ T cells converts in vivo over several months after viral infection from an early population of proliferating, $CD45RA^-$

/CD45RO$^+$ effector T cells to mostly quiescent, CD45RA$^+$ memory T cells with a high replicative capacity (111, 133). Consistent with these results we found higher CD45RA$^+$ frequencies in the proliferated fraction during day 5 and day 6, where the CD45RA$^-$ fraction increased over the same period to become the dominant phenotype within the BrdU$^+$ population at day 7 (Figure 4.1.C).

The results for the virus-specific CD8$^+$ T cells were similar to the findings in virus-specific CD4$^+$ T cells (Figure 4.2.A and B). However, interpretation of the TL in CD8$^+$ T cells warrants caution. The normal CD4$^+$: CD8$^+$ ratios in PBMC result in lower total numbers of cells to analyze in flowFISH, and the use of viral antigen preparations rather than peptide mixtures may have produced sub-optimal virus-specific CD8$^+$ stimulation. For these reasons we excluded CD8$^+$ results from further cross-sectional and longitudinal modeling.

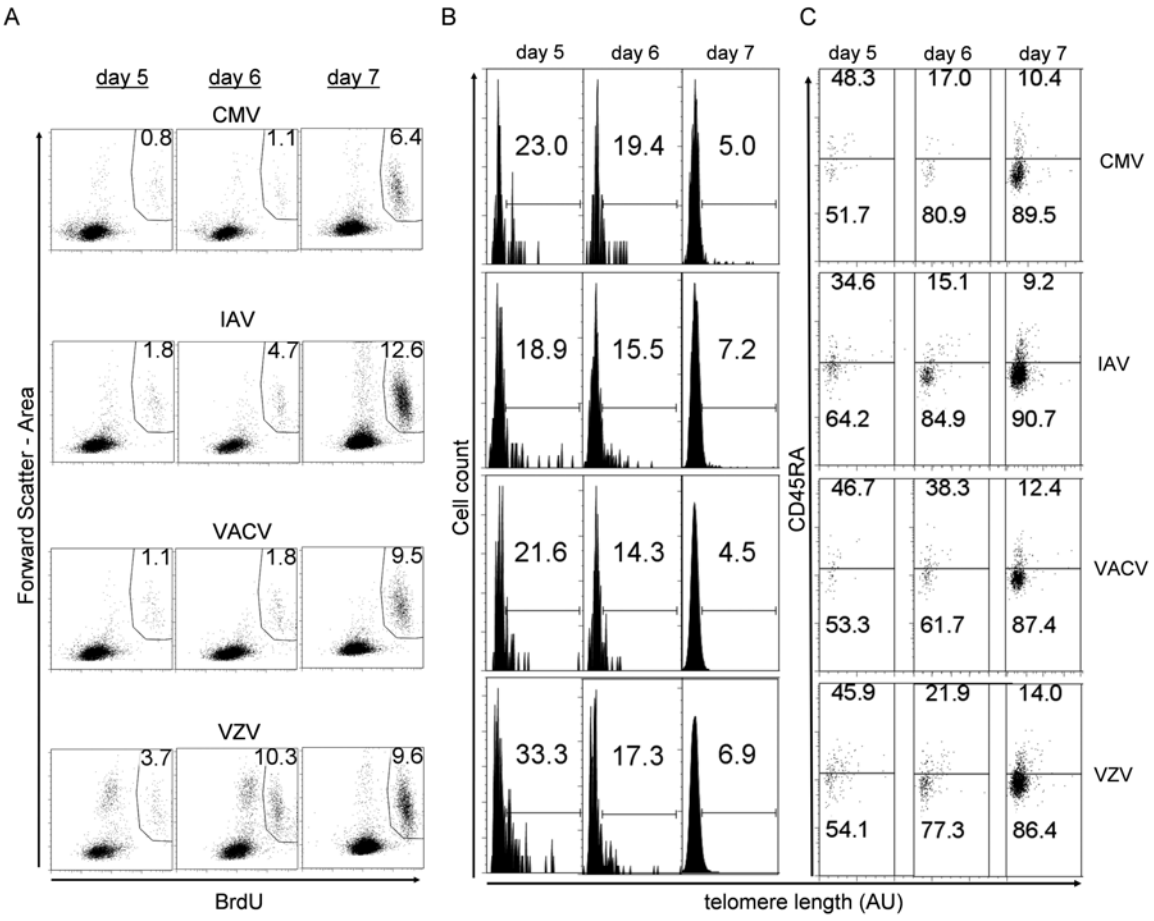


**Figure 4.1 TL and CD45RA$^+$ frequencies in proliferating CD4$^+$ T cells**

(A) BrdU+ CD4$^+$ T cells were enumerated on the indicated days after in vitro stimulation with viral antigens. BrdU was added to wells 3 days before harvest in all cases. (B) Histograms of TL in BrdU+ cell populations from A. Values indicate the frequencies of long telomere cells. (C) Distribution of TL and CD45RA staining in BrdU+ cells from A. Values indicate the percentages of CD45RA$^-$ and CD45RA$^+$ cells in each sample. Data are representative of two independent experiments.

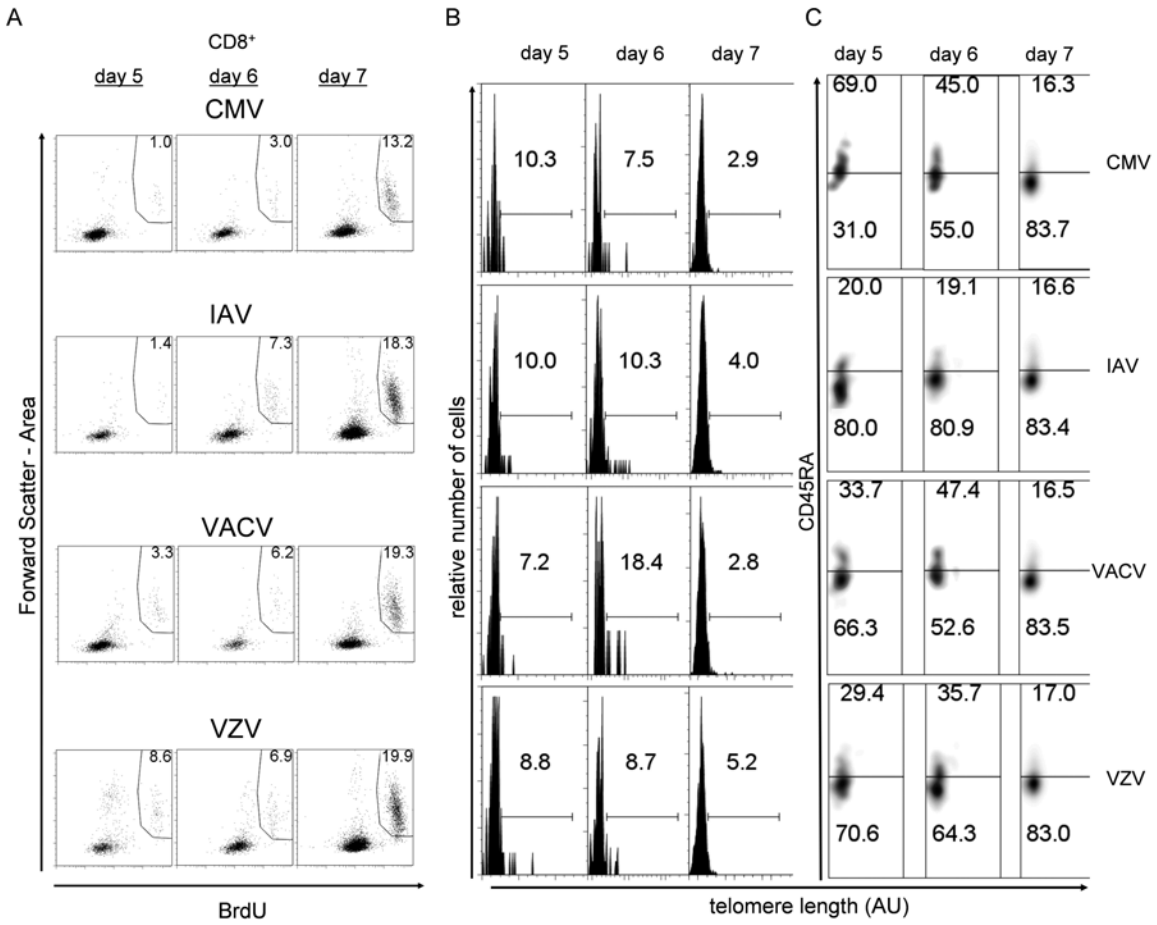


**Figure 4.2 TL and CD45RA$^+$ frequencies in proliferating CD8$^+$ T cells**

(A) BrdU+ CD8$^+$ T cells were enumerated on the indicated days after in vitro stimulation with viral antigens. BrdU was added to wells 3 days before harvest in all cases.
(B) Histograms of TL in BrdU+ cell populations from A. Values indicate the frequencies of long telomere cells. (C) Distribution of TL and CD45RA staining in BrdU+ cells from A. Values indicate the percentages of CD45RA$^-$ and CD45RA$^+$ cells in each sample. Data are representative of two independent experiments.

**B. CMV-specific and VACV-specific $CD4^+$ T cells have longer mean telomere lengths than IAV-specific $CD4^+$ T cells**

Nine of ten subjects had $CD4^+$ T cells that proliferated to CMV, and all ten subjects had $CD4^+$ T cells that proliferated to IAV, VACV and VZV (Table 4.1). Our analysis of PBMC from these ten healthy adult subjects indicated that stimulation with IAV produced the highest frequency of proliferating $CD4^+$ memory T cells (percent BrdU+) (Figure 4.3.A, $p<0.05$ by Wilcoxon paired analysis). Frequencies of $CD4^+$ T cells that proliferated to CMV were generally lower than for the other three viruses, but were very high in two subjects.

Analysis of naïve (non-proliferated, $CD45RA^+$ from media-only cultures) and virus-specific $CD4^+$ T cells in our cohort of ten healthy subjects, who ranged in age from 26 to 61 years, produced a wide range of mean TL (Figure 4.3.B). In pair-wise comparisons, VACV-specific $CD4^+$ T cell TL were significantly longer than IAV-specific $CD4^+$ T cells, in both absolute TL ($p<0.01$, Figure 4.3.C) and as a ratio to the subject's naïve T cell TL (Figure 4.3.D). Counter to our hypothesis, we found that CMV-specific $CD4^+$ T cell TL was also significantly longer than IAV-specific $CD4^+$ T cell TL ($p<0.05$) in both absolute TL and as a ratio to naïve T cell TL. Important to the interpretation of these results, TL in proliferating T cells showed no correlation with the percent BrdU+ cells (Figure 4.3.E), indicating that the differences in TL were not an artifact of the amount in vitro expansion.

**Table 4.1 $CD4^+$ T cell proliferation responses in ten healthy donors to the four tested viruses**

| | $CD4^+$ T Cells | | Fold over background* | | | |
|---|---|---|---|---|---|---|
| Donor # | Background proliferation (%) | | CMV | H3N2 flu | VacV | VZV |
| 1 | 2.1 | | (2.7) | 23.4 | 13.8 | 8.5 |
| 2 | 0.6 | | 20.0 | 76.6 | 65.2 | 41.3 |
| 3 | 0.7 | | 7.1 | 40.4 | 5.1 | 73.3 |
| 4 | 0.5 | | 162.8 | 69.4 | 66.8 | 60.2 |
| 5 | 0.2 | | 24.5 | 146.0 | 75.6 | 122.5 |
| 6 | 0.4 | | 125.5 | 67.3 | 23.3 | 29.3 |
| 7 | 0.7 | | 16.1 | 64.1 | 19.6 | 58.0 |
| 8 | 1.4 | | 9.1 | 24.1 | 19.3 | 29.4 |
| 9 | 0.1 | | 92.0 | 96.0 | 230.0 | 283.0 |
| 10 | 0.5 | | 15.4 | 106.0 | 35.8 | 69.0 |
| | | **min** | **2.7** | **23.4** | **5.1** | **8.5** |
| | | **max** | **162.8** | **146.0** | **230.0** | **283.0** |
| | | **number positive** | **9** | **10** | **10** | **10** |

*Notes:*
** Fold over background is the virus-specific (BrdU+) proliferation frequency divided by the media-only (BrdU+) proliferation frequency.*
*Number in parentheses ( ) indicates a response that did not meet the positive response criteria.*

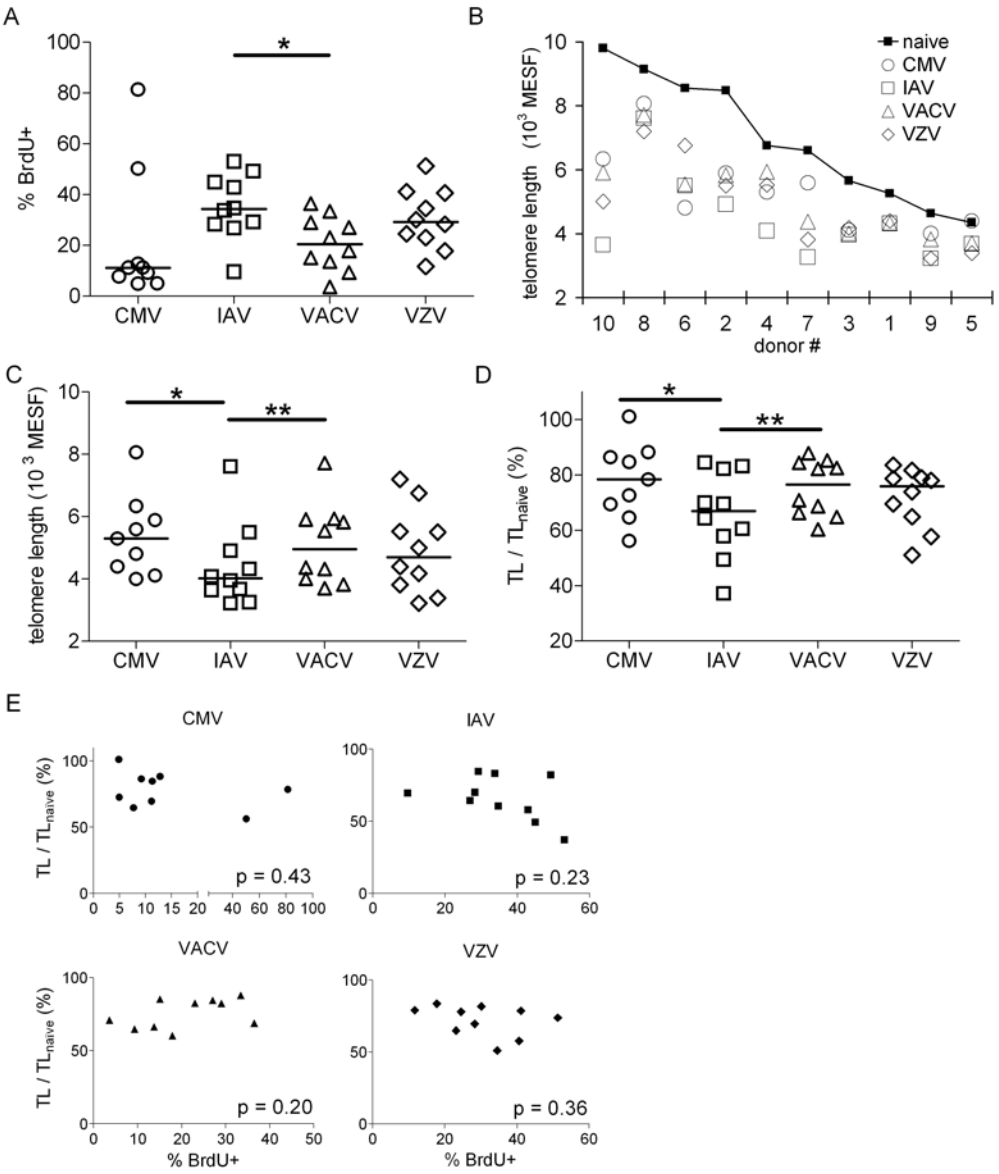


**Figure 4.3 TL in CMV- and VACV-specific CD4$^+$ T cells are longer than TL in IAV-specific CD4$^+$ T cells**

(A) Frequencies of BrdU+ CD4$^+$ T cells in ten healthy adults. (B) Mean TL measured in CD4$^+$ T cells grouped by subject in units of molecules of equivalent soluble fluorescence (MESF). (C) Absolute TL in CD4$^+$ T cells grouped by virus. (D) TL in CD4$^+$ T cells that proliferated to viral antigen normalized to TL in naïve CD4$^+$ T cells (BrdU$^{neg}$ CD45RA$^+$) (TL/TL$_{naïve}$) in the same subject. Statistical analyses: ** $p < 0.01$, * $p < 0.05$ by Wilcoxon paired, signed rank test. (E) Linear regression analyses for correlations between virus-specific proliferation frequencies (% BrdU+) and TL/TL$_{naive}$. P values are from linear regression testing. For CMV, n=9; all others, n=10.

**C. CMV-specific and VACV-specific $CD4^+$ T cells have a more effector-like phenotype**

Standard flow cytometry surface phenotype analyses were performed in parallel with the flow-FISH TL analysis on these BrdU-labeled in vitro cultures (Figure 4.4.A). VACV-specific $CD4^+$ T cells had a higher frequency of $CD62L^{low}$ cells than IAV-specific and VZV-specific $CD4^+$ T cells (Figure 4.4.B). Additionally, CMV-specific $CD4^+$ T cells had a higher frequency of $CD62L^{low}$ phenotype cells compared to IAV-specific $CD4^+$ T cells. These data suggest that VACV-specific and CMV-specific $CD4^+$ T cells have a more effector-like phenotypes than IAV-specific $CD4^+$ T cells.

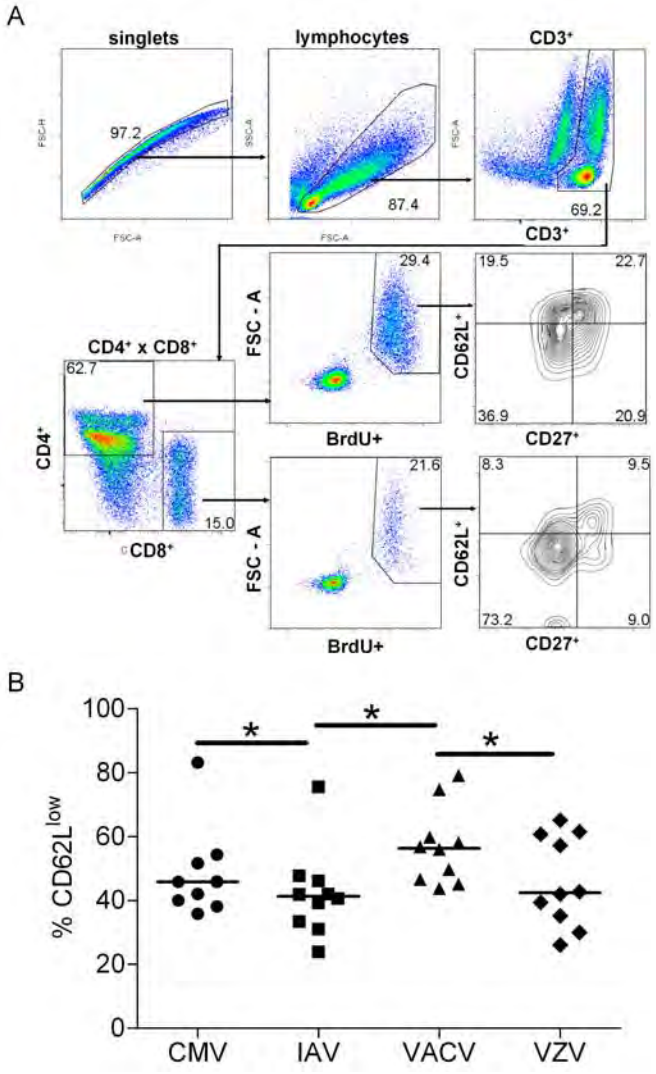


**Figure 4.4 In vitro expanded CMV- and VACV-specific CD4$^+$ T cells display a more effector-like phenotype than IAV-specific CD4$^+$ T cells**

Surface phenotyping was performed on all day 7 cultures using standard flow cytometry staining. (A) Flow cytometry gating of virus-specific memory (BrdU+) T cells employed the analysis of CD62L and CD27 surface expression as shown. (B) Frequency of CD62L$^{low}$ (effector memory phenotype) T cells within BrdU+ CD4$^+$ CD3$^+$ T cells. CD62L$^{low}$ frequency (in percent) is the sum of the lower two quadrants of the CD27 by CD62L flow plots shown in A. * $p < 0.05$ by Wilcoxon paired, signed rank test. Horizontal bars are median values. CMV, n = 9, all other virus-specific results, n = 10.

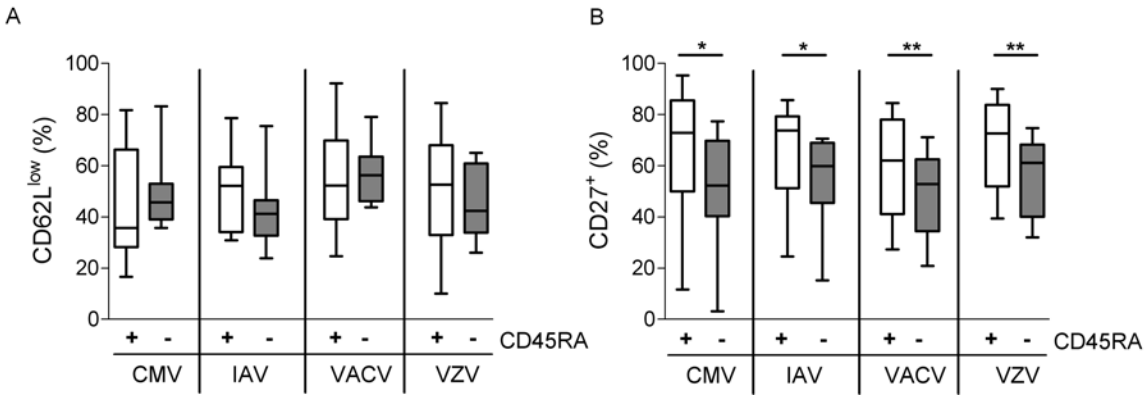


**Figure 4.5 Surface phenotypes of virus-specific memory BrdU+ $CD4^+$ $CD45RA^+$ T cells**

(A) CD62L expression was not different between $CD45RA^+$ and $CD45RA^-$ virus-specific $CD4^+$ T cells. $P > 0.1$ for all pair-wise ($CD45RA^+$ versus $CD45RA^-$) comparisons in A. (B) CD27 expression was higher in $CD45RA^+$ than $CD45RA^-$ virus-specific $CD4^+$ T cells. Note: CD27 data was only available for 8 of 10 donors. Statistical tests by Wilcoxon paired analyses, * $p < 0.05$, ** $p < 0.01$. Plots are box-whisker min to max plots.

**D. VACV-specific memory $CD4^+$ T cells include a higher frequency of $CD45RA^+$ cells with long telomeres.**

In the course of these studies, we observed the consistent presence of BrdU+ cells with long telomeres in day 7 virus-stimulated cultures (Figure. 4.1.B), nearly all of which were $CD45RA^+$. Surface phenotype analysis showed that the proliferated (BrdU+) $CD45RA^+$ T cells had CD62L expression equivalent to the larger $CD45RA^-$ fraction of virus-specific T cells (Figure 4.5.A). Compared to the virus-specific $CD45RA^-$ T cells, $CD27^+$ expression was higher in the $CD45RA^+$ virus-specific T cells, suggestive of a cellular phenotype receptive to co-stimulation (Figure 4.5.B). The $CD45RA^+$ fraction typically constituted 5-15% of BrdU+ cells in all four virus-stimulated cultures at day 7 (Figure 4.6.A), and was skewed toward longer TL compared to the $CD45RA^-$ population (Figure 4.6.B histograms). Skewing of the TL distributions in the $CD45RA^+$ sub-population is further indicated by mean fluorescence intensities higher than the median values (Figure 4.6.B), in contrast to the $CD45RA^-$ population.

We compared the frequency of long telomere $CD4^+$ $CD45RA^+$ cells in our cohort. For this analysis, we applied an arbitrary, but consistent telomere probe cutoff value for each subject (Figure 4.6.C). We found that the frequencies of long telomere $CD45RA^+$ cells were significantly greater in VACV-specific T cells than in IAV-specific T cells ($p=0.03$, Figure 4.6.D).

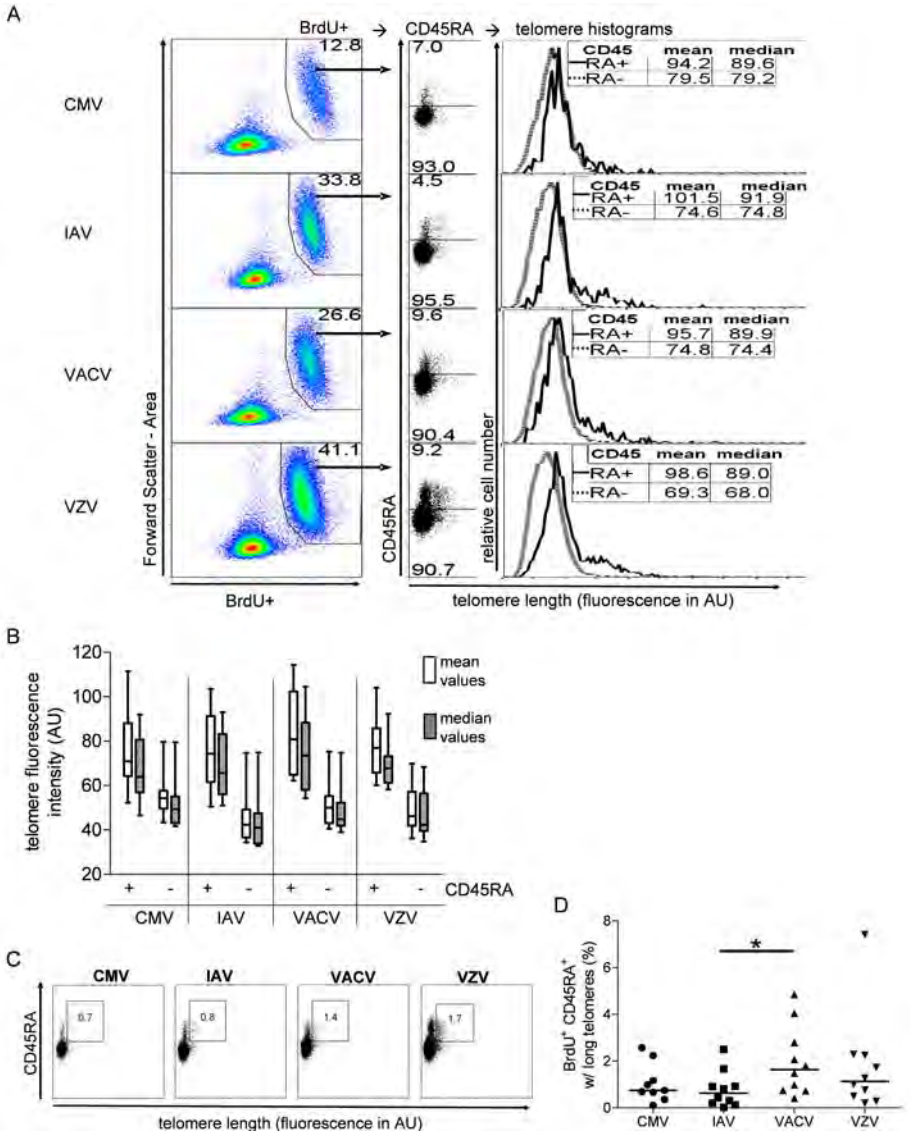


**Figure 4.6 VACV-specific memory CD4$^+$ T cells have a higher frequency of CD45RA$^+$ cells with long telomeres**

(A) CD4$^+$ T cell proliferative responses (BrdU$^+$) gated by CD45RA$^{+/-}$from 1 subject. Histograms of TL in CD45RA$^-$ and CD45RA$^+$ cells are overlaid, and mean and median fluorescence intensities for each population are shown. (B) Mean and median telomere probe fluorescence intensity values for all subjects' grouped by virus. Box and whisker plots indicate minimum to maximum values with the lines inside the boxes depicting the median values for each set of measurements. (C) Frequencies of BrdU$^+$ CD45RA$^+$ CD4$^+$ T cells with long telomeres in a representative subject. (D) Frequency of CD45RA$^+$ CD4$^+$ T cells with long telomere within the BrdU+ population for 10 subjects. * $p < 0.05$ by Wilcoxon paired, signed rank test. Fluorescence is shown in arbitrary units (AU).

**E. Longitudinal analysis of virus-specific $CD4^+$ T cell telomere dynamics in healthy subjects.**

For five of our subjects, we had multiple PBMC samples collected over an 8 to 10 year interval. We compared TL of naïve ($CD45RA^+$ $BrdU^{neg}$) and virus-specific $CD4^+$ T cells from the first and last time points grouped by subject (Figure 4.7.A) and by virus (Figure 4.7.B). We also used the average slopes and y-intercepts to graph the average TL kinetics (dashed lines in Figure 4.7.B). Naïve ($CD45RA^+$ $BrdU^{neg}$) $CD4^+$ T cells in all subjects showed a downward slope, consistent with age-dependent TL erosion (88). Virus-specific $CD4^+$ T cells also showed declining mean TL in the cohort as a whole; however, TL in CMV-, IAV-, or VZV-specific CD4+ T cells increased from the first to last time point in at least 1 subject.

The mean TL slopes (rate of TL decay) in both CMV- and IAV-specific $CD4^+$ T cells were similar, while both the VACV- and VZV-specific slopes were steeper and similar to the naïve TL decay rate (Figure 4.7.C). The differences in TL slopes did not reach statistical significance in this small cohort, however ($n=5$, $p=0.06$).

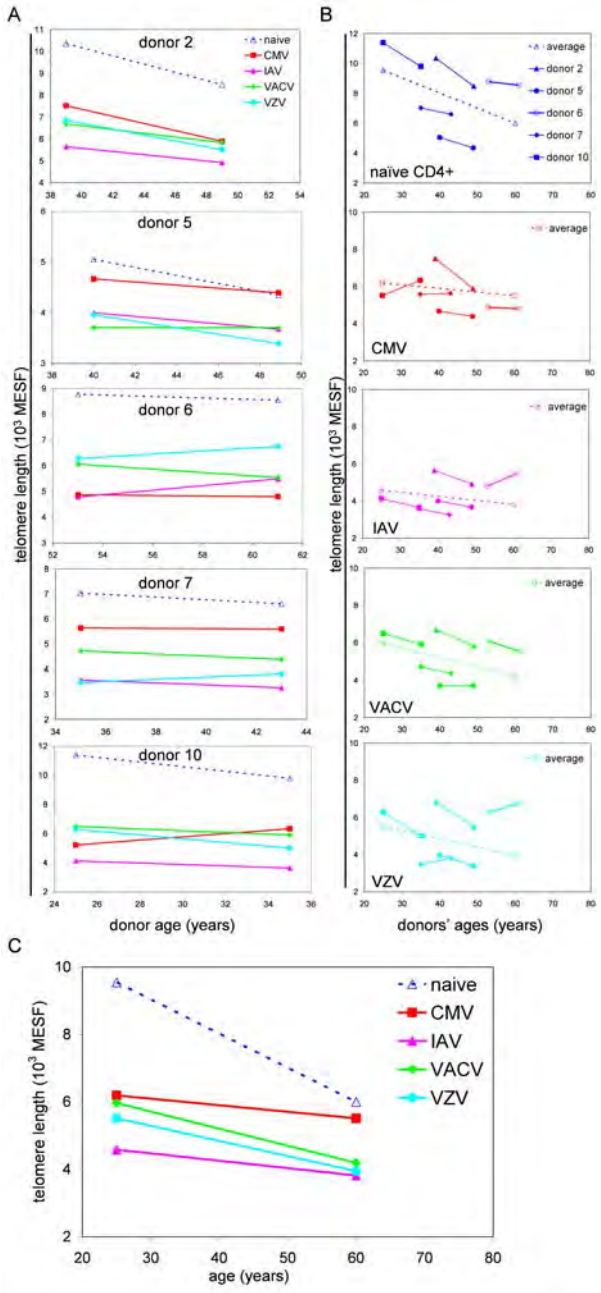


**Figure 4.7 Longitudinal analysis of TL in virus-specific CD4$^+$ memory T cells.**

(A) TL was measured in naïve CD4$^+$ (BrdU$^{neg}$ CD45RA$^+$) (dotted lines) and BrdU+ CD4$^+$ T cells (solid lines) from five healthy subjects. PBMC samples were obtained 8 to 10 years apart. (B) The data from A were grouped according to different virus-specific T cell populations for all 5 subjects. Dotted lines derive from the average slopes and y-intercepts. (C) Average TL kinetics of each virus-specific T cell population and naïve T cells are redrawn from B.

**F. VZV reactivation was associated with an increase in VZV-specific T cell telomere lengths and proliferative responses**

From one healthy subject, we had obtained three PBMC samples over a period of three and a half years. We observed an increase in both the frequency and mean TL in the VZV-specific $CD4^+$ (Figure 4.8.A, C) and $CD8^+$ (Figure 4.8.B, D) T cells at the middle time point in this subject. This individual reported an episode of shingles approximately 2-3 weeks prior to the blood draw for the middle time point. These results suggest that a herpesvirus reactivation can lead not only to a boost in the memory T cell frequency but also to increased TL in T cells.

We further analyzed the $CD45RA^{+/-}$ expression in VZV-specific $CD4^+$ and $CD8^+$ T cells in this subject (Figure 4.8.E). While TL in $CD4^+$ $CD45RA^+$ BrdU+ T cells was not different from TL in $CD4^+$ $CD45RA^-$ BrdU+ T cells before VZV reactivation, it was significantly higher after VZV reactivation (Figure 4.8.F), indicating that prior to reactivation the long telomere characteristic of the VZV-specific CD45RA+ CD4+ T cell was lost. Overall, these results suggest a picture of waning $CD4^+$ assisted T cell control to VZV reactivation is not simply a decline in virus-specific T cell frequency. Reduced proliferative capacity as TLs diminish would eventually lead to loss of the high replicative capacity $CD45RA^+$ component. Robust VZV reactivation in the form of shingles with active viral replication may then lead to recruitment of naïve T cells to re-establish T cell control of viral replication with a corresponding increase in proliferative frequency and TL, as seen in this subject.

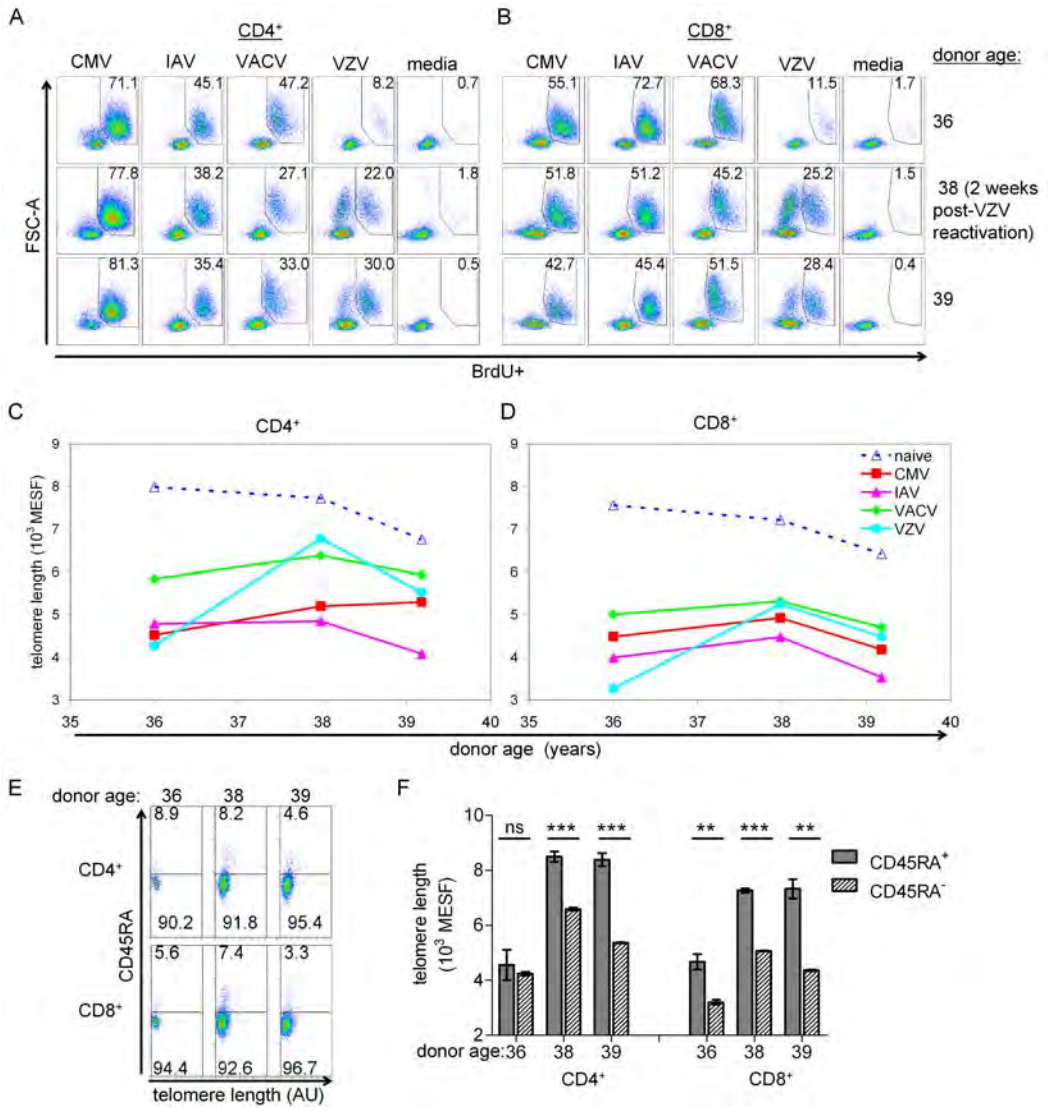


**Figure 4.8 VZV reactivation was associated with an increase in proliferative responses and TL in VZV-specific CD4$^+$ and CD8$^+$ T cells**

Dot plots show virus-specific (A) CD4$^+$ and (B) CD8$^+$ proliferative responses across three time points in the same subject. BrdU+ frequencies (percent) are shown in the gate. PBMC were collected approximately two years prior (top row), two weeks after (middle row) or fourteen months after (bottom row) VZV reactivation. Graphs depict mean TL in (C) CD4$^+$ and (D) CD8$^+$ T cells along with TL in naïve T cells (media-only culture BrdU$^{neg}$CD45RA$^+$) (dashed line) across the three time points. (E) VZV-specific CD4$^+$ and CD8$^+$ T cell from A and B are further delineated by CD45RA expression. (F) Mean TL for VZV-specific T cells by CD45RA expression. Error bars are standard errors from triplicate hybridizations of the same sample. By unpaired *t*-test, *** $p < 0.001$, ** $p < 0.01$, ns = not significantly different.

**G. Chapter Summary**

Declining telomere length (TL) is associated with age-related T cell senescence, but there are few data on TL in virus-specific T cells. Using BrdU-flowFISH and PBMC from ten healthy adults, we tested the hypothesis that recurring-acute (IAV) or reactivating (VZV and CMV) viruses would generate memory T cells with shorter TL than a non-recurring acute viral infection (VACV); five subjects provided multiple PBMC samples separated by up to 10 years. Our results indicate that VACV-specific and CMV-specific $CD4^+$ memory T cells had longer telomeres than IAV-specific $CD4^+$ T cells. Although most virus-specific (BrdU+) cells were $CD45RA^-$, we observed a minor population (5-15%) of BrdU+ $CD45RA^+$ T cells characterized by long telomeres. Analysis of sequential PBMC samples demonstrated a slow decline in TL in virus-specific T cells, even in the absence of re-exposure. However, in one subject, VZV reactivation led to a significant increase in TL in virus-specific T cells, suggesting recruitment of longer telomere naïve cells to memory.

Declining TL with age was reproduced in the cross-sectional/longitudinal model. TL in virus-specific memory T cells generally declined as in the naïve T cell compartment, but the kinetics of these declines appeared to differ – a topic more fully explored in Chapter VI. The observation that herpesvirus reactivation can substantially refresh specific T cell memory TLs has important implications that are also explored in Chapter VI. We conclude that TL in memory T cells that are able to proliferate to viral antigens is dynamic, and that TL distribution is important to understanding the maintenance of long-lived T cell memory.

# CHAPTER V

## EXTENDED INTERFERON-ALPHA THERAPY ACCELERATES TELOMERE LENGTH LOSS IN HUMAN PERIPHERAL BLOOD T LYMPHOCYTES

Type I interferons have pleiotropic effects on host cells, including inhibiting telomerase in lymphocytes and antiviral activity. Combination pegylated-IFNα (peg-IFNα) with ribavirin is the standard therapy for subjects with chronic hepatitis C virus (cHCV) infection. There are additional clinical settings where extended interferon therapy is utilized, such as relapsing-remitting multiple sclerosis and melanoma (134, 135). How IFN modulates TL in peripheral naïve and memory T cells is currently unclear.

The aim of this study was to examine the effects of long-term peg-IFNα therapy on TL in peripheral blood T lymphocytes. The PBMC used in this study were obtained from patients enrolled in the Hepatitis-C Antiviral Long-term Treatment against Cirrhosis (HALT-C) trial (113). We used a flowFISH assay described in Chapter III, Section D to measure TLs in naïve and memory T cells at baseline (S00) and at months 21 (M21) and 45 (M45) of the trial in 29 HCV-infected subjects. The subjects included in our study had failed to achieve a sustained virologic response following 24 weeks of pegylated- IFNα plus ribavirin treatment and were subsequently randomized to either a no additional therapy group (no therapy group) or a maintenance dose of pegylated-IFNα group (peg-IFNα group) for an additional 3.5 years as described in Chapter II, Figure 2.1. Additionally, we used a commercial telomerase repeat activity protocol (TRAP) assay on

*in vitro* stimulated PBMC samples, as detailed in Chapter II, Materials and Methods, to assess telomerase activity between the therapy group and control group samples.

**A. Baseline characteristics of patients**

The clinical characteristics of the subjects involved in this study are shown in Chapter II, Table 2.1. There were no significant differences in these clinical characteristics at baseline between the peg-IFNα and the no-therapy group. We measured baseline TL in T cell subsets from this cohort. TLs in naïve ($CD45RA^+$ $CD57^-$) T cells were greater than TLs in memory ($CD45RA^-$ $CD57^-$) T cells, consistent with prior reports (88, 119). Average TLs in $CD57^+$ T cell subsets were shorter than their corresponding $CD57^-$ subsets (Figure 5.1.A). The percentage of $CD57^+$ cells was higher in the $CD8^+$ T cell compartment than in the $CD4^+$ T cell compartment (Figure 5.2.B), consistent with published results (129). No correlation existed between subject age and TL in the cHCV cohort (Figure 5.1.B left panel). In contrast, we found an expected inverse correlation of age and TL in a separate cohort of 19 healthy subjects (Fig 5.1.B right panel) (88, 136). There were no significant differences in TL for any of the T cell subpopulations between the peg-IFNα group and the no-therapy group at baseline (Figure 5.2.A).

We next compared viremia levels and body mass index (BMI) with TLs in T cells at baseline. HCV viremia levels inversely correlated with TL in total $CD4^+$ and $CD8^+$ T cells (Figure 5.3.A), naïve T cells (Figure 5.3.B), and memory T cells (Figure 5.3.C) at baseline. BMI at baseline also inversely correlated with TL in naïve $CD4^+$ and $CD8^+$ T cells (Figure 5.3.D). However, there was no significant correlation between HCV viremia

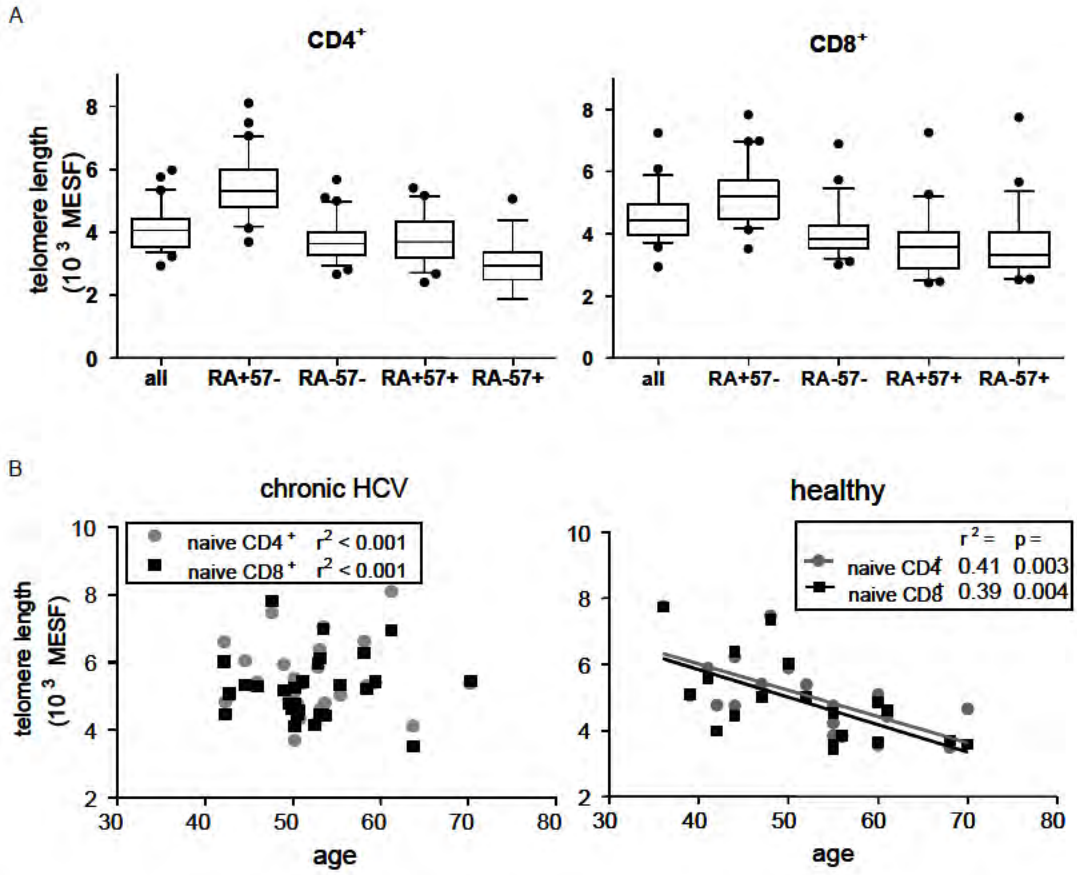


**Figure 5.1 Telomere length (TL) in T cells from cHCV healthy subjects and healthy control donors**

(A) TL estimates within total $CD4^+$ and $CD8^+$ T lymphocytes and indicated subpopulations for all 29 HALT-C subjects at baseline. Graphs are box-whisker 10-90 percentile with outliers. $RA^+$ or $RA^-$ indicates $CD45RA^+$ or $CD45RA^-$ respectively, $57^+$ or 57- indicates $CD57^+$ or $CD57^-$ respectively. Subpopulations are naïve (RA+57-), memory (RA-57-), $T_{EMRA}$ (RA+57+), and effector memory (RA-57+). (B) Linear regression analysis of naïve ($CD45RA^+$ $CD57^-$) $CD4^+$ (circles) and naïve $CD8^+$ (squares) TL at baseline for cHCV subjects (n=29, left panel) and a separate cohort of healthy, age-matched donors (n=19, right panel) versus age at blood draw.

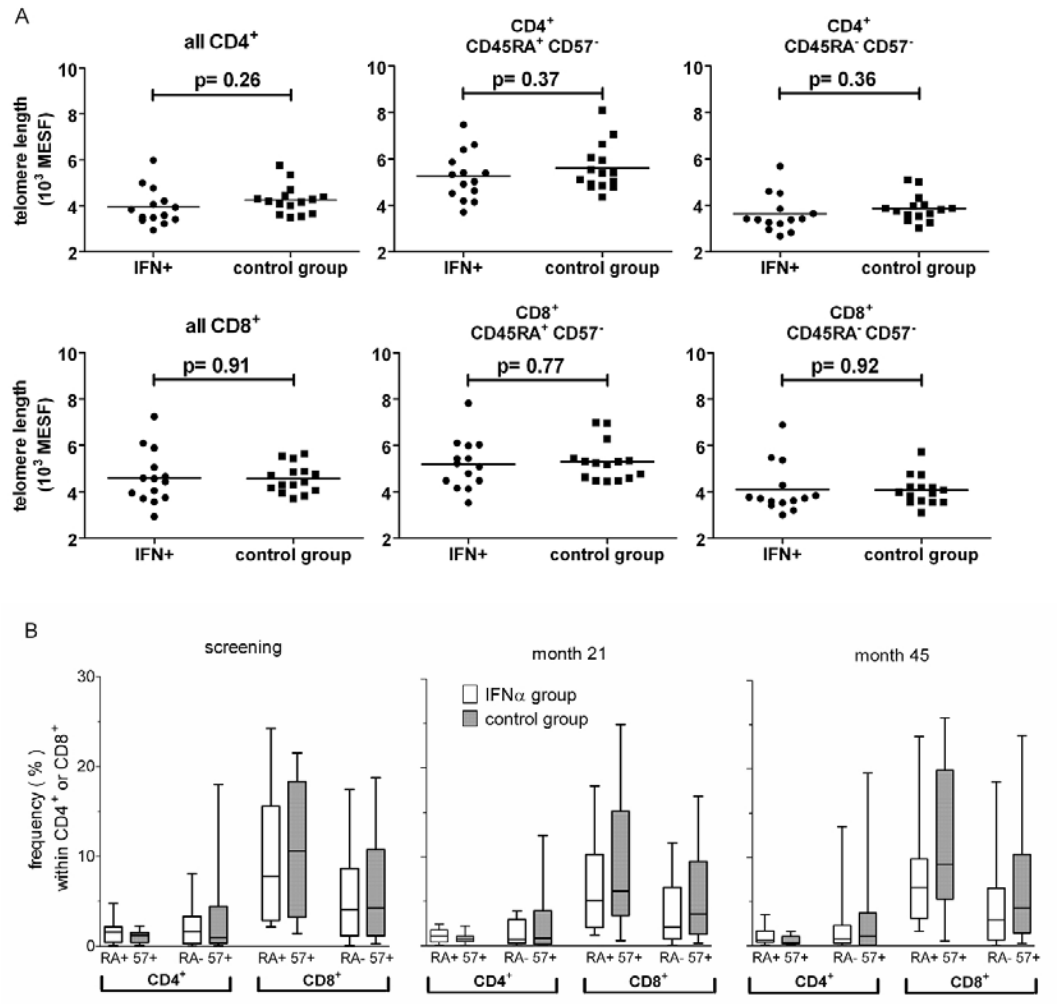


**Figure 5.2 Baseline telomere lengths were not different between the IFN treatment and control groups**

(A) Subject telomere lengths at baseline. Each symbol is an individual subject's TL measured by flowFISH in that T cell subset. P values are from unpaired *t* test analysis. Horizontal bars are mean values. (B) $CD57^+$ subset distribution within respective $CD4^+$ and $CD8^+$ T cell populations from baseline (S00), month 21 (M21), and month 45 (M45). Plots are box and whiskers 5-95 percentile bar graphs showing outlier values; peg-IFNα therapy subjects shown as empty bars; control group subjects, filled bars. $RA^+$ or $RA^-$ indicates $CD45RA^+$ or $CD45RA^-$ respectively, $57^+$ indicates $CD57^+$.

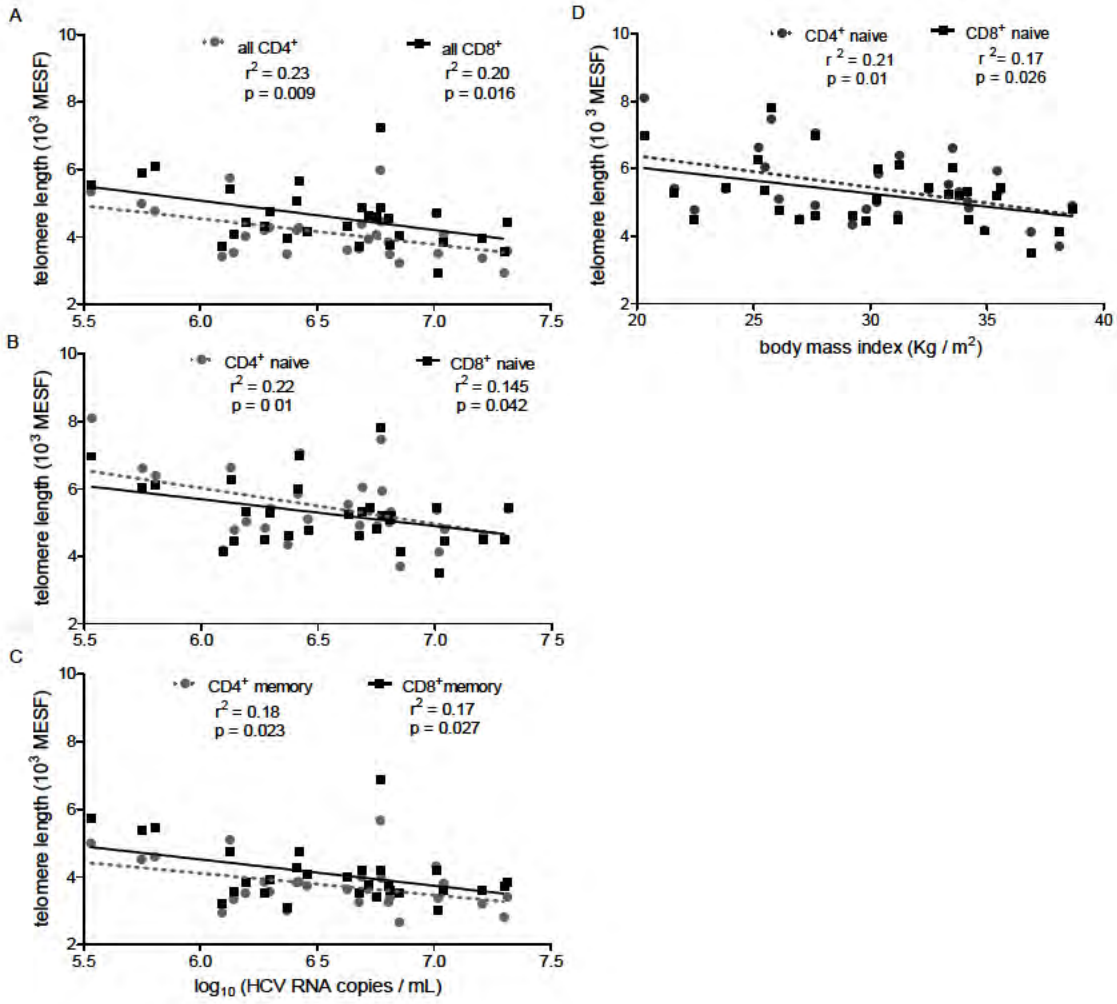


**Figure 5.3 Baseline T cell telomere lengths inversely correlated with hepatitis C viral RNA levels and BMI**

(A) TL in total $CD4^+$ (gray circles) and total $CD8^+$ (black squares) T cells from the baseline (S00) time point versus baseline HCV RNA levels, (B) TL in naïve $CD4^+$ (circles) and $CD8^+$ (squares) $CD45RA^+$ $CD57^-$ subsets versus baseline HCV RNA levels, and (C) TL in memory $CD4^+$ (circles) and $CD8^+$ (squares) $CD45RA^-$ $CD57^-$ subset versus baseline HCV RNA levels. (D) Baseline body-mass index (BMI, in kilograms per meter squared) from baseline assessment inversely correlated with naïve phenotype $CD4^+$ (gray circles) and $CD8^+$ (filled squares) T cells. Correlation (r-squared) and p values are from linear regression testing with best-fit lines as shown.

levels and BMI (data not shown), suggesting that BMI and viremia are independent factors associating with T cell TL in chronic HCV infection.

**B. Sustained IFNα therapy was associated with increased loss of telomere length**

To determine whether IFN therapy affected telomere erosion, the rate of change in TL in $CD4^+$ and $CD8^+$ T lymphocyte subsets between baseline (S00), month 21 (M21) and month 45 (M45) was determined for both groups (Figure 5.4). The average slopes derived from the linear regression equations for each subject (delta TL/year in units of MESF) showed declining TL for all T cell subsets. The average linear regression slopes between S00 and M45 show higher average rates of TL loss in the peg-IFNα treatment group for total $CD4^+$ T cells (Figure 5.4.A), total $CD8^+$ T cells (Figure 5.4.D), naïve CD4+ and CD8+ T cell subsets (Figs. 5.4.B, E) and memory CD4+ and CD8+ T cell subsets (Figs. 5.4.C, F), although this difference was statistically significant only for naïve $CD8^+$ T cells ($p=0.005$). $CD57^+$ T cells within both $CD4^+$ $CD45RA^{+/-}$ and $CD8^+$ $CD45RA^{+/-}$ subsets showed no difference in TL between treatment groups (data not shown).

The mid-point (M21) samples allowed assessment of whether the peg-IFNα effect on TL was linear over the four year study period. Within the peg-IFNα group, TL loss was greater in the first interval, S00 to M21, in the naïve $CD8^+$ ($p=0.002$), memory $CD8^+$ ($p=0.03$) and naive $CD4^+$ subsets ($p=0.02$) compared to the M21 to M45 interval (Figure 5.5). Naïve $CD8^+$ T cell TL loss was higher in the treatment compared to control group in

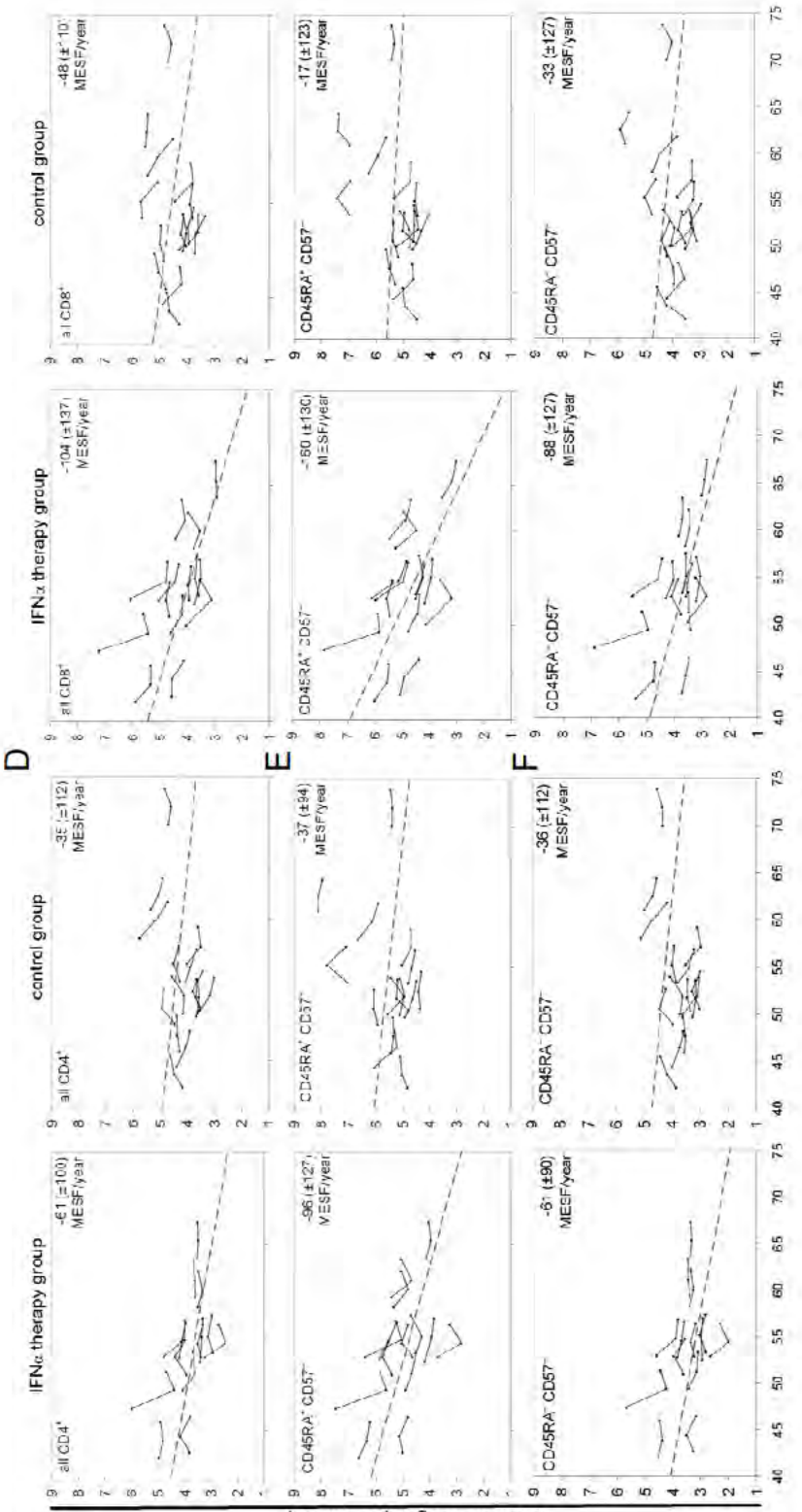


**Figure 5.4 Accelerated telomere length (TL) loss in naïve T cell subsets for the IFN group**
*(legend continues next page)*

**Figure 5.4 Accelerated telomere length (TL) loss in naïve T cell subsets for the IFN group** *(figure previous page)*

Individual TL trajectories for (A) all $CD4^+$, (B) naïve $CD4^+$ ($CD45RA^+$ $CD57^-$), (C) memory $CD4^+$ ($CD45RA^-$ $CD57^-$), (D) all $CD8^+$, (E) naïve $CD8^+$ ($CD45RA^+$ $CD57^-$), and (F) memory $CD8^+$ ($CD45RA^-$ $CD57^-$) T cell subsets are shown for peg-IFNα subjects (left panels) and the no-therapy, control subjects (right panels). Solid lines connect the TL of each subject at three time points plotted by age at blood draw. The dashed line on each plot derives from a linear regression based on the averaged slope and y-intercept from each individual's linear regression equation, with the average slope (± standard. deviation) in MESF per year of age shown in the upper right corner.

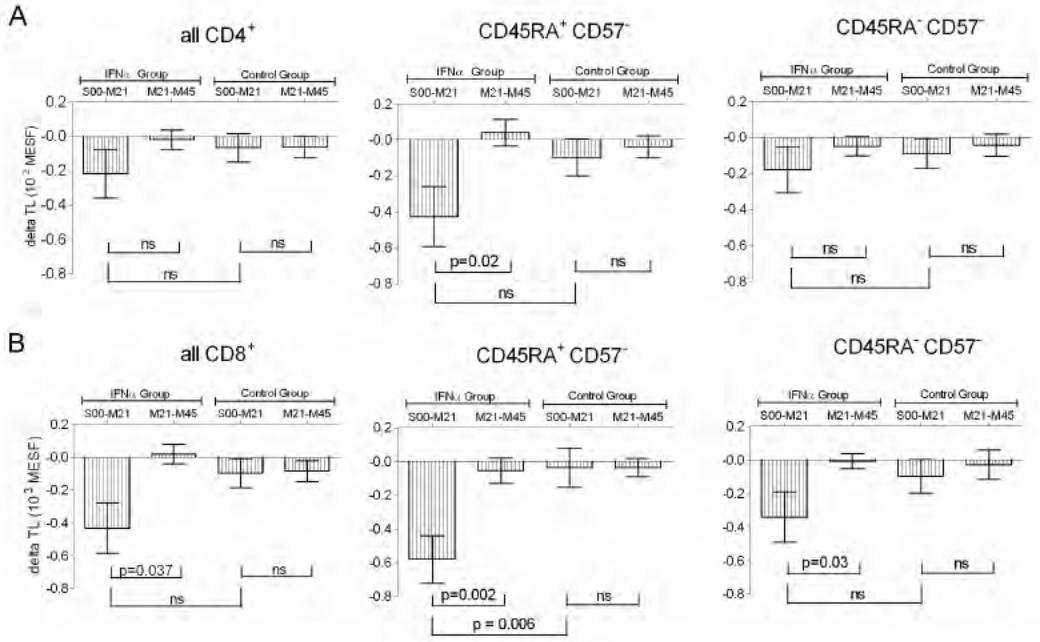


**Figure 5.5 Accelerated telomere length loss (delta TL) occurs in the first 21 months**

Delta TL analysis between treatment and control groups for (A) $CD4^+$ and (B) $CD8^+$ T cells and their naïve (CD45RA+ CD57-) and memory (CD45RA- CD57-) subsets for the baseline (S00) to month 21 (M21), and month 21 (M21) to month 45 (M45) intervals. P values are from Mann-Whitney testing. Error bars are mean ± standard error. ns = not significantly different.

the first interval ($p = 0.006$), but not different in the second interval. Taken together, these analyses indicate that TL loss accelerated with peg-IFNα treatment, but only in the first study interval.

**C. Age dependence of accelerated telomere length loss**

To assess the effects of age, treatment group, and TL changes, mixed-effects statistical analyses were performed with results indicating a significant age-related IFN-effect on TLs (data not shown). However, linear model fitting assumptions inherent to a multivariate, mixed effects model were not consistent with the non-linear TL loss data across the three time points. We therefore partitioned the data set into three age categories: <50 years, 50 to 55 years, and >55 years of age at baseline (Figure 5.6.). The 50-55 year partition was centered on the average age of our subjects (Chapter II, Table 2.1), with the age partition boundaries selected to roughly balance the numbers of subjects in each partition. This age-partitioned analysis corroborated the mixed-effects model results in that accelerated TL loss in the peg-IFNα group was seen in subjects <50 years old and that the effect was lost with increasing age in both $CD4^+$ and $CD8^+$ naïve and memory compartments.

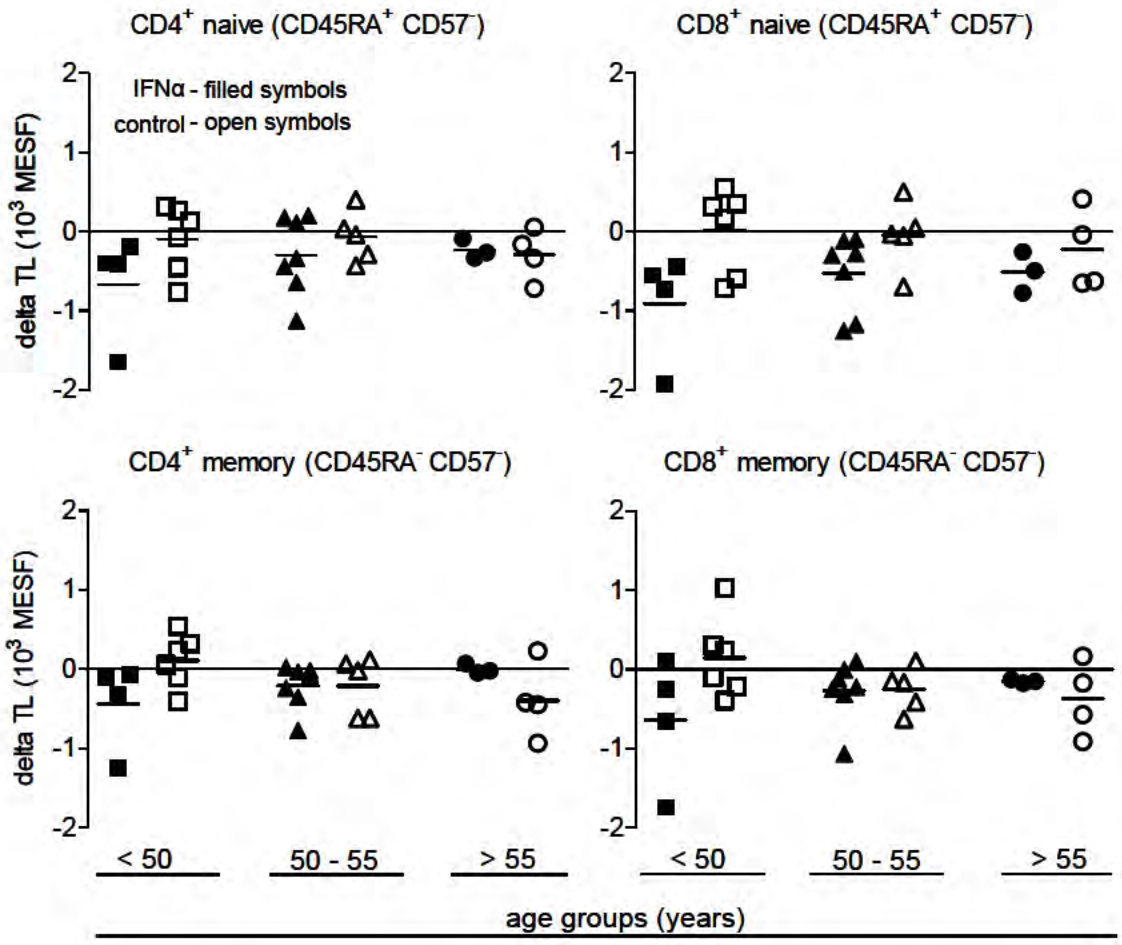


**Figure 5.6 TL loss with therapy was lost with increasing age in a T cell subset-dependent manner**

Change in telomere length in T cells (delta TL) from baseline to month 45 from subjects in both treatment groups. Each symbol is an individual subject's delta TL for that T cell subset. Filled symbols are subjects in the IFNα treatment, open symbols are control group subjects. Horizontal bars are mean values.

**D. Telomerase activity in T cells activated in vitro**

We asked whether effects of long-term IFN therapy on telomerase activity (TA) could explain the accelerated TL loss. As resting peripheral blood T cells express little or no TA (88), we analyzed TA after in vitro activation as an indication of a possible durable effect of peg-IFNα therapy. No difference was detected in TA after in vitro activation between the two treatment groups (Figure 5.7).

**E. Serum ALT-AST values inversely correlated with TL changes in the control group**

Serum alanine aminotransferase (ALT) and serum aspartate aminotransferase (AST) levels are commonly measured in the clinical setting to monitor liver pathology. Since liver injury in cHCV is hypothesized to be related to T cell activation (50, 52), we examined the relationship between serum ALT and AST and T cell TL. We found that TL change (S00 to M45) in naïve $CD4^+$ T cells and $CD8^+$ T cells negatively correlated with the average serum ALT levels ($p=0.016$ and $p=0.006$, respectively) during the randomization phase in the control but not the peg-IFNα group (Figure 5.8). Average AST levels during randomization also inversely correlated with TL loss in naïve $CD4^+$ T cells and $CD8^+$ T cells ($p=0.03$ and $p=0.006$, respectively) during the randomization phase in the control but not the peg-IFNα group (data not shown). These ALT-AST associations with telomere loss were not seen in the memory ($CD45RA^-$ $CD57^-$) subsets ($p >0.1$, data not shown). These data suggest that TL loss is related to on-going liver disease activity, but only in the absence of exogenous IFN therapy.

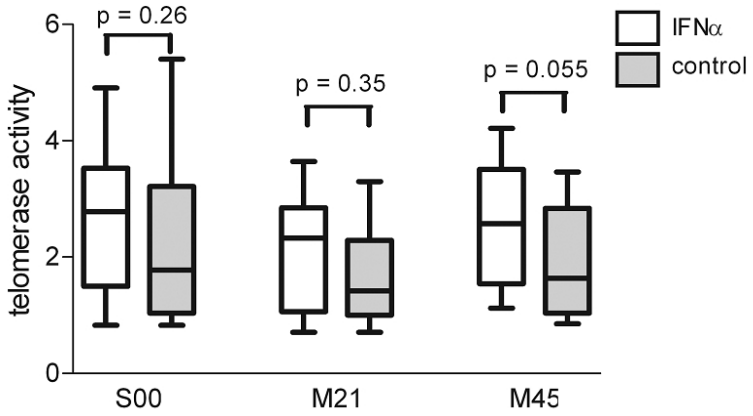


**Figure 5.7 Induced telomerase activity in PBMC between treatment groups was not different at any time point**

Telomerase activity (TA) was assessed in *in vitro* stimulated PBMC from each of the three time points, baseline (S00), month 21 (M21), and month 45 (M45), and the results analyzed between treatment groups as shown. Statistical p values are from Mann-Whitney non-parametric analysis. PBMC were stimulated with plate-bound anti-CD3 plus anti-CD28 for 3 days and then tested for TA by a commercial real-time PCR-based TRAP assay as described in supplemental methods.

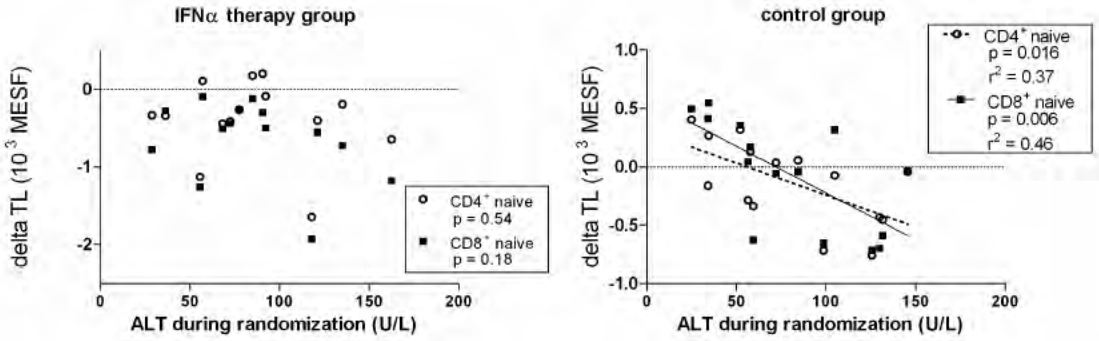


**Figure 5.8 Serum ALT correlates with changes in naïve T cell telomere lengths in the control group**

Average serum alanine aminotransferase (ALT) levels during the randomization phase correlated with telomere length loss (delta TL) in the no-therapy control group (right-hand panel), but not in the IFN therapy group (left-hand panel). Delta TL shown is from baseline (S00) to month 45 (M45).

**F. Sustained IFNα therapy suppressed $T_{EMRA}$ expansion**

Analysis of the $CD57^+$ T cell subsets indicated these $CD4^+$ and $CD8^+$ T cell sub-populations did not incur accelerated TL loss in the IFNα therapy group (data not shown). This result is consistent with previously published reports that $CD57^+$ is a marker for T cells with limited replicative capacity, and thus a limited ability to further erode telomere length (31, 128). Oligoclonal $CD8^+$ $CD57^+$ T cell expansions have been reported as a marker for reduced responses to IFNα therapy in cHCV patients (137). Thus we undertook further analyses of the changes in the frequency of the $CD57^+$ subsets within our cHCV cohort. The $CD8^+$ $CD45RA^+$ $CD57^+$ subset, which is primarily a $T_{EMRA}$ population of highly differentiated T cells (31), declined in frequency ($p=0.042$) in the peg-IFNα group between S00 and M21, followed by no significant change from M21 to M45 (Figure 5.9, left panel). In contrast, the control group showed no significant change in the $CD8^+$ $CD45RA^+$ $CD57^+$ T cell frequency between S00 and M21, followed by an increase between M21 and M45 ($p=0.0001$; Figure 5.9, right panel). These data suggest sustained therapy suppressed the accumulation of highly differentiated $CD8^+$ T cell memory oligoclonal expansions, results consistent with the ability of type I interferon to induce lymphopenia (87, 138, 139).

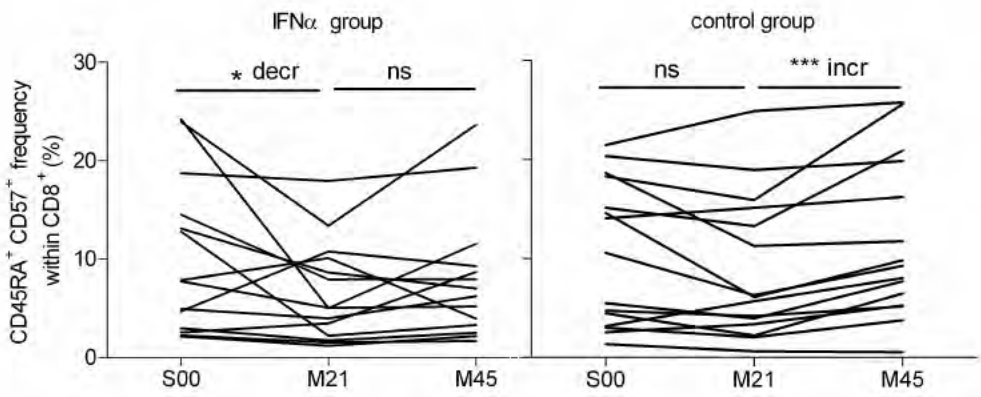


**Figure 5.9 Sustained interferon therapy associated with suppression of $CD8^+$ $CD45RA^+$ $CD57^+$ expansions**

$CD45RA^+$ $CD57^+$ subset frequency (%) within $CD8^+$ T lymphocytes across the three time points for the peg-IFNα subjects (left panel) and the no-therapy, control subjects (right panel). Individual lines on the plots represent values from each subject across the three time points. * $p < 0.05$; *** $p = 0.0001$ by Wilcoxon paired analysis (decr = decrease; incr = increase; ns = not significant).

**G. Chapter Summary**

Our data demonstrate significant telomere loss in naïve T cells in the first 21 months in the interferon-alpha group. Telomere losses were similar in both groups during the final two years. Expansion of $CD8^+CD45RA^+CD57^+$ memory T cells and an inverse correlation of alanine aminotransferase levels with naïve $CD8^+$ T cell telomere loss were observed in the control group but not in the interferon-alpha group. Telomere length at baseline inversely correlated with hepatitis-C viral load and body mass index.

The implications of our findings on the maintenance of T cell replicative capacity, both naïve and memory, are explored further in Chapter VI.

# CHAPTER VI

# DISCUSSION

How memory T cells are maintained in our bodies for decades is a puzzle that has long intrigued immunologists. The focus of this work was to understand the maintenance of T cell memory through the analysis of T cell telomere length (TL) dynamics. We used samples from two cohorts in this research to address our aims: 1) PBMC obtained during sustained IFN treatment in individuals with chronic HCV infection, and 2) PBMC obtained from healthy donors with memory T cells specific for common viral infections, CMV, VZV, IAV, and VACV. These viruses were selected to reflect diverse patterns of viral exposure, including a single acute infection (VACV), recurrent acute infections (IAV), viral latency with in-frequent reactivation (VZV), and viral latency with frequent reactivation (CMV) (41, 43, 47, 69, 94). In contrast, IFN treatment was an experimental model that could reflect the "bystander" effects on T cells that would be seen during acute infections with unrelated viruses (60, 61).

We first had to develop the appropriate experimental tools to measure TL in T cell populations of interest. We initially followed published methods for flowFISH analysis (140); however, several modifications were necessary in order to make this approach suitable for our studies, which included a fixation-permeabilization protocol for RNA nuclease treatment.

Using this flowFISH assay, we first analyzed TL in serial PBMC samples from chronic HCV (cHCV) patients receiving IFN-alpha therapy and a control group that did not receive IFN-alpha. These experiments were performed to understand how TL in T cells was affected by type I IFN. The studies permitted us to associate effects on TL with both exogenous IFN as well as cHCV itself (Chapter V). Lastly, using flowFISH in combination with BrdU labeling to detect virus-specific T cells, we performed a novel study on PBMC from ten healthy adults. We compared TL in $CD4^+$ T cells that proliferated to viruses with different patterns of exposure to understand the maintenance of TL in memory T cells. These studies revealed an unappreciated heterogeneity in the distribution of TL in polyclonal T cell populations, as well as unexpected relationships between T cell TL and the frequency and pattern of viral re-exposure (Chapter IV). While the previous chapters document these findings, the present chapter attempts to interpret and evaluate them in a wider context. Finally, models for virus-specific TL dynamics during aging and its relationship to the maintenance of T cell memory are presented.

**A. Insights from the flowFISH experimental approach along with recent findings on telomere biology in highly activated, proliferating T cells**

We measured TL in T cells that proliferated in vitro to viral antigens using a novel combination of the BrdU proliferation assay with a modified flow-FISH TL assay. Under these conditions of activation-induced proliferation, highly proliferative T cells strongly up-regulate telomerase (79, 95). In light of these telomere dynamics of T cells, TL changes during in vitro culture needed to be examined in order to understand how the

observed lengths evolved. Initially, we performed experiments to optimize parameters for fixation-permeabilization and RNA nuclease treatment to produce a TL measurement in agreement with Southern blot TRF results.

**i. Understanding the inflated telomere signal in un-modified flowFISH**

TL measured by flowFISH in *in vitro*-stimulated T cells was initially found to be significantly higher than TL measured by Southern blot TRF; only when steps were added for fixation-permeabilization and RNA nuclease treatment did we find good agreement between these assays. These steps were included after the presence of telomeric RNA in lymphocytes was reported by others in late-2007 (124, 125). This reported discovery and our realization that telomeric RNA could provide non-DNA binding targets for our telomere probe prompted us to begin experiments to remove this signal component. Very recently work by Picket, *et al.* demonstrated that high levels of telomerase in T cell blasts result in elongated telomeres at day 3. However, in their data by day 6 of culture, TLs returned to more normal lengths by a process they termed "telomere trimming" (131). Picket, *et al.* showed that trimming of elongated telomeres resulted in the formation of extrachromosomal telomeric circles (T-circles), likely by homologous recombination using a Rad51C/XRCC3-dependent mechanism. The T-circles are closed circles of telomeric DNA, which would present binding sites for the telomere probe under the standard flowFISH assay conditions. These extrachromosomal T-circles are one likely candidate source for the "inflated" telomere signals we observed in the un-modified flowFISH assay (no fixation-permeabilization, Fig 3.1) that fixation-

permeabilization alone corrected. Inclusion of a permeabilization step in our modified flowFISH assay could have allowed un-tethered T circles to diffuse out of the cell and be diluted away during the multiple wash steps prior to hybridization. Although this mechanism had not been reported at the time we performed these experiments, that work now provides an explanation as to how fixation-permeabilization alone could have reduced the telomere probe signal in our flowFISH, bringing it closer in line with the TRF Southern blot results. The additional removal of telomeric RNA by the RNA nuclease treatment further corrected the flowFISH TL signal to bring it into agreement with the Southern blot TRF-derived TL (Chapter III, Figure 3.1).

**ii. T cell telomere length changes during activation-induced proliferation**

The findings of Picket *et al.* offer a fundamentally altered view of the early increase and later decrease, i.e. trimming, in telomere probe florescence in proliferating, activated normal T cells (131). Our interpretations of the flowFISH data during in vitro proliferation (Chapter IV, Figure 4.1) are also supported and more fully understood by this telomere trimming-T circle paradigm. The loss of mean TL in the BrdU+ cells of Figure 4.1 between day 5 and day 6 of in vitro proliferation was greater than could be explained by the amount of observed proliferation between these time points. Telomere trimming provides an explanation for this problem. At day 7, we found the predominance of a near normal distribution of TLs in the virus-specific proliferating (BrdU+) T cells. Based on the day 6 where the elongated telomere signal was absent, Picket *et al* concluded that trimming to create T circles occurred between days 3 and day 6 in vitro.

Based on the Picket, *et al.* conclusions and our data, we conclude that we are likely measuring the remaining true chromosomal TL at day 7. Our observation that in vitro proliferation did not correlate with the observed day 7 telomere lengths (Chapter IV, figure 4.3.E) strengthens the argument that the telomere lengths measured at day 7 are not merely artifacts of in vitro culture. From these lines of evidence, we conclude that the differences in TL between virus-specific T cell populations at day 7 reflect true differences in telomere length in virus-specific memory T cells at the time of blood collection.

**B. CMV-specific and VACV-specific $CD4^+$ T cells have higher mean telomere length than IAV-specific $CD4^+$ T cells**

Our finding that TL in $CD4^+$ T cells specific for the non-recurring acute virus infection, VACV, was longer than TL in T cells specific for acute but recurring IAV supports our initial hypothesis. We had also predicted that TL in CMV-specific T cells would be shorter than TL in T cells specific for acute virus infections. Counter to our prediction for CMV, we found that TL in CMV-specific $CD4^+$ T cells with high replicative capacity was longer than TL in IAV-specific $CD4^+$ T cells. There are likely several explanations for these observations. We did not survey an older (aged >60 years) adult cohort where clonal expansions of CMV-specific T cells with short TL are most prominent (66). Importantly, as described by others, CMV-specific $CD4^+$ T cells may be continuously driven to replicative exhaustion in vivo (107); therefore, it is possible that findings in an older population would more closely follow our original hypothesis.

Another possible explanation for our results is that the experimental approach used limited the measurement of TL to T cells that proliferated in vitro in response to viral antigen stimulation. Thus our results, showing lower frequency (figure 4.3) and longer TL in CMV-specific $CD4^+$ T cells are consistent with the possibility that the cells captured in our proliferation assay are T cells more recently recruited from the naive repertoire with correspondingly longer telomeres, whereas circulating T cells with short telomeres that were unable to proliferate in vitro would not have contributed to the TL measurement.

**C. Combined longitudinal and cross-sectional modeling enhances the study of virus-specific memory T cell telomere kinetics in aging populations**

Our longitudinal modeling, although based on a small cohort of five healthy donors, offers some insights into the kinetics of TL of differing virus-specific T cell populations. This model indicates that TL differences between virus-specific T cell populations may be greater at younger ages and diminish as we age. This would suggest that follow-on studies using this proliferative assay approach of an older age cohort (> 60 years) may not observe significant differences in virus-specific memory T cell populations, or that it would necessitate many more subjects in an aged cohort to reach statistically significant conclusions. This could be an important consideration in the selection and sizing of age cohorts in studies designed to explore differences in memory T cell TL differences to a range of viruses or vaccine formulations in age stratified populations. The data further suggest caution in interpreting TL kinetics derived from

purely cross-sectional data, because survivorship bias, where study participants with short telomeres die earlier (141), would lead to an underestimation of age-related TL loss in purely cross-sectional data.

Interestingly, this hybrid longitudinal/cross-sectional model suggests that declining naïve T cell TL with age will have an impact on the control of CMV reactivation. If existing memory T cells are continually driven to replicative exhaustion (107), new recruitment from naïve T cells would be necessary for CMV-specific T cells to maintain control of viral replication. Thus our finding here of relatively long telomeres in the CMV-specific $CD4^+$ memory T cells, rather than the short telomeres we predicted, could be explained in that 1) all our donors were under age 60, 2) our assay only captures T cells with a high proliferative capacity, and/or 3) these may be more recently activated from the naïve repertoire and had not yet lost significant TL.

**D. VZV reactivation re-established VZV-specific long telomere $CD45^+$ T cells**

Our observations that TL increased by more than 50% in both VZV-specific $CD4^+$ and $CD8^+$ cells in one subject after virus reactivation in vivo have interesting implications both for basic lymphocyte biology and use of VZV vaccine for secondary prophylaxis (boosting at an older age). There are at least two models to explain this increase in TL in VZV-specific T cells: elongation of shortened telomeres in pre-existing memory T cells, or recruitment of new naïve T cells (with longer TL) into memory. Human T cells undergoing activation-induced proliferation have been shown to up-regulate telomerase, which has been proposed to maintain TL, but in general does not

lead to significant telomere elongation in lymphocytes (84). On the other hand, the recruitment of new naïve VZV-specific T cells with longer TL better explains this TL increase and is the explanation that best fits our data based on our current understandings of T cell biology. With regard to VZV prophylactic boosting, this interpretation would recommend re-vaccination before the age-related decline in naïve T cell TL compromises the recruitment and formation of new long-lived memory T cells.

The lack of a significant population of cells with long TL in $CD45RA^+$ VZV-specific $CD4^+$ T cells in the blood sample collected prior to VZV reactivation (Figure 4.8.F) provides an intriguing opportunity for the study of T cell-mediated control of latent-reactivating herpesviruses using the imprint that reactivation may leave on its virus-specific memory T cell TLs. Our findings support a model where a gradual loss of TL in a long-lived reserve of memory T cells would lead to a loss of in vivo effector T cell replicative capacity and a waning frequency of effector T cells, finally becoming insufficient in quantity and quality to suppress reactivation (142). The clinically evident reactivation with replicating virus in turn would drive a strong immune response, including the recruitment of additional naive T cells.

**E. Accelerated T cell TL loss under sustained IFN therapy**

The study of subjects from the HALT-C trial (Chapter V) indicated that sustained peg-IFNα therapy (90 μg/week) was associated with an increased rate of TL loss in both naïve $CD4^+$ and $CD8^+$ T cell subsets. Additionally, based on a single intermediate time-point, the enhanced TL loss related to IFNα therapy was fully concentrated in the initial

21 months of the trial. The delineation of TL changes in T cell $CD45RA^{+/-}/CD57^{-}$ subsets showed that declines in T cell TL did not represent shifts between naïve (long TL) versus memory (shortened TL) T cell proportions, but true decreases in TL with the greatest impact on the naïve T cell subsets. The lack of an accelerated TL loss in naïve T cells in the second interval in the peg-IFNα group suggests that a new homeostasis was reached. These findings are consistent with the telomere erosion effects of increased lymphocyte turn-over in response to a sustained lymphopenic signal as predicted from the mathematical models of de Boer and Noest (143). Increased T cell turn-over would also account for our observation that sustained peg-IFNα treatment inhibited the expansion of $CD8^{+}$ $CD45RA^{+}$ $CD57^{+}$ $T_{EMRA}$ cells, a phenomenon that was observed in the control group.

Based on the design of the HALT-C trial, subjects in both groups received combination therapy with peg-IFNα (180 μg/week) plus ribavirin for the initial 24 weeks of the study (113). PBMC were not available from other intermediate time points. Therefore, it is possible that accelerated TL loss occurred in both groups during the initial phase of lead-in therapy. Average TL could then have rebounded in the control group between the end of therapy at week 24 and month 21, whereas ongoing, lower-dose peg-IFNα therapy maintained the lower average TL (or suppressed a TL recovery) in the therapy group. Consistent with this interpretation, the decline in TL was slower during the second interval than in the earlier interval in the therapy group. If this interpretation is correct, it is impossible to determine whether the effect of the initial therapy on TL is attributable to the higher dose of peg-IFNα or to ribavirin. Nevertheless, sustained peg-

IFNα was clearly associated with accelerated TL loss during the subsequent 3½ years in comparison with the control group.

**F. Baseline TL correlates with viremia and obesity in cHCV subjects**

An important finding from the interferon study was the correlation of baseline T cell TL in cHCV subjects with viremia and BMI. It should be noted that subjects in the randomization phase of the trial had endured HCV viremia for decades (range: 14-51 years) and failed to achieve SVR during combination peg-IFNα-ribavirin therapy. The absence of a negative correlation of baseline T cell TL with age in this cohort may therefore reflect stronger impacts of long-term viremia and the generally high levels of obesity in these subjects.

We speculated that the inverse association between serum viral RNA levels and baseline TL may reflect chronic elevated T cell activation, cell death, and proliferation due to persistent presentation of HCV antigens in a dose-dependent manner (58). Alternatively, higher circulating viral RNA levels may also drive greater endogenous type I IFN production. A negative correlation of BMI with baseline TL in naïve T cells could also reflect chronic inflammation in obesity (144). Chronic inflammation as a result of obesity may lead to decreased thymic output (145), inducing increased homeostatic proliferation of naïve T lymphocytes and thus a decrease in TL through replicative erosion.

Another possible explanation for the lack of an age-dependent TL association in this cohort relates to evidence that short telomeres play a causal role in a variety of age-

related diseases (146-149). The HALT-C study inclusion criteria limited enrollment to cHCV without other co-morbidities, such as a history of cardiovascular disease, neoplasia, or other chronic condition which might have prevented a subject from competing the 4 year long trial (113). Thus it is plausible that the study inclusion criteria biased the enrolled study population away from subjects with very short telomeres.

**G. Serum transaminases as indicators of hepatocyte killing and loss of naive T cell TL**

Elevated ALT and AST levels in cHCV are indicative of hepatocellular inflammation and necrosis (150). Our finding of a correlation of serum ALT and AST levels with naïve T cell TL loss in the control group possibly reflects T cell responses to infected HCV-infected hepatocytes and the extended time frame over which telomere lengths were analyzed. This relationship was possibly obscured in the peg-IFNα group by the effects of continuous therapy. The correlation between TL changes and ALT/AST, which could be due to T cell clonal exhaustion, immuno-senescence, or a combination of these and/or other immunological factors (151, 152), suggests that normalization of liver enzyme levels in the blood may coincide with a reduction in T cell turn-over and thus reduced telomere erosion.

**H. Telomerase inhibition was not seen with interferon therapy**

We hypothesized that maintenance peg-IFNα therapy would cause increased TL loss in T cells as a result of inhibition of telomerase activity (82, 86). However, we did

not find a significant difference between the peg-IFNα and control groups in telomerase activity in PBMC stimulated in vitro. It is possible that, using in vitro-stimulated PBMC, the telomerase assay failed to detect an inhibitory effect of peg-IFNα therapy that existed in vivo. In any case, as naive T cells do not express telomerase and are antigen inexperienced and thus have not gone through a telomerase-inducing clonal expansion, a telomerase inhibition mechanism falls short in explaining the predominance of an accelerated TL loss on naïve T cells. Further in these older adults where thymic output of new, longer telomere naïve T cells may be negligible, a reduced thymopoesis explanation is also not a likely source of TL loss in the naïve T cell compartment. Taken together, our data suggest a telomerase inhibition mechanism by IFN does not explain the accelerated TL erosion in the naïve T cell compartment.

**I. Interferon-induced TL loss may reveal a hierarchy of onset of T cell subset senescence**

We found a decline in the effect of peg-IFNα on TL loss with increasing age. Increasing age is associated with increased failure rates of IFN therapy for cHCV (55). This may suggest that elevated TL erosion caused by peg-IFNα is counteracted by replicative senescence occurring at different rates within different T cell compartments. The results of the analysis of IFNα-induced TL loss in $CD4^+$ and $CD8^+$ T cell subsets in the different age groups suggest a hierarchy of age-dependent T cell senescence in chronic HCV patients, occurring in the order: memory $CD4^+$ > memory $CD8^+$ > naïve $CD4^+$ > naïve $CD8^+$. This result and our conclusion are consistent with the finding by

Hoare, *et al*. that TL in $CD4^+$ $CD45RO^+$ memory T cells was a stronger predictor of SVR with IFN therapy than TL in any other T cell subset (153). Refractoriness to TL loss in memory $CD4^+$ T cells under the influence of type I interferon stimulation (as seen in the older age group in our study) may signal the onset of immunosenescence that affects the clearance of virus from a chronic infection state.

**J. Strengths and Limitations of the Studies**

Several additional points are worth noting regarding the methodological approach described in this thesis. An inherent limitation of flow-FISH is the limited number of cellular phenotype markers that survive the hybridization conditions (119). A further limitation of our approach to study virus-specific T cells using BrdU staining is the measurement of TL only in cells that proliferated in vitro. Therefore we were not able to perform a robust cross-sectional analysis of TL in $CD8^+$ T cells with the experimental conditions we used.

On the other hand, metrics of TL distribution such as median TL or skewness, which can be derived from single cell methods such as flow-FISH, may be quite informative to understanding long-lived T cell memory. TL distribution parameters of single cells are not captured in Southern blotting and PCR-based methods of TL measurement (109). Using the additional information available from flow cytometry, we identified a subset of BrdU+ cells with long TL that were CD45RA+ and CD27+. The long TL in these cells could be advantageous in maintaining long-term immunologic memory, but further studies would be needed to confirm such a role.

**K. Virus-specific memory T cell study: Summary, Implications, Models**

We hypothesized that virus-specific memory T cells that proliferate to acute, non recurring infections have longer telomere lengths than T cells that proliferate to recurring or reactivating viral infections. In line with our hypothesis, we found that TLs in VACV-specific $CD4^+$ T cells were longer than TLs in IAV-specific $CD4^+$ T cells. Since re-exposure to VACV is not likely, there would be fewer opportunities for activation-induced erosion or accelerated depletion of memory T cells. In contrast, yearly re-exposure to IAV could slowly erode the proliferative reserve of memory T cells while maintaining elevated circulating frequencies of effector memory, leading to the shorter telomeres and higher BrdU+ frequencies observed in IAV-specific $CD4^+$ T cells. Longer TL in CMV-specific $CD4^+$ T cells and the data from others that CMV reactivation may continuously drive T cells to replicative exhaustion (107) would imply that regular recruitment of naive T cells would be needed to sustain viral control from reactivation. A proposed model of maintenance of CMV-specific $CD4^+$ T cells against the backdrop of age-related declining naïve T cell TL and its impact on host T cell immunity is presented in Figure 6.1. The longer telomeres of the CMV-specific $CD4^+$ T cells that proliferate in conjunction with the lower slope of TL loss in this population relative to that of naïve T cells predicts that the TL of CMV-specific CD4+ T cells will intersect with the TL of naïve T cells 20 years earlier than for the other three viruses studied. This could have significant implications for host T cell maintenance.

This data-derived model provides a possible explanation of the CMV-specific T cell functional defects seen in the elderly, as observed by others (71, 154-156). These functional defects have been described as clonal expansions of CMV-reactive $CD8^+$ T cells which are apoptosis resistant, but lack many anti-viral functional characteristics such as robust interferon-gamma secretion. An explanation of these CMV-reactive $CD8^+$ memory T cell functional defects may lie in TL limitation of proliferative capacity in the naïve T cell compartment. A truncated proliferation program due to the Hayflick limit could translate to an inadequately completed differentiation program with the observed result being the described dysfunctional memory T cell. As the TL of the naïve T cell compartment further declines with advancing age, the proliferative response becomes progressively more truncated by this unyielding Hayflick limit. In this scenario the inability of dysfunctional effector T cells to fully restrain CMV replication would lead to heightened innate inflammatory cytokine signaling such as IL-6, TNF, or type I IFNs. This sustained chronic low level inflammation would lead to non-specific bystander effects to all circulating T cells in a self-reinforcing feedback loop as proposed by others (156-158).

Additional longitudinal studies of T cell TL dynamics in a larger number of healthy individuals are clearly needed, both to validate these preliminary models of memory maintenance, and to further extend the data set to older subjects. Longitudinal studies of TL in HIV-, HBV-, and HCV-specific T cells would shed light on the relationship between exhaustion of virus-specific T cell memory and declining TL in virus-specific and naïve T cells, against the backdrop of age-related T cell senescence

(66, 154, 156, 158-161). The visualization of TL distribution in an ensemble of individual virus-specific T cells, made possible with flow cytometry, may provide clearer insights to the factors affecting the generation of T cell memory replicative capacity to different pathogens and vaccines.

Additionally, we consistently noted a small fraction of long telomere CD45RA$^{+}$ T cells that arose in each of the four virus-specific responses tested for all ten donors. The CD45RA$^{-}$ fraction, in contrast, consisted of cells with shorter telomeres and lower levels of CD27 -- both characteristics of effector memory T cells. Recently published work by others have provided support for the presence of highly proliferative CD45RA+ memory T cells with limited differentiation in humans (11). Our data here provide insight of how human T cells, with different functional fates arising during activation and expansion, can provide both the differentiated effector CD62L$^{-}$ CD45RA$^{-}$ responses needed for antiviral effects, while simultaneously establishing a smaller pool of long telomere CD45RA$^{+}$ T cells with high replicative potential. These ideas of long telomere T cell generation during an acute viral response are embodied in the proposed models shown in Figure 6.2.

During the response to primary (1$^{o}$) viremia, T cell recruitment and activation produces a large population of virus-specific T cells. The differentiation status of these virus-specific T cells rapidly increases during activation and expansion, leading to shortened telomere lengths in the large effector population. Once viremia resolves, T cell numbers dramatically contract, as most are short lived, highly differentiated effectors and undergo apoptosis.

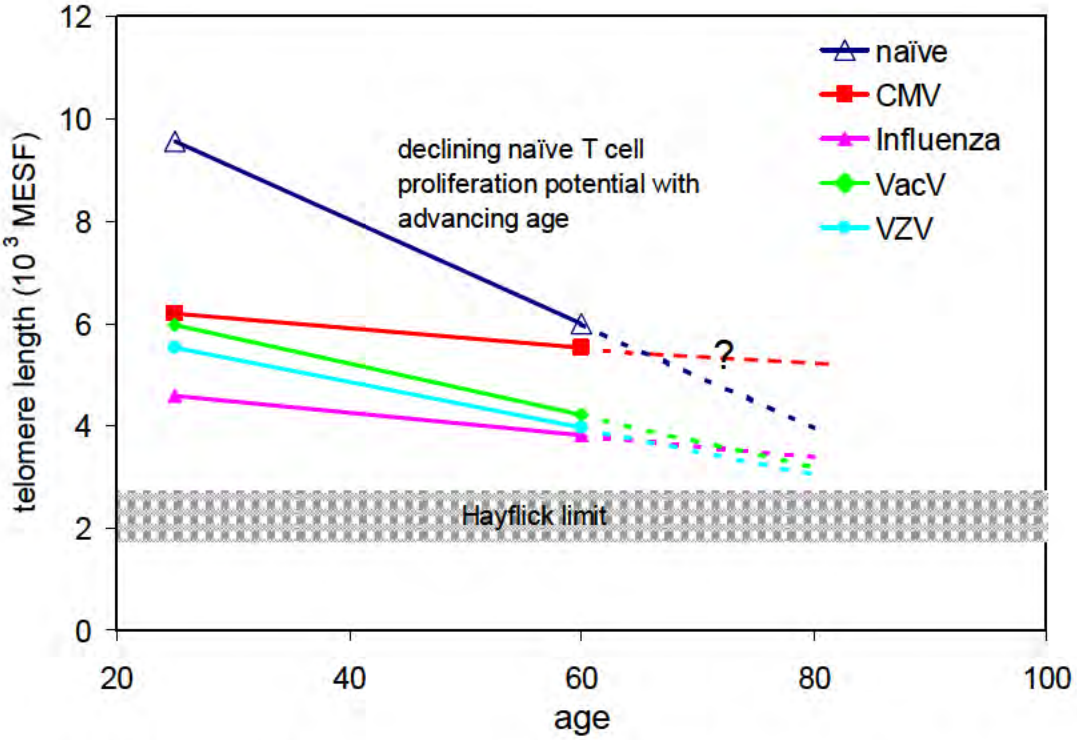


**Figure 6.1 A model for age-dependent declining virus-specific memory T cell telomere length**

Telomere length decline over decades of aging reduces proliferative potential. This modeling predicts that T cell recruitment from the naïve repertoire will affect the response to CMV much earlier than for IAV, VZV, or VACV. The Hayflick Limit (critical telomere length) is estimated and is shown as a wide band because it likely varies between individuals.

Over periods of years to decades, the total number of circulating effectors slowly declines during homeostatic maintenance as long-lived T cells slowly consume their telomere length to support homeostatic maintenance.This small population of $CD45RA^{high}$ T cells with long telomeres, established during activation-dependent induction of memory, maintains the circulating effector memory population through slow homeostatic proliferation to maintain a small but steady level of circulating virus-specific T cells that have immediate effector function if stimulated by their cognate antigen via TCR stimulation. Sustained memory maintenance during homeostatic proliferation leads to slow, but steady telomere loss. Re-infection or reactivation leads to antigen-driven activation, clonal proliferation, and increased differentiation. Large scale recruitment of memory T cells leads to a diminished telomere length within the long-lived, long telomere $CD45RA^{+}$ T cell memory.

As speculation, telomere maintenance related to high telomerase expression combined with a suppression (or avoidance) of homologous recombination-dependent telomere trimming (131) during activation-induced memory induction could create small number of $CD45RA^{+}$ memory with long telomeres. As we found with the VZV-specific response shown in Figure 4.8, the characteristic long-telomere $CD45RA^{+}$ $CD4^{+}$ T cell reserve was not observed prior to VZV-reactivation in this donor. Others have shown that VZV-reactivation occurs when circulating VZV-specific T cells falls below critical levels (69, 70, 162). This strong reactivation likely led to recruitment of new VZV-specific T cells from the naïve repertoire with long telomeres and high proliferative capacity,

restored VZV T cell-mediated control, and replenished the long telomere $CD45RA^{+}$ $CD4^{+}$ T cell population.

During homeostatic maintenance of T cell memory, the replicative capacity contained within a single $CD4^{+}$ $CD45RA^{high}$ long telomere memory T cell supports maintenance of a large number of differentiated clonal daughter cells. Daughter cells differentiate to establish more differentiated effector functions following programmed fates (Th1, Th2, Tfh, etc.) as they proliferate. Differentiation and division simultaneously induces telomere erosion. Early differentiated T cells maintain poly-functional responses and the capacity for proliferation and IL-2 secretion, while more differentiated daughter cells have shorter telomeres and limited replicative capacity.

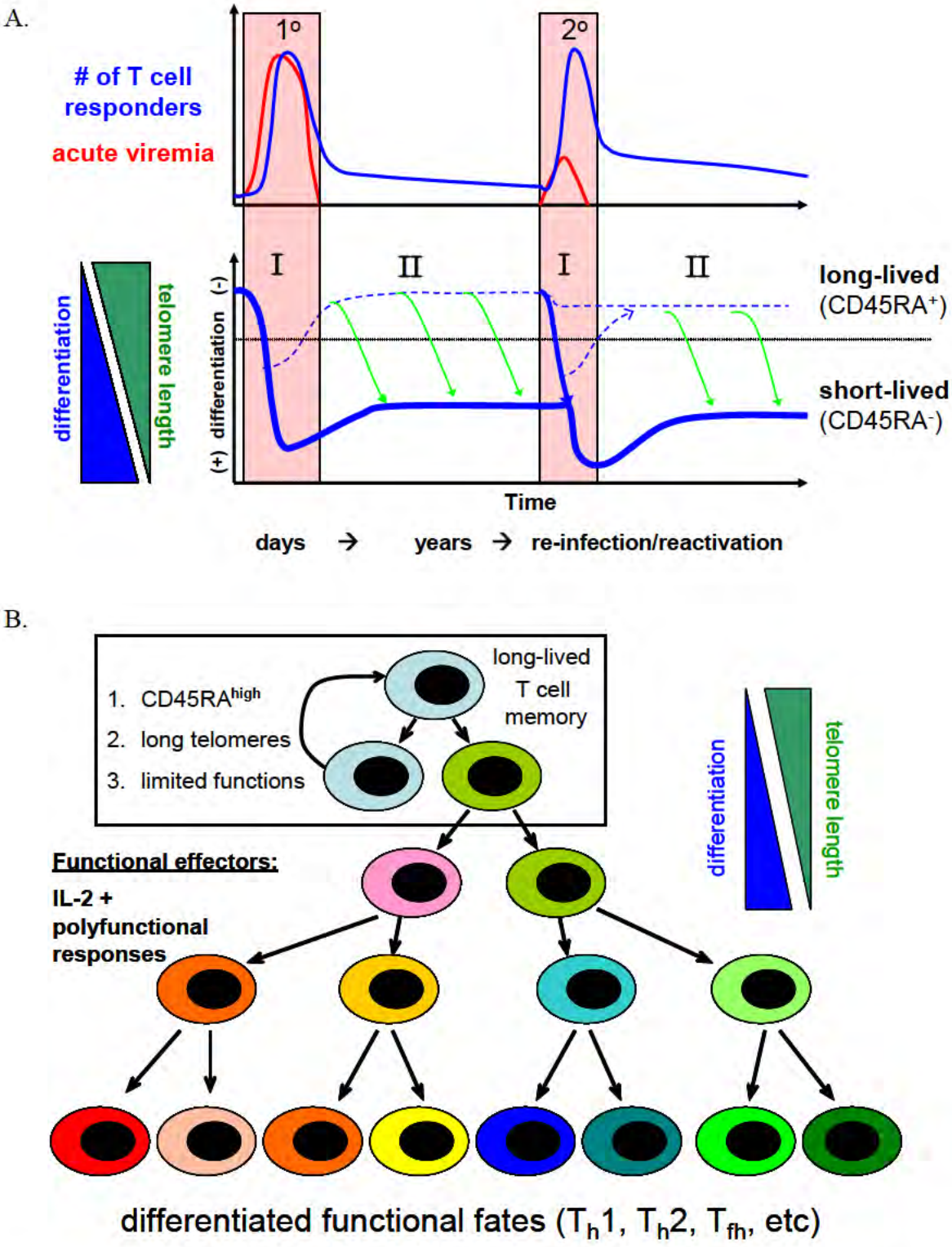


**Figure 6.2 A model for the role of CD4$^+$ CD45RA$^+$ T cells with long telomeres in maintenance of virus-specific memory** *(continued next page)*

**Figure 6.2** *(continued from previous page)*

(A) In response to primary ($1^{o}$) virus infection (red line), a large population of antigen-specific T cells (blue line, upper graph) become activated during the acute phase. During activation and expansion of these virus-specific T cells (shaded area I, lower graph), a the majority differentiate to shorter lived-effectors and their average telomere lengths decline (thick blue line). Once viremia resolves, T cell numbers dramatically contract. Unknown mechanisms or pathways during the periods of activation-induced memory induction create a small population of $CD45RA^{high}$ T cells with long telomeres (blue dashed line, lower graph). During homeostatic proliferation (green lines in area II), some $CD45RA^{+}$ T cells with long telomeres steadily produce daughter cells to maintain a population of more numerous shorter-lived, more differentiated effector memory cells. Re-infection or reactivation (second shaded area I) can also lead to loss of telomere length within the long-lived, long telomere CD45RA T cell population as clonal expansion results in large clonal burst of differentiated, short lived effectors being produced. Renewal and maintenance of the long telomere T cell memory may increasingly become compromised due to increasing telomerase repression after several rounds of clonal activation. Once the long-telomere T cell reserve is depleted, recruitment of new clones from the naïve repertoire, with long telomeres and high proliferative capacity, would then be needed for host protection.
(B) The enhanced replicative capacity contained within a single $CD4^{+}$ $CD45RA^{high}$ long telomere memory T cell supports homeostatic maintenance of an army of more differentiated clonal daughter cells (area II in A above). Telomere lengths in all cells would slowly decline due to replication-dependent telomere erosion as telomerase expression is low to non-existent during homeostatic proliferation. Daughter cells become more differentiated with effector functions following programmed fates as they proliferate. Early differentiated T cells maintain poly-functional responses and proliferative capacity and IL-2 secretion, while fully differentiated daughter cells have shorter telomeres and limited replicative capacity.

**L. Interferon therapy telomere length study: Summary, Implications, Model**

From the HALT-C study we found data to support the hypothesis that sustained IFN therapy enhanced loss of telomere length. However, we found no data to support telomerase inhibition as a mechanism for this effect. Instead, the data showed TL loss was concentrated in naïve T cells, and a steady $CD8^+$ $CD57^+$ $T_{EMRA}$ expansion occurred in the control group and not in the therapy group which implies that IFN suppressed these memory expansions in the therapy group. These data, along with the known ability of IFN to cause lymphopenia, led us to conclude that greater homeostatic proliferation, resulting in elevated TL erosion, was a likely mechanism that best fit our data.

Enhanced naïve T cell TL loss in cHCV subjects who received long-term peg-IFNα therapy suggests that T cells in these subjects have reduced proliferative reserve. Subjects receiving type I IFN therapy are known to be more susceptible to bacterial infections; this has been attributed to neutropenia, but several studies have shown no temporal correlation between neutrophil count and infections (163, 164). Diminished memory T cells and proliferative reserve related to naïve T cell TL loss, as shown in this study, could contribute to the increased susceptibility to infection and disease while on IFN therapy. Importantly, diminished naive T cell proliferative TL reserve incurred under sustained IFN therapy may persist well beyond the end of therapy. Indeed, as age-related thymic involution severely limits the production of new, long-telomere, naïve T cells (153), a sustained accelerated TL erosion may leave a permanently degraded naïve T cell compartment. Support for this possibility comes from a recent analysis of a subset of patients from the HALT-C cohort prospectively followed for more than 5 years after the

trial. That study showed that rates of non-liver-related death were significantly higher ($p=0.01$) among patients with liver fibrosis who received the 3½ year peg-IFNα therapy compared to similar patients in the control arm (165). A model of the effects of an accelerated naïve T cell TL loss that may explain this increased mortality is proposed in Figure 6.3. Accelerated telomere loss in the naïve T cell compartment would result in earlier impacts on the ability to maintain T cell responses to recurring infections due to a diminished naive T cell proliferative potential. Accelerated onset of memory T cell immunosenescence thus would compromise T cell mediated immunity at an earlier age, providing the explanation for the increased mortality seen in the HALT-C long-term interferon therapy patients.

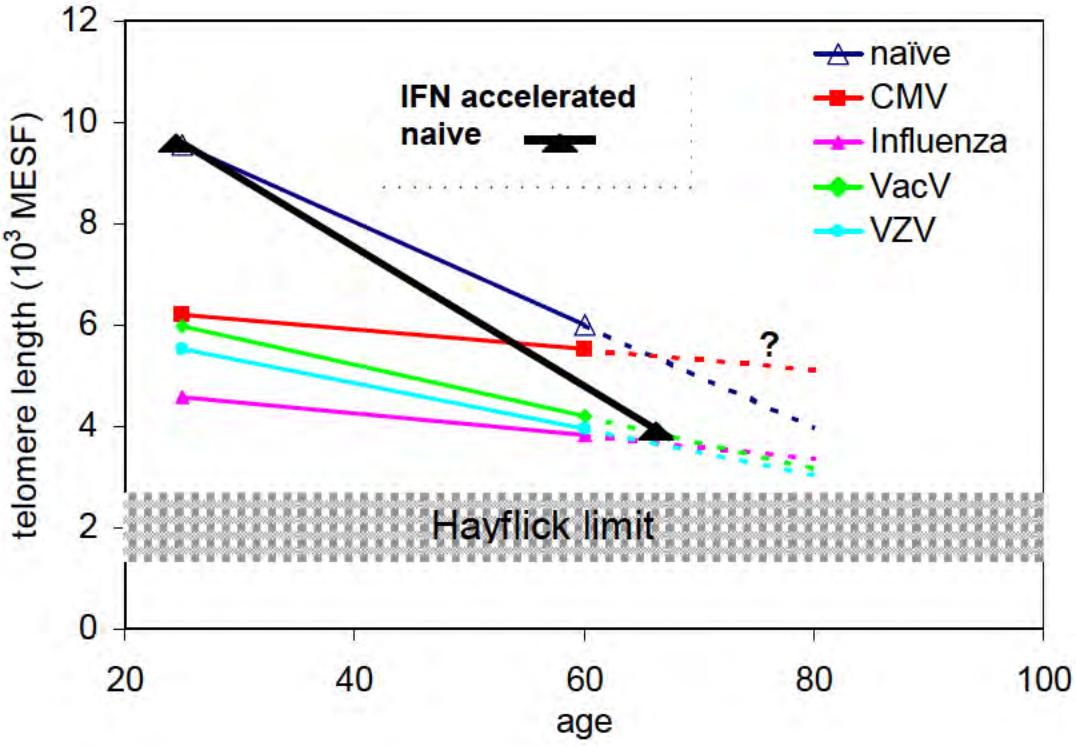


**Figure 6.3 Consequences of sustained IFN-induced lymphopenia -- accelerated telomere loss in the naïve T cell compartment**

Accelerated telomere loss in the naïve T cell compartment due to IFN treatment (dark black line) leads to earlier impacts on the ability to maintain T cell responses to recurring infection due to a diminished proliferative potential. The accelerated onset of T cell immunosenescence across naïve and memory T cell compartments compromises virus-specific T cell maintenance at an earlier age, and provides an explanation for the increased mortality seen in the HALT-C long-term IFN therapy patients.

**M. Conclusions**

These studies of T cell telomere lengths extend prevailing models of the formation and maintenance of T cell memory with insights on long telomere T cells, and open up novel approaches for further study. In the process of this thesis research, several of the initial hypotheses were ultimately supported by the data (e.g. VACV-specific TLs were longer than IAV-specific TL and IFN accelerated TL loss) and others refuted (CMV-specific TL were longer than IAV-specific TL). The complexity of this picture of T cell telomere length dynamics against the background of age-related decline in TL suggests that re-vaccinations such as for VZV should be undertaken before the onset of naïve T cell senescence for greatest efficacy. Further it suggests that efforts to slow or prevent excessive TL loss in the naïve T cell compartment may be vital for healthy longevity. Importantly, the telomere length assay methods used here may enable future studies using T cell telomere dynamics as a "reporter" for understanding the kinetics of viral reactivation from latency, which are not easily quantifiable in otherwise healthy individuals.

# CHAPTER VII

## REFERENCES


1. Doherty, P. C., D. J. Topham, R. A. Tripp, R. D. Cardin, J. W. Brooks, and P. G. Stevenson. 1997. Effector CD4+ and CD8+ T-cell mechanisms in the control of respiratory virus infections. *Immunol Rev* 159:105-117.

2. Taylor, J. J., and M. K. Jenkins. 2011. CD4+ memory T cell survival. *Curr Opin Immunol* 23:319-323.

3. Cui, W., and S. M. Kaech. 2010. Generation of effector CD8+ T cells and their conversion to memory T cells. *Immunol Rev* 236:151-166.

4. Wakim, L. M., and M. J. Bevan. 2010. From the thymus to longevity in the periphery. *Curr Opin Immunol* 22:274-278.

5. Aspinall, R., and D. Andrew. 2000. Thymic involution in aging. *J Clin Immunol* 20:250-256.

6. Davis, M. M., and P. J. Bjorkman. 1988. T-cell antigen receptor genes and T-cell recognition. *Nature* 334:395-402.

7. Mackay, C. R. 1992. Migration pathways and immunologic memory among T lymphocytes. *Semin Immunol* 4:51-58.

8. Reiner, S. L. 2005. Epigenetic control in the immune response. *Hum Mol Genet* 14 Spec No 1:R41-46.

9. Boyman, O., S. Letourneau, C. Krieg, and J. Sprent. 2009. Homeostatic proliferation and survival of naive and memory T cells. *Eur J Immunol* 39:2088-2094.

10. Macallan, D. C., B. Asquith, A. J. Irvine, D. L. Wallace, A. Worth, H. Ghattas, Y. Zhang, G. E. Griffin, D. F. Tough, and P. C. Beverley. 2003. Measurement and modeling of human T cell kinetics. *Eur J Immunol* 33:2316-2326.

11. Gattinoni, L., E. Lugli, Y. Ji, Z. Pos, C. M. Paulos, M. F. Quigley, J. R. Almeida, E. Gostick, Z. Yu, C. Carpenito, E. Wang, D. C. Douek, D. A. Price, C. H. June, F. M. Marincola, M. Roederer, and N. P. Restifo. 2011. A human memory T cell

subset with stem cell-like properties. *Nat Med* Advance Online Publication, available online Sep 18, 2011.

12. Bird, J. J., D. R. Brown, A. C. Mullen, N. H. Moskowitz, M. A. Mahowald, J. R. Sider, T. F. Gajewski, C. R. Wang, and S. L. Reiner. 1998. Helper T cell differentiation is controlled by the cell cycle. *Immunity* 9:229-237.

13. Deenick, E. K., C. S. Ma, R. Brink, and S. G. Tangye. 2011. Regulation of T follicular helper cell formation and function by antigen presenting cells. *Curr Opin Immunol* 23:111-118.

14. Matloubian, M., R. J. Concepcion, and R. Ahmed. 1994. CD4+ T cells are required to sustain CD8+ cytotoxic T-cell responses during chronic viral infection. *J Virol* 68:8056-8063.

15. Marzo, A. L., B. F. Kinnear, R. A. Lake, J. J. Frelinger, E. J. Collins, B. W. Robinson, and B. Scott. 2000. Tumor-specific CD4+ T cells have a major "post-licensing" role in CTL mediated anti-tumor immunity. *J Immunol* 165:6047-6055.

16. King, C., S. G. Tangye, and C. R. Mackay. 2008. T follicular helper (TFH) cells in normal and dysregulated immune responses. *Annu Rev Immunol* 26:741-766.

17. Sallusto, F., D. Lenig, R. Forster, M. Lipp, and A. Lanzavecchia. 1999. Two subsets of memory T lymphocytes with distinct homing potentials and effector functions. *Nature* 401:708-712.

18. Hamann, D., P. A. Baars, M. H. Rep, B. Hooibrink, S. R. Kerkhof-Garde, M. R. Klein, and R. A. van Lier. 1997. Phenotypic and functional separation of memory and effector human CD8+ T cells. *J Exp Med* 186:1407-1418.

19. Bouneaud, C., Z. Garcia, P. Kourilsky, and C. Pannetier. 2005. Lineage relationships, homeostasis, and recall capacities of central- and effector-memory CD8 T cells in vivo. *J Exp Med* 201:579-590.

20. Kanegane, H., Y. Kasahara, Y. Niida, A. Yachie, S. Sughii, K. Takatsu, N. Taniguchi, and T. Miyawaki. 1996. Expression of L-selectin (CD62L) discriminates Th1- and Th2-like cytokine-producing memory CD4+ T cells. *Immunology* 87:186-190.

21. Gamadia, L. E., R. J. Rentenaar, R. A. van Lier, and I. J. ten Berge. 2004. Properties of CD4(+) T cells in human cytomegalovirus infection. *Hum Immunol* 65:486-492.

22. Richards, H., M. P. Longhi, K. Wright, A. Gallimore, and A. Ager. 2008. CD62L (L-selectin) down-regulation does not affect memory T cell distribution but failure to shed compromises anti-viral immunity. *J Immunol* 180:198-206.

23. Yang, S., F. Liu, Q. J. Wang, S. A. Rosenberg, and R. A. Morgan. 2011. The shedding of CD62L (L-selectin) regulates the acquisition of lytic activity in human tumor reactive T lymphocytes. *PLoS One* 6:e22560.

24. Kagamu, H., and S. Shu. 1998. Purification of L-selectin(low) cells promotes the generation of highly potent CD4 antitumor effector T lymphocytes. *J Immunol* 160:3444-3452.

25. Obar, J. J., and L. Lefrancois. 2010. Early signals during CD8 T cell priming regulate the generation of central memory cells. *J Immunol* 185:263-272.

26. Ahmed, R., M. J. Bevan, S. L. Reiner, and D. T. Fearon. 2009. The precursors of memory: models and controversies. *Nat Rev Immunol* 9:662-668.

27. Gerlach, C., J. W. van Heijst, E. Swart, D. Sie, N. Armstrong, R. M. Kerkhoven, D. Zehn, M. J. Bevan, K. Schepers, and T. N. Schumacher. 2010. One naive T cell, multiple fates in CD8+ T cell differentiation. *J Exp Med* 207:1235-1246.

28. Obar, J. J., and L. Lefrancois. 2010. Early events governing memory CD8+ T-cell differentiation. *Int Immunol* 22:619-625.

29. Zhu, J., H. Yamane, and W. E. Paul. 2010. Differentiation of effector CD4 T cell populations (*). *Annu Rev Immunol* 28:445-489.

30. Tomiyama, H., T. Matsuda, and M. Takiguchi. 2002. Differentiation of human CD8(+) T cells from a memory to memory/effector phenotype. *J Immunol* 168:5538-5550.

31. Le Priol, Y., D. Puthier, C. Lecureuil, C. Combadiere, P. Debre, C. Nguyen, and B. Combadiere. 2006. High cytotoxic and specific migratory potencies of senescent CD8+ CD57+ cells in HIV-infected and uninfected individuals. *J Immunol* 177:5145-5154.

32. MacLennan, I. C., Y. J. Liu, and G. D. Johnson. 1992. Maturation and dispersal of B-cell clones during T cell-dependent antibody responses. *Immunol Rev* 126:143-161.

33. Sprent, J., and D. F. Tough. 2001. T cell death and memory. *Science* 293:245-248.

34. Welsh, R. M., J. W. Che, M. A. Brehm, and L. K. Selin. 2010. Heterologous immunity between viruses. *Immunol Rev* 235:244-266.

35. Vezys, V., A. Yates, K. A. Casey, G. Lanier, R. Ahmed, R. Antia, and D. Masopust. 2009. Memory CD8 T-cell compartment grows in size with immunological experience. *Nature* 457:196-199.

36. Boyman, O., J. F. Purton, C. D. Surh, and J. Sprent. 2007. Cytokines and T-cell homeostasis. *Curr Opin Immunol* 19:320-326.

37. Fry, T. J., and C. L. Mackall. 2005. The many faces of IL-7: from lymphopoiesis to peripheral T cell maintenance. *J Immunol* 174:6571-6576.

38. Kastenmuller, W., G. Gasteiger, N. Subramanian, T. Sparwasser, D. H. Busch, Y. Belkaid, I. Drexler, and R. N. Germain. 2010. Regulatory T Cells Selectively Control CD8+ T Cell Effector Pool Size via IL-2 Restriction. *J Immunol* 187:3186-3197.

39. Malek, T. R., A. Yu, L. Zhu, T. Matsutani, D. Adeegbe, and A. L. Bayer. 2008. IL-2 family of cytokines in T regulatory cell development and homeostasis. *J Clin Immunol* 28:635-639.

40. Virgin, H. W., E. J. Wherry, and R. Ahmed. 2009. Redefining chronic viral infection. *Cell* 138:30-50.

41. Nikolich-Zugich, J. 2008. Ageing and life-long maintenance of T-cell subsets in the face of latent persistent infections. *Nat Rev Immunol* 8:512-522.

42. Ferguson, N. M., A. P. Galvani, and R. M. Bush. 2003. Ecological and immunological determinants of influenza evolution. *Nature* 422:428-433.

43. Lofgren, E., N. H. Fefferman, Y. N. Naumov, J. Gorski, and E. N. Naumova. 2007. Influenza seasonality: underlying causes and modeling theories. *J Virol* 81:5429-5436.

44. Crotty, S., P. Felgner, H. Davies, J. Glidewell, L. Villarreal, and R. Ahmed. 2003. Cutting edge: long-term B cell memory in humans after smallpox vaccination. *J Immunol* 171:4969-4973.

45. Combadiere, B., A. Boissonnas, G. Carcelain, E. Lefranc, A. Samri, F. Bricaire, P. Debre, and B. Autran. 2004. Distinct time effects of vaccination on long-term proliferative and IFN-gamma-producing T cell memory to smallpox in humans. *J Exp Med* 199:1585-1593.

46. Committee on Smallpox Vaccination Program Implementation, B. A., Anason AP, Stratton K, Strom B, editors. 2005. The smallpox vaccination program: public health in an age of terrorism. *National Academies Press.* Available at: http://www.nap.edu.

47. Hammarlund, E., M. W. Lewis, S. G. Hansen, L. I. Strelow, J. A. Nelson, G. J. Sexton, J. M. Hanifin, and M. K. Slifka. 2003. Duration of antiviral immunity after smallpox vaccination. *Nat Med* 9:1131-1137.

48. Douek, D. C. 2003. Disrupting T-cell homeostasis: how HIV-1 infection causes disease. *AIDS Rev* 5:172-177.

49. McCune, J. M. 2001. The dynamics of CD4+ T-cell depletion in HIV disease. *Nature* 410:974-979.

50. Gremion, C., and A. Cerny. 2005. Hepatitis C virus and the immune system: a concise review. *Rev Med Virol* 15:235-268.

51. Neumann-Haefelin, C., H. E. Blum, F. V. Chisari, and R. Thimme. 2005. T cell response in hepatitis C virus infection. *J Clin Virol* 32:75-85.

52. Pawlotsky, J. M. 2004. Pathophysiology of hepatitis C virus infection and related liver disease. *Trends Microbiol* 12:96-102.

53. Liang, T. J. 2009. Hepatitis B: the virus and disease. *Hepatology* 49:S13-21.

54. Jafri, S. M., and A. S. Lok. 2010. Antiviral therapy for chronic hepatitis B. *Clin Liver Dis* 14:425-438.

55. Romeo, R., M. Rumi, and M. Colombo. 1995. Alpha interferon treatment of chronic hepatitis C. *Biomed Pharmacother* 49:111-115.

56. Sandberg, J. K., K. Falconer, and V. D. Gonzalez. 2010. Chronic immune activation in the T cell compartment of HCV/HIV-1 co-infected patients. *Virulence* 1:177-179.

57. Chang, J. J., and M. Altfeld. 2010. Innate immune activation in primary HIV-1 infection. *J Infect Dis* 202 Suppl 2:S297-301.

58. Catalfamo, M., C. Wilhelm, L. Tcheung, M. Proschan, T. Friesen, J. H. Park, J. Adelsberger, M. Baseler, F. Maldarelli, R. Davey, G. Roby, C. Rehm, and C. Lane. 2011. CD4 and CD8 T cell immune activation during chronic HIV infection: roles of homeostasis, HIV, type I IFN, and IL-7. *J Immunol* 186:2106-2116.

59. Boasso, A., and G. M. Shearer. 2008. Chronic innate immune activation as a cause of HIV-1 immunopathogenesis. *Clin Immunol* 126:235-242.

60. Marshall, H. D., S. L. Urban, and R. M. Welsh. 2011. Virus-induced transient immune suppression and the inhibition of T cell proliferation by type I interferon. *J Virol* 85:5929-5939.

61. McNally, J. M., C. C. Zarozinski, M. Y. Lin, M. A. Brehm, H. D. Chen, and R. M. Welsh. 2001. Attrition of bystander CD8 T cells during virus-induced T-cell and interferon responses. *J Virol* 75:5965-5976.

62. Kim, P. S., and R. Ahmed. 2010. Features of responding T cells in cancer and chronic infection. *Curr Opin Immunol* 22:223-230.

63. Knipe, D. M. 1989. The role of viral and cellular nuclear proteins in herpes simplex virus replication. *Adv Virus Res* 37:85-123.

64. Plafker, S. M., and W. Gibson. 1998. Cytomegalovirus assembly protein precursor and proteinase precursor contain two nuclear localization signals that mediate their own nuclear translocation and that of the major capsid protein. *J Virol* 72:7722-7732.

65. Deutsch, M. J., E. Ott, P. Papior, and A. Schepers. 2010. The latent origin of replication of Epstein-Barr virus directs viral genomes to active regions of the nucleus. *J Virol* 84:2533-2546.

66. Koch, S., A. Larbi, D. Ozcelik, R. Solana, C. Gouttefangeas, S. Attig, A. Wikby, J. Strindhall, C. Franceschi, and G. Pawelec. 2007. Cytomegalovirus infection: a driving force in human T cell immunosenescence. *Ann N Y Acad Sci* 1114:23-35.

67. Sinclair, J. 2008. Human cytomegalovirus: Latency and reactivation in the myeloid lineage. *J Clin Virol* 41:180-185.

68. Kennedy, P. G., and R. J. Cohrs. 2010. Varicella-zoster virus human ganglionic latency: a current summary. *J Neurovirol* 16:411-418.

69. Gershon, A. A., M. D. Gershon, J. Breuer, M. J. Levin, A. L. Oaklander, and P. D. Griffiths. 2010. Advances in the understanding of the pathogenesis and epidemiology of herpes zoster. *J Clin Virol* 48 Suppl 1:S2-7.

70. Asanuma, H., M. Sharp, H. T. Maecker, V. C. Maino, and A. M. Arvin. 2000. Frequencies of memory T cells specific for varicella-zoster virus, herpes simplex

virus, and cytomegalovirus by intracellular detection of cytokine expression. *J Infect Dis* 181:859-866.

71. Vasto, S., G. Colonna-Romano, A. Larbi, A. Wikby, C. Caruso, and G. Pawelec. 2007. Role of persistent CMV infection in configuring T cell immunity in the elderly. *Immun Ageing* 4:2.

72. Misri, S., S. Pandita, R. Kumar, and T. K. Pandita. 2008. Telomeres, histone code, and DNA damage response. *Cytogenet Genome Res* 122:297-307.

73. Allen, C., A. K. Ashley, R. Hromas, and J. A. Nickoloff. 2011. More forks on the road to replication stress recovery. *J Mol Cell Biol* 3:4-12.

74. de Lange, T. 2005. Shelterin: the protein complex that shapes and safeguards human telomeres. *Genes Dev* 19:2100-2110.

75. Denchi, E. L., and T. de Lange. 2007. Protection of telomeres through independent control of ATM and ATR by TRF2 and POT1. *Nature* 448:1068-1071.

76. Hug, N., and J. Lingner. 2006. Telomere length homeostasis. *Chromosoma* 115:413-425.

77. Harley, C. B., A. B. Futcher, and C. W. Greider. 1990. Telomeres shorten during ageing of human fibroblasts. *Nature* 345:458-460.

78. Levy, M. Z., R. C. Allsopp, A. B. Futcher, C. W. Greider, and C. B. Harley. 1992. Telomere end-replication problem and cell aging. *J Mol Biol* 225:951-960.

79. Weng, N. P., B. L. Levine, C. H. June, and R. J. Hodes. 1996. Regulated expression of telomerase activity in human T lymphocyte development and activation. *J Exp Med* 183:2471-2479.

80. Effros, R. B. 2004. Impact of the Hayflick Limit on T cell responses to infection: lessons from aging and HIV disease. *Mech Ageing Dev* 125:103-106.

81. Hodes, R. J., K. S. Hathcock, and N. P. Weng. 2002. Telomeres in T and B cells. *Nat Rev Immunol* 2:699-706.

82. Reed, J. R., M. Vukmanovic-Stejic, J. M. Fletcher, M. V. Soares, J. E. Cook, C. H. Orteu, S. E. Jackson, K. E. Birch, G. R. Foster, M. Salmon, P. C. Beverley, M. H. Rustin, and A. N. Akbar. 2004. Telomere erosion in memory T cells induced by telomerase inhibition at the site of antigenic challenge in vivo. *J Exp Med* 199:1433-1443.

83. Fritsch, R. D., X. Shen, G. P. Sims, K. S. Hathcock, R. J. Hodes, and P. E. Lipsky. 2005. Stepwise differentiation of CD4 memory T cells defined by expression of CCR7 and CD27. *J Immunol* 175:6489-6497.

84. Hathcock, K. S., Y. Jeffrey Chiang, and R. J. Hodes. 2005. In vivo regulation of telomerase activity and telomere length. *Immunol Rev* 205:104-113.

85. Akbar, A. N., and M. Vukmanovic-Stejic. 2007. Telomerase in T lymphocytes: use it and lose it? *J Immunol* 178:6689-6694.

86. Xu, D., S. Erickson, M. Szeps, A. Gruber, O. Sangfelt, S. Einhorn, P. Pisa, and D. Grander. 2000. Interferon alpha down-regulates telomerase reverse transcriptase and telomerase activity in human malignant and nonmalignant hematopoietic cells. *Blood* 96:4313-4318.

87. Hirsch, R. L., and K. P. Johnson. 1986. The effects of long-term administration of recombinant alpha-2 interferon on lymphocyte subsets, proliferation, and suppressor cell function in multiple sclerosis. *J Interferon Res* 6:171-177.

88. Weng, N. P., B. L. Levine, C. H. June, and R. J. Hodes. 1995. Human naive and memory T lymphocytes differ in telomeric length and replicative potential. *Proc Natl Acad Sci U S A* 92:11091-11094.

89. Van Ziffle, J. A., G. M. Baerlocher, and P. M. Lansdorp. 2003. Telomere length in subpopulations of human hematopoietic cells. *Stem Cells* 21:654-660.

90. Vrisekoop, N., I. den Braber, A. B. de Boer, A. F. Ruiter, M. T. Ackermans, S. N. van der Crabben, E. H. Schrijver, G. Spierenburg, H. P. Sauerwein, M. D. Hazenberg, R. J. de Boer, F. Miedema, J. A. Borghans, and K. Tesselaar. 2008. Sparse production but preferential incorporation of recently produced naive T cells in the human peripheral pool. *Proc Natl Acad Sci U S A* 105:6115-6120.

91. Wallace, D. L., Y. Zhang, H. Ghattas, A. Worth, A. Irvine, A. R. Bennett, G. E. Griffin, P. C. Beverley, D. F. Tough, and D. C. Macallan. 2004. Direct measurement of T cell subset kinetics in vivo in elderly men and women. *J Immunol* 173:1787-1794.

92. Valenzuela, H. F., and R. B. Effros. 2002. Divergent telomerase and CD28 expression patterns in human CD4 and CD8 T cells following repeated encounters with the same antigenic stimulus. *Clin Immunol* 105:117-125.

93. Hammarlund, E., M. W. Lewis, J. M. Hanifin, M. Mori, C. W. Koudelka, and M. K. Slifka. 2010. Antiviral immunity following smallpox virus infection: a case-control study. *J Virol* 84:12754-12760.

94. Amara, R. R., P. Nigam, S. Sharma, J. Liu, and V. Bostik. 2004. Long-lived poxvirus immunity, robust CD4 help, and better persistence of CD4 than CD8 T cells. *J Virol* 78:3811-3816.

95. Son, N. H., S. Murray, J. Yanovski, R. J. Hodes, and N. Weng. 2000. Lineage-specific telomere shortening and unaltered capacity for telomerase expression in human T and B lymphocytes with age. *J Immunol* 165:1191-1196.

96. Zhou, J., X. Shen, J. Huang, R. J. Hodes, S. A. Rosenberg, and P. F. Robbins. 2005. Telomere length of transferred lymphocytes correlates with in vivo persistence and tumor regression in melanoma patients receiving cell transfer therapy. *J Immunol* 175:7046-7052.

97. Tran, K. Q., J. Zhou, K. H. Durflinger, M. M. Langhan, T. E. Shelton, J. R. Wunderlich, P. F. Robbins, S. A. Rosenberg, and M. E. Dudley. 2008. Minimally cultured tumor-infiltrating lymphocytes display optimal characteristics for adoptive cell therapy. *J Immunother* 31:742-751.

98. D'Souza, M., A. P. Fontenot, D. G. Mack, C. Lozupone, S. Dillon, A. Meditz, C. C. Wilson, E. Connick, and B. E. Palmer. 2007. Programmed death 1 expression on HIV-specific CD4+ T cells is driven by viral replication and associated with T cell dysfunction. *J Immunol* 179:1979-1987.

99. Zhang, J. Y., Z. Zhang, X. Wang, J. L. Fu, J. Yao, Y. Jiao, L. Chen, H. Zhang, J. Wei, L. Jin, M. Shi, G. F. Gao, H. Wu, and F. S. Wang. 2007. PD-1 up-regulation is correlated with HIV-specific memory CD8+ T-cell exhaustion in typical progressors but not in long-term nonprogressors. *Blood* 109:4671-4678.

100. Freeman, G. J., E. J. Wherry, R. Ahmed, and A. H. Sharpe. 2006. Reinvigorating exhausted HIV-specific T cells via PD-1-PD-1 ligand blockade. *J Exp Med* 203:2223-2227.

101. Day, C. L., D. E. Kaufmann, P. Kiepiela, J. A. Brown, E. S. Moodley, S. Reddy, E. W. Mackey, J. D. Miller, A. J. Leslie, C. DePierres, Z. Mncube, J. Duraiswamy, B. Zhu, Q. Eichbaum, M. Altfeld, E. J. Wherry, H. M. Coovadia, P. J. Goulder, P. Klenerman, R. Ahmed, G. J. Freeman, and B. D. Walker. 2006. PD-1 expression on HIV-specific T cells is associated with T-cell exhaustion and disease progression. *Nature* 443:350-354.

102. Trautmann, L., L. Janbazian, N. Chomont, E. A. Said, S. Gimmig, B. Bessette, M. R. Boulassel, E. Delwart, H. Sepulveda, R. S. Balderas, J. P. Routy, E. K. Haddad, and R. P. Sekaly. 2006. Upregulation of PD-1 expression on HIV-specific CD8+ T cells leads to reversible immune dysfunction. *Nat Med* 12:1198-1202.

103. Ejrnaes, M., C. M. Filippi, M. M. Martinic, E. M. Ling, L. M. Togher, S. Crotty, and M. G. von Herrath. 2006. Resolution of a chronic viral infection after interleukin-10 receptor blockade. *J Exp Med* 203:2461-2472.

104. Roth, A., G. M. Baerlocher, M. Schertzer, E. Chavez, U. Duhrsen, and P. M. Lansdorp. 2005. Telomere loss, senescence, and genetic instability in CD4+ T lymphocytes overexpressing hTERT. *Blood* 106:43-50.

105. Dagarag, M., T. Evazyan, N. Rao, and R. B. Effros. 2004. Genetic manipulation of telomerase in HIV-specific CD8+ T cells: enhanced antiviral functions accompany the increased proliferative potential and telomere length stabilization. *J Immunol* 173:6303-6311.

106. Andersen, H., E. V. Barsov, M. T. Trivett, C. M. Trubey, L. D. Giavedoni, J. D. Lifson, D. E. Ott, and C. Ohlen. 2007. Transduction with human telomerase reverse transcriptase immortalizes a rhesus macaque CD8+ T cell clone with maintenance of surface marker phenotype and function. *AIDS Res Hum Retroviruses* 23:456-465.

107. Fletcher, J. M., M. Vukmanovic-Stejic, P. J. Dunne, K. E. Birch, J. E. Cook, S. E. Jackson, M. Salmon, M. H. Rustin, and A. N. Akbar. 2005. Cytomegalovirus-specific CD4+ T cells in healthy carriers are continuously driven to replicative exhaustion. *J Immunol* 175:8218-8225.

108. Khan, N., N. Shariff, M. Cobbold, R. Bruton, J. A. Ainsworth, A. J. Sinclair, L. Nayak, and P. A. Moss. 2002. Cytomegalovirus seropositivity drives the CD8 T cell repertoire toward greater clonality in healthy elderly individuals. *J Immunol* 169:1984-1992.

109. Aubert, G., M. Hills, and P. M. Lansdorp. 2011. Telomere length measurement-Caveats and a critical assessment of the available technologies and tools. *Mutat Res*.

110. Rufer, N., W. Dragowska, G. Thornbury, E. Roosnek, and P. M. Lansdorp. 1998. Telomere length dynamics in human lymphocyte subpopulations measured by flow cytometry. *Nat Biotechnol* 16:743-747.

111. Dunne, P. J., J. M. Faint, N. H. Gudgeon, J. M. Fletcher, F. J. Plunkett, M. V. Soares, A. D. Hislop, N. E. Annels, A. B. Rickinson, M. Salmon, and A. N. Akbar. 2002. Epstein-Barr virus-specific CD8(+) T cells that re-express CD45RA are apoptosis-resistant memory cells that retain replicative potential. *Blood* 100:933-940.

112. van Baarle, D., N. M. Nanlohy, S. Otto, F. J. Plunkett, J. M. Fletcher, and A. N. Akbar. 2008. Progressive telomere shortening of Epstein-Barr virus-specific memory T cells during HIV infection: contributor to exhaustion? *J Infect Dis* 198:1353-1357.

113. Lee, W. M., J. L. Dienstag, K. L. Lindsay, A. S. Lok, H. L. Bonkovsky, M. L. Shiffman, G. T. Everson, A. M. Di Bisceglie, T. R. Morgan, M. G. Ghany, C. Morishima, E. C. Wright, and J. E. Everhart. 2004. Evolution of the HALT-C Trial: pegylated interferon as maintenance therapy for chronic hepatitis C in previous interferon nonresponders. *Control Clin Trials* 25:472-492.

114. Rothman, A. L., C. Morishima, H. L. Bonkovsky, S. J. Polyak, R. Ray, A. M. Di Bisceglie, K. L. Lindsay, P. F. Malet, M. Chang, D. R. Gretch, D. G. Sullivan, A. K. Bhan, E. C. Wright, and M. J. Koziel. 2005. Associations among clinical, immunological, and viral quasispecies measurements in advanced chronic hepatitis C. *Hepatology* 41:617-625.

115. Delgado-Borrego, A., S. H. Jordan, B. Negre, D. Healey, W. Lin, Y. Kamegaya, M. Christofi, D. A. Ludwig, A. S. Lok, and R. T. Chung. 2010. Reduction of insulin resistance with effective clearance of hepatitis C infection: results from the HALT-C trial. *Clin Gastroenterol Hepatol* 8:458-462.

116. Everhart, J. E., E. C. Wright, Z. D. Goodman, J. L. Dienstag, J. C. Hoefs, D. E. Kleiner, M. G. Ghany, A. S. Mills, S. R. Nash, S. Govindarajan, T. E. Rogers, J. K. Greenson, E. M. Brunt, H. L. Bonkovsky, C. Morishima, and H. J. Litman. 2010. Prognostic value of Ishak fibrosis stage: Findings from the hepatitis C antiviral long-term treatment against cirrhosis trial. *Hepatology* 51:585-594.

117. Van Herreweghe, E., S. Egloff, I. Goiffon, B. E. Jady, C. Froment, B. Monsarrat, and T. Kiss. 2007. Dynamic remodelling of human 7SK snRNP controls the nuclear level of active P-TEFb. *Embo J* 26:3570-3580.

118. Wassarman, D. A., and J. A. Steitz. 1991. Structural analyses of the 7SK ribonucleoprotein (RNP), the most abundant human small RNP of unknown function. *Mol Cell Biol* 11:3432-3445.

119. Baerlocher, G. M., I. Vulto, G. de Jong, and P. M. Lansdorp. 2006. Flow cytometry and FISH to measure the average length of telomeres (flow FISH). *Nat Protoc* 1:2365-2376.

120. Yehezkel, S., Y. Segev, E. Viegas-Pequignot, K. Skorecki, and S. Selig. 2008. Hypomethylation of subtelomeric regions in ICF syndrome is associated with abnormally short telomeres and enhanced transcription from telomeric regions. *Hum Mol Genet* 17:2776-2789.

121. Goldman, F. D., G. Aubert, A. J. Klingelhutz, M. Hills, S. R. Cooper, W. S. Hamilton, A. J. Schlueter, K. Lambie, C. J. Eaves, and P. M. Lansdorp. 2008. Characterization of primitive hematopoietic cells from patients with dyskeratosis congenita. *Blood* 111:4523-4531.

122. Alter, B. P., G. M. Baerlocher, S. A. Savage, S. J. Chanock, B. B. Weksler, J. P. Willner, J. A. Peters, N. Giri, and P. M. Lansdorp. 2007. Very short telomere length by flow fluorescence in situ hybridization identifies patients with dyskeratosis congenita. *Blood* 110:1439-1447.

123. Baerlocher, G. M., and P. M. Lansdorp. 2003. Telomere length measurements in leukocyte subsets by automated multicolor flow-FISH. *Cytometry A* 55:1-6.

124. Azzalin, C. M., P. Reichenbach, L. Khoriauli, E. Giulotto, and J. Lingner. 2007. Telomeric repeat containing RNA and RNA surveillance factors at mammalian chromosome ends. *Science* 318:798-801.

125. Schoeftner, S., and M. A. Blasco. 2008. Developmentally regulated transcription of mammalian telomeres by DNA-dependent RNA polymerase II. *Nat Cell Biol* 10:228-236.

126. Xu, Y., K. Kaminaga, and M. Komiyama. 2008. Human telomeric RNA in G-quadruplex structure. *Nucleic Acids Symp Ser (Oxf)*:175-176.

127. Martadinata, H., and A. T. Phan. 2009. Structure of propeller-type parallel-stranded RNA G-quadruplexes, formed by human telomeric RNA sequences in K+ solution. *J Am Chem Soc* 131:2570-2578.

128. Brenchley, J. M., N. J. Karandikar, M. R. Betts, D. R. Ambrozak, B. J. Hill, L. E. Crotty, J. P. Casazza, J. Kuruppu, S. A. Migueles, M. Connors, M. Roederer, D. C. Douek, and R. A. Koup. 2003. Expression of CD57 defines replicative senescence and antigen-induced apoptotic death of CD8+ T cells. *Blood* 101:2711-2720.

129. Koch, S., A. Larbi, E. Derhovanessian, D. Ozcelik, E. Naumova, and G. Pawelec. 2008. Multiparameter flow cytometric analysis of CD4 and CD8 T cell subsets in young and old people. *Immun Ageing* 5:6.

130. Morley, J. K., F. M. Batliwalla, R. Hingorani, and P. K. Gregersen. 1995. Oligoclonal CD8+ T cells are preferentially expanded in the CD57+ subset. *J Immunol* 154:6182-6190.

131. Pickett, H. A., J. D. Henson, A. Y. Au, A. A. Neumann, and R. R. Reddel. 2011. Normal mammalian cells negatively regulate telomere length by telomere trimming. *Hum Mol Genet* Advance Online Publication, available Sep 8, 2011.

132. Hanna-Wakim, R., L. L. Yasukawa, P. Sung, A. M. Arvin, and H. A. Gans. 2008. Immune responses to mumps vaccine in adults who were vaccinated in childhood. *J Infect Dis* 197:1669-1675.

133. Miller, J. D., R. G. van der Most, R. S. Akondy, J. T. Glidewell, S. Albott, D. Masopust, K. Murali-Krishna, P. L. Mahar, S. Edupuganti, S. Lalor, S. Germon, C. Del Rio, M. J. Mulligan, S. I. Staprans, J. D. Altman, M. B. Feinberg, and R. Ahmed. 2008. Human effector and memory CD8+ T cell responses to smallpox and yellow fever vaccines. *Immunity* 28:710-722.

134. Hauschild, A., H. Gogas, A. Tarhini, M. R. Middleton, A. Testori, B. Dreno, and J. M. Kirkwood. 2008. Practical guidelines for the management of interferon-alpha-2b side effects in patients receiving adjuvant treatment for melanoma: expert opinion. *Cancer* 112:982-994.

135. Lam, S., S. Wang, and M. Gottesman. 2008. Interferon-beta1b for the treatment of multiple sclerosis. *Expert Opin Drug Metab Toxicol* 4:1111-1117.

136. Aubert, G., and P. M. Lansdorp. 2008. Telomeres and aging. *Physiol Rev* 88:557-579.

137. Manfras, B. J., H. Weidenbach, K. H. Beckh, P. Kern, P. Moller, G. Adler, T. Mertens, and B. O. Boehm. 2004. Oligoclonal CD8+ T-cell expansion in patients with chronic hepatitis C is associated with liver pathology and poor response to interferon-alpha therapy. *J Clin Immunol* 24:258-271.

138. Kaser, A., S. Nagata, and H. Tilg. 1999. Interferon alpha augments activation-induced T cell death by upregulation of Fas (CD95/APO-1) and Fas ligand expression. *Cytokine* 11:736-743.

139. Jiang, J., D. Gross, S. Nogusa, P. Elbaum, and D. M. Murasko. 2005. Depletion of T cells by type I interferon: differences between young and aged mice. *J Immunol* 175:1820-1826.

140. Baerlocher, G. M., and P. M. Lansdorp. 2004. Telomere length measurements using fluorescence in situ hybridization and flow cytometry. *Methods Cell Biol* 75:719-750.

141. Ehrlenbach, S., P. Willeit, S. Kiechl, J. Willeit, M. Reindl, K. Schanda, F. Kronenberg, and A. Brandstatter. 2009. Influences on the reduction of relative

telomere length over 10 years in the population-based Bruneck Study: introduction of a well-controlled high-throughput assay. *Int J Epidemiol* 38:1725-1734.

142. Ahlers, J. D., and I. M. Belyakov. 2010. Memories that last forever: strategies for optimizing vaccine T-cell memory. *Blood* 115:1678-1689.

143. De Boer, R. J., and A. J. Noest. 1998. T cell renewal rates, telomerase, and telomere length shortening. *J Immunol* 160:5832-5837.

144. Hotamisligil, G. S., and E. Erbay. 2008. Nutrient sensing and inflammation in metabolic diseases. *Nat Rev Immunol* 8:923-934.

145. Dixit, V. D. 2008. Adipose-immune interactions during obesity and caloric restriction: reciprocal mechanisms regulating immunity and health span. *J Leukoc Biol* 84:882-892.

146. Gilley, D., B. S. Herbert, N. Huda, H. Tanaka, and T. Reed. 2008. Factors impacting human telomere homeostasis and age-related disease. *Mech Ageing Dev* 129:27-34.

147. Farzaneh-Far, R., J. Lin, E. Epel, K. Lapham, E. Blackburn, and M. A. Whooley. 2009. Telomere length trajectory and its determinants in persons with coronary artery disease: longitudinal findings from the heart and soul study. *PLoS One* 5:e8612.

148. Huzen, J., R. A. de Boer, D. J. van Veldhuisen, W. H. van Gilst, and P. van der Harst. 2010. The emerging role of telomere biology in cardiovascular disease. *Front Biosci* 15:35-45.

149. Zee, R. Y., S. E. Michaud, S. Germer, and P. M. Ridker. 2009. Association of shorter mean telomere length with risk of incident myocardial infarction: a prospective, nested case-control approach. *Clin Chim Acta* 403:139-141.

150. Jamal, M. M., A. Soni, P. G. Quinn, D. E. Wheeler, S. Arora, and D. E. Johnston. 1999. Clinical features of hepatitis C-infected patients with persistently normal alanine transaminase levels in the Southwestern United States. *Hepatology* 30:1307-1311.

151. Tillmann, H. L., M. P. Manns, and K. L. Rudolph. 2005. Merging models of hepatitis C virus pathogenesis. *Semin Liver Dis* 25:84-92.

152. Ferri, S., C. Lalanne, G. Lanzoni, M. Bassi, S. Asioli, V. Cipriano, G. Pappas, P. Muratori, M. Lenzi, and L. Muratori. 2011. Redistribution of regulatory T-cells across the evolving stages of chronic hepatitis C. *Dig Liver Dis* 43:807-813.

153. Hoare, M., W. T. Gelson, A. Das, J. M. Fletcher, S. E. Davies, M. D. Curran, S. L. Vowler, M. K. Maini, A. N. Akbar, and G. J. Alexander. 2010. CD4+ T-lymphocyte telomere length is related to fibrosis stage, clinical outcome and treatment response in chronic hepatitis C virus infection. *J Hepatol* 53:252-260.

154. Pawelec, G., M. Adibzadeh, A. Rehbein, K. Hahnel, W. Wagner, and A. Engel. 2000. In vitro senescence models for human T lymphocytes. *Vaccine* 18:1666-1674.

155. Ouyang, Q., W. M. Wagner, A. Wikby, E. Remarque, and G. Pawelec. 2002. Compromised interferon gamma (IFN-gamma) production in the elderly to both acute and latent viral antigen stimulation: contribution to the immune risk phenotype? *Eur Cytokine Netw* 13:392-394.

156. Pawelec, G., A. Akbar, C. Caruso, R. Solana, B. Grubeck-Loebenstein, and A. Wikby. 2005. Human immunosenescence: is it infectious? *Immunol Rev* 205:257-268.

157. Nikolich-Zugich, J., and B. D. Rudd. 2010. Immune memory and aging: an infinite or finite resource? *Curr Opin Immunol* 22:535-540.

158. Akbar, A. N., and S. M. Henson. 2011. Are senescence and exhaustion intertwined or unrelated processes that compromise immunity? *Nat Rev Immunol* 11:289-295.

159. O'Bryan, J. M., J. A. Potts, H. L. Bonkovsky, A. Mathew, and A. L. Rothman. 2011. Extended Interferon-Alpha Therapy Accelerates Telomere Length Loss in Human Peripheral Blood T Lymphocytes. *PLoS One* 6:e20922.

160. Collado, M., M. A. Blasco, and M. Serrano. 2007. Cellular senescence in cancer and aging. *Cell* 130:223-233.

161. Shawi, M., and C. Autexier. 2008. Telomerase, senescence and ageing. *Mech Ageing Dev* 129:3-10.

162. Weinberg, A., and M. J. Levin. 2010. VZV T cell-mediated immunity. *Curr Top Microbiol Immunol* 342:341-357.

163. Soza, A., J. E. Everhart, M. G. Ghany, E. Doo, T. Heller, K. Promrat, Y. Park, T. J. Liang, and J. H. Hoofnagle. 2002. Neutropenia during combination therapy of interferon alfa and ribavirin for chronic hepatitis C. *Hepatology* 36:1273-1279.

164. Antonini, M. G., S. Babudieri, I. Maida, C. Baiguera, B. Zanini, L. Fenu, G. Dettori, D. Manno, M. S. Mura, G. Carosi, and M. Puoti. 2008. Incidence of neutropenia and infections during combination treatment of chronic hepatitis C with pegylated interferon alfa-2a or alfa-2b plus ribavirin. *Infection* 36:250-255.

165. Di Bisceglie, A. M., A. M. Stoddard, J. L. Dienstag, M. L. Shiffman, L. B. Seeff, H. L. Bonkovsky, C. Morishima, E. C. Wright, K. K. Snow, W. M. Lee, R. J. Fontana, T. R. Morgan, and M. G. Ghany. 2011. Excess mortality in patients with advanced chronic hepatitis C treated with long-term peginterferon. *Hepatology* 53:1100-1108.